

Copyright Undertaking

This thesis is protected by copyright, with all rights reserved.

By reading and using the thesis, the reader understands and agrees to the following terms:

1. The reader will abide by the rules and legal ordinances governing copyright regarding the use of the thesis.
2. The reader will use the thesis for the purpose of research or private study only and not for distribution or further reproduction or any other purpose.
3. The reader agrees to indemnify and hold the University harmless from and against any loss, damage, cost, liability or expenses arising from copyright infringement or unauthorized usage.

If you have reasons to believe that any materials in this thesis are deemed not suitable to be distributed in this form, or a copyright owner having difficulty with the material being included in our database, please contact lbsys@polyu.edu.hk providing details. The Library will look into your claim and consider taking remedial action upon receipt of the written requests.

Some New Approaches to Alkene Epoxidation with Manganese Catalyst

A Thesis

forward to

Department of Applied Biology and Chemical Technology

in

Partial Fulfilment of the Requirements

for

the Degree of Doctor of Philosophy

at

The Hong Kong Polytechnic University

by

Ho Kam Piu

October, 2005

Declaration

I hereby declare that this thesis is my own work and that, to the best of my knowledge and belief, it reproduces no material previously published or written, nor material that has been accepted for the award of any other degree or diploma, except where due acknowledgement has been made in the text.

Ho Kam Piu

October, 2005.

Acknowledgments

I wish to express my deepest gratitude to my supervisor, Prof. K. Y. Wong, for his valuable suggestions, encouragement and discussion throughout the course of my work, and for his valuable comments on the draft of this thesis. It is a pleasure to work with him in the past 4 years.

I wish to thank all my postgraduate colleagues in FG701 for their help and support throughout my study: Prof. Z. K. He, Dr. C. Huang, Dr. C. M. Chan, Dr. K. C. Chan, Dr. K. C. Cheung, Dr. N. Y. Kwok, Dr. K. H. Tong, Mr. H. L. Pang, Mr. C. Y. Tang, Ms. S. N. Pun, Mr. P. H. Chan, Mr. K. M. Lam and Mr. W. H. Chung. Thanks are also given to the colleagues in Prof. Bill Chan's group in U506, Dr. A. B. Brendan, Dr. K. F. Chan, Dr. B. Wan, Mr. M. C. Law and Mr. T. C. Chan, for their helpful discussion throughout my study.

I am also greatly indebted to my family especially my mum for their consistent support, concern and encouragement over these four years.

Last but not least, I would like to thank the Research Committee of The Hong Kong

Polytechnic University for the award of a research studentship and a tuition scholarship in 2001-2005 and for the traveling grant supporting my conference presentation in the 207th Electrochemical Society Meeting held in Quebec City, Canada in May 2005.

Abstract of thesis entitled “Some New Approaches to Alkene Epoxidation with
Manganese Catalyst”

Submitted by Ho Kam Piu

for the Degree of Doctor of Philosophy

at The Hong Kong Polytechnic University in October, 2005

Abstract

Epoxides are important starting materials in organic synthesis, as they can be easily transformed into other useful functionalities. Although there are many existing routes to prepare epoxides, many of these processes involve toxic chemicals and volatile organic solvents that cause pollution to the environment. The objective of this study is to develop some new approaches for alkene epoxidation that can minimize the use of toxic chemicals and solvents in the synthetic process. Manganese catalysts are chosen in this study because they are relatively non-toxic and many manganese compounds are known to be good catalysts for epoxidation.

In the first part of the thesis, hydrogen peroxide (H_2O_2) was generated in aqueous bicarbonate solutions electrochemically for the *in-situ* epoxidation of alkenes. Dioxygen (O_2) was directly reduced at the cathode to generate hydrogen peroxide, while epoxide was formed *in-situ* with a catalytic amount of manganese(II) sulfate (MnSO_4). Water-soluble alkenes were epoxidized with excellent yields and high efficiencies. The system can be adapted for the epoxidation of lipophilic alkenes in a *tert*-butanol/water/ $\text{Mn}^{2+}/\text{HCO}_3^-$ mixture.

In the second part of the thesis, ionic liquids (ILs) were employed as reaction media to generate hydrogen peroxide electrochemically for the epoxidation of alkenes. Ionic liquids are non-volatile and highly conductive solvents in which hydrogen peroxide could be generated by electrochemical reduction of dioxygen in the presence of suitable amount of water. The active oxidant peroxydicarbonate (HCO_4^-) was generated in the hydrogen peroxide/ionic liquid mixture by purging with carbon dioxide. Lipophilic alkenes were effectively epoxidized with the assistance of a catalytic amount of manganese(II) sulfate. The ionic liquids can be reused without any diminution in the efficiency of electrosynthesis and catalysis.

In the third part of the thesis, a catalytic system based on simple manganese salt was developed for the efficient epoxidation of terminal aliphatic alkenes with peracetic acid. Terminal aliphatic alkenes are a challenging class of substrates in epoxidation because of their poor nucleophilicity. We found that terminal aliphatic alkenes are efficiently and selectively epoxidized at ambient temperature by peracetic acid/ $\text{Mn}^{2+}/\text{NH}_4\text{HCO}_3$ in acetonitrile/water mixture with low catalyst loading. The reaction is stereospecific with retention of the cis/trans configuration of the alkenes in the epoxide products.

Table of Contents

DECLARATION	ii
ACKNOWLEDGMENTS	iii
ABSTRACT	vi
TABLE OF CONTENTS	viii
CHAPTER 1	1
INTRODUCTION	1
1.1. Background	2
1.1.1. Applications of epoxides	2
1.1.2. Production of epoxides and its impact on the environment	7
1.2. Some Green Approaches to Produce Epoxides	11
1.2.1. Green Solvents	11
1.2.2. Green Oxidants and Catalysts	21
1.3. Electrogeneration of Hydrogen Peroxide and Its Application to the Epoxidation of Alkenes	23
1.3.1. Electrogeneration of hydrogen peroxide	23
1.3.2. <i>In-situ</i> epoxidation with electrogenerated hydrogen peroxide	27
1.4. Metal-assisted Epoxidations with Hydrogen Peroxide and Peracetic Acid	32
1.4.1. Hydrogen peroxide as terminal oxidant	32
1.4.2. Peracetic acid as terminal oxidant	38
1.5. Aims and Objectives of this Project	41

CHAPTER 2	43
MANGANESE-MEDIATED EPOXIDATION OF ALKENES WITH HYDROGEN PEROXIDE ELECTROGENERATED <i>IN-SITU</i> IN BICARBONATE SOLUTIONS	43
2.1. Introduction	44
2.2. Experimental Section	47
2.2.1. Materials	47
2.2.2. Synthesis of epoxides	47
2.2.3. Instrumentation	49
2.2.4. Hydrogen peroxide electrogeneration	51
2.2.5. Epoxidation of alkenes with hydrogen peroxide electrogenerated <i>in-situ</i>	51
2.3. Results and Discussion	55
2.3.1. Preparation of calibration curves for the determination of hydrogen peroxide concentration	55
2.3.2. Voltammetric studies for the electrochemical reduction of dioxygen to hydrogen peroxide	60
2.3.3. Electrogeneration of hydrogen peroxide in bicarbonate solution	64
2.3.3.1. The effect of applied potential on the electrogeneration of hydrogen peroxide	64
2.3.3.2. The effect of catholyte alkalinity on the current efficiency of hydrogen peroxide electrogeneration	68
2.3.4. Electrogeneration of hydrogen peroxide in <i>tert</i> -butanol/H ₂ O/NaHCO ₃ mixture	71
2.3.4.1. Optimal amount of <i>tert</i> -butanol in bicarbonate solution for hydrogen peroxide electrogeneration	71
2.3.4.2. Optimal applied potential for the electrogeneration of hydrogen peroxide in <i>tert</i> -butanol/H ₂ O/NaHCO ₃ mixture	76
2.3.5. The role of anolyte in controlling the catholyte alkalinity	80
2.3.6. Epoxidation of water soluble alkenes with hydrogen peroxide electrogenerated <i>in-situ</i> in bicarbonate solutions	84
2.3.6.1. The effect of applied potential on the current	

efficiency of epoxide production	84
2.3.6.2. The effect of catalyst loading on the current efficiency of epoxide production	87
2.3.6.3. Epoxidation of various water-soluble alkenes	91
2.3.7. Epoxidation of lipophilic alkenes with hydrogen peroxide electrogenerated in <i>tert</i> -butanol/H ₂ O/NaHCO ₃ mixture	93
2.4. Conclusion	98
 CHAPTER 3	 100
 INDIRECT CATALYTIC EPOXIDATION WITH HYDROGEN PEROXIDE ELECTROGENERATED IN IONIC LIQUIDS	 100
3.1. Introduction	101
3.2. Experimental Section	104
3.2.1. Materials	104
3.2.2. Synthesis of ionic liquids	104
3.2.3. Instrumentation	106
3.2.4. Electrogeneration of hydrogen peroxide in ionic liquid/NaOH _(aq) mixture	109
3.2.5. Epoxidation of lipophilic alkenes with hydrogen peroxide electrogenerated in ionic liquid	109
3.2.6. Recovery and reuse of ionic liquid	110
3.3. Results and Discussion	112
3.3.1. Voltammetric studies on the reduction of oxygen in [bdmim][BF ₄]	112
3.3.2. The effect of water content in [bdmim][BF ₄] on the current efficiency of hydrogen peroxide electrogeneration	117
3.3.3. The effect of catholyte and anolyte composition in hydrogen peroxide electrogeneration	122
3.3.4. The effect of current density on the current efficiency of hydrogen peroxide electrogeneration	125
3.3.5. Epoxidation of alkenes with hydrogen peroxide	

electrogenerated in the [bdmim][BF ₄]/NaOH _(aq) mixture	129
3.3.5.1. <i>In-situ</i> generation of peroxymonocarbonate by purging CO _{2(g)} into the [bdmim][BF ₄]/NaOH _(aq) /HO ₂ ⁻ mixture	129
3.3.5.2. The effect of catalyst loading and CO ₂ sources on the efficiency of alkene epoxidation	132
3.3.6. Catalytic epoxidation of alkenes	137
3.3.7. Recycling of the ionic liquid	142
3.4. Conclusion	149
 CHAPTER 4	 150
 MANGANESE-CATALYZED EPOXIDATION OF TERMINAL ALIPHATIC ALKENES WITH PERACETIC ACID	 150
 4.1. Introduction	 151
 4.2. Experimental Section	 153
4.2.1. Materials	153
4.2.2. Synthesis	153
4.2.3. Instrumentation	155
4.2.4. Reaction conditions for epoxidation	156
4.2.5. Gram-scale preparation of epoxide	156
 4.3. Results and Discussion	 158
4.3.1. Manganese-mediated epoxidation of alkenes with peracetic acid	158
4.3.2. The role of additives in the reaction	165
4.3.3. The effect of metal catalysts	173
4.3.4. The effect of solvents	181
4.3.5. Epoxidation of various alkenes with this catalytic system	186
4.3.6. Stereoselectivity of the reaction system	192
4.3.7. Proposed mechanism for the catalytic reaction	195
 4.4. Conclusion	 197

CHAPTER 5	198
CONCLUSIONS	198
REFERENCES	202

Chapter 1

Introduction

1.1. Background

1.1.1. Applications of epoxides

Epoxides are useful intermediates for the manufacture of a wide range of commercial products [1]. They can be easily modified to other functionalized compounds and conjugated to other building blocks. What makes epoxides so reactive is the high strain of the three membered ring structure (Figure 1.1) [2]. In this ring structure, an oxygen atom is tenuously connected to two neighboring carbon atoms by single bonds. The resulting strain weakens the carbon-oxygen bond, allowing epoxides to undergo ring-opening readily.

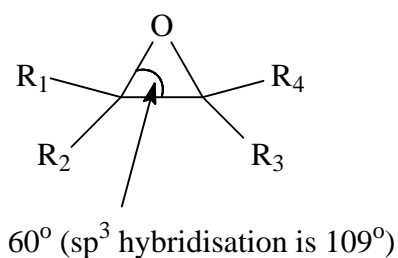
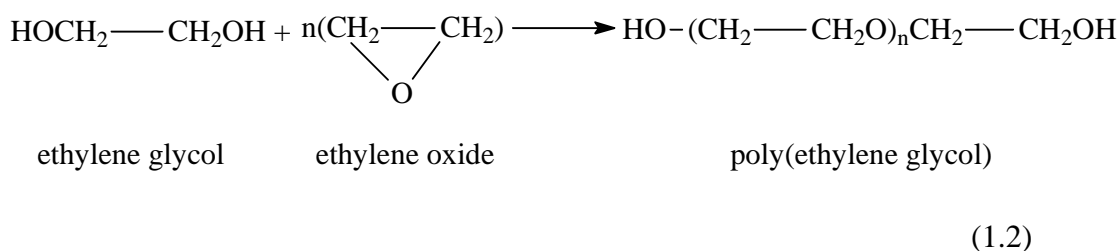
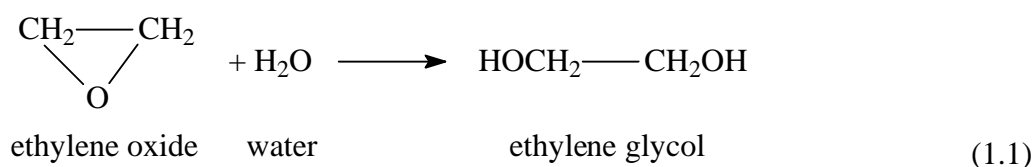


Figure 1.1 Structure of epoxides.

Epoxides such as ethylene oxide, propylene oxide, butylene oxide and epichlorohydrin are widely applicable in chemical and pharmaceutical industries

(Table 1.1) [3-5]. For instance, ethylene glycol formed by hydrolyzing ethylene oxide (eq. 1.1) is used for antifreeze formulations and polyester fibres manufacture. Polymerization of ethylene glycol (eq. 1.2) gives polymers of low molecular weight which find applications in cosmetics, lubricants, paints and drugs. Moreover, ethylene glycol ethers from ethylene oxide are used as brake fluids and solvents.



The largest single use of epoxides is in the manufacture of epoxy resins (Figure 1.2) [6]. These high strength polymers are created by the reaction of one-dimensional polymers with epoxides. By mixing with epoxy-curing agents (e.g. amines and derived polyamides), more rigid three-dimensional polymers are formed by cross-linking. Because of their low shrinkage rate, strength, excellent adhesion and resistance to chemicals, epoxide resins are ubiquitously used in the electronic industry,

where they are often used to encapsulate or embed electronic components. They are also used in boating and automotive manufacture as protective coatings and sealants and in the construction industry as components in many tough and durable structures.

Table 1.1 Applications of epoxides.

Epoxide	World production/ million tons y ⁻¹	Applications
Ethylene oxide	11	Fibers, films (decorative, packaging and photographic), containers, surfactants, functional fluids (brake fluids, hydraulic fluids and lubricants), cosmetics, emollients and vinyl plasticizers
Propylene oxide	2	Insulator (refrigerator and building), epoxy resins, cosmetics, drugs, lubricants, humectants, paints, hydraulic fluids, textile lubricants, surfactants and adhesives
Butylene oxide	4	Dry-cleaning solvent, metal-cleaning solvent, drugs, surfactants and gasoline additives
Epichlorohydrin	0.9	Epoxy resins, pesticide, coatings, adhesives, electrical casting, reinforced plastics and elastomers
Styrene oxide	-	Epoxy resins, electrical insulation, electronic, paper coating and surgical instruments

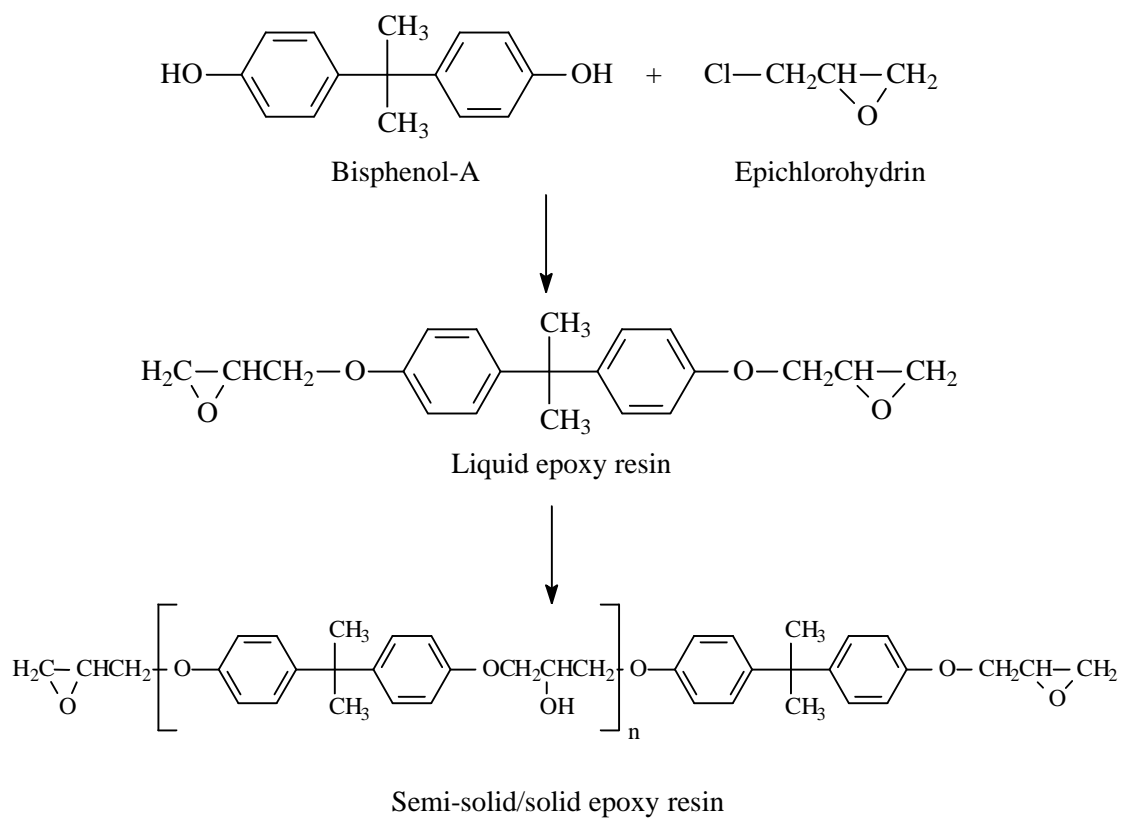
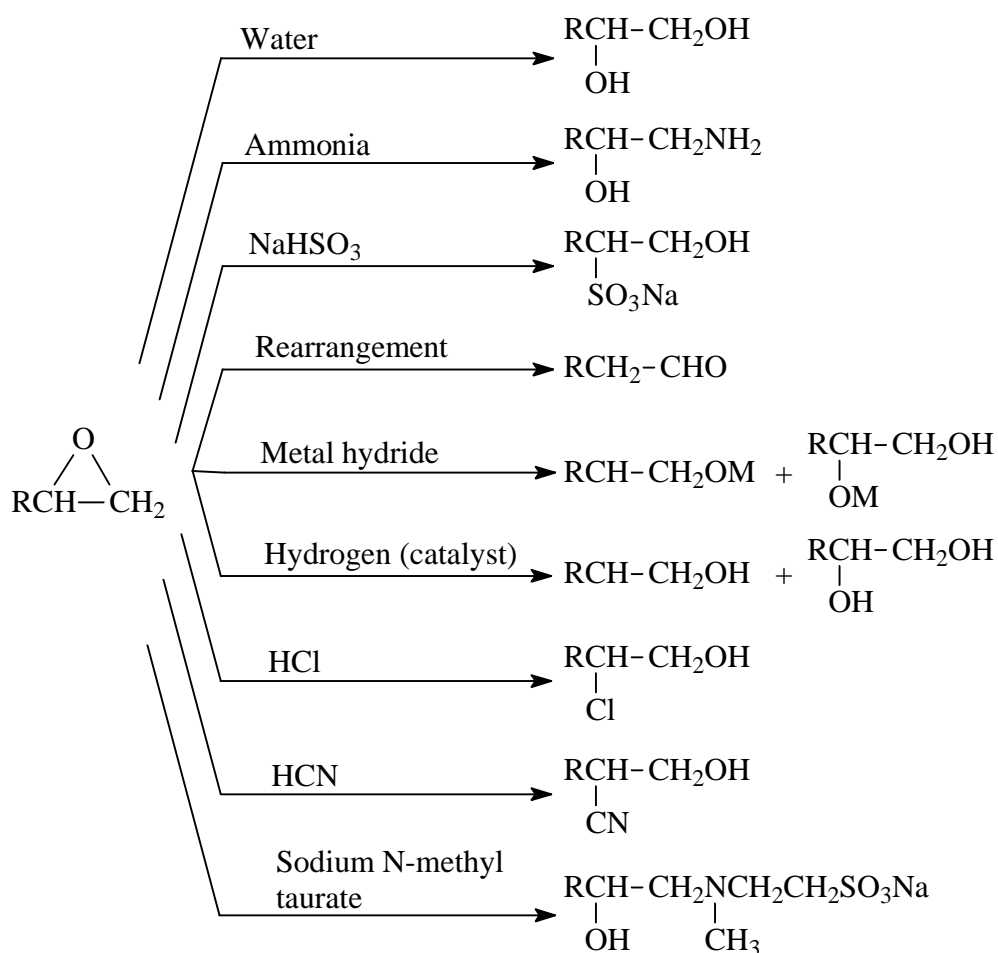


Figure 1.2 Production of epoxy resins.

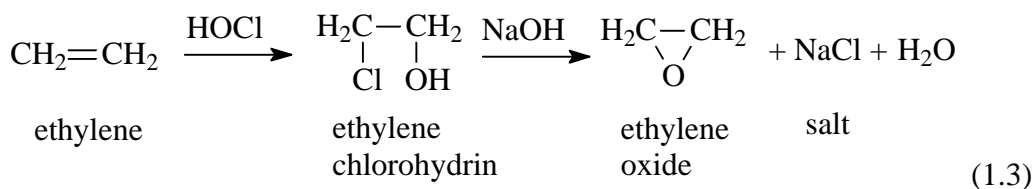
Besides polymerization, epoxides also undergo various reactions as shown in Scheme 1.1 [7]. The potential versatility and applications for these chemicals from epoxides vary and are extremely diverse. Obviously, most epoxides are attacked by nucleophiles (e.g. metal hydride and ammonia) because of the oxiranyl carbon susceptibility. Ring-opening reactions are dominant because of their tendencies to form 'open' alkyl chain structure.



Scheme 1.1 Reactions involving epoxides.

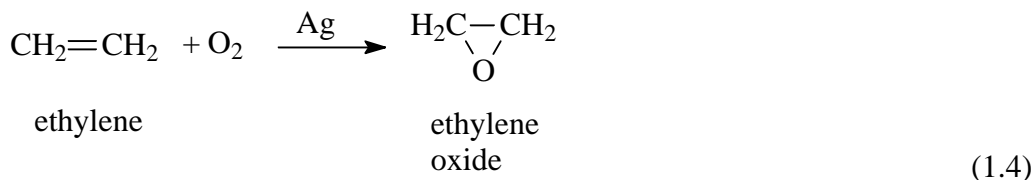
1.1.2. Production of epoxides and its impact on the environment

In the chemical industries, epoxides are produced via two ways - direct oxidation and the chlorohydrin process [2]. For many years, epoxides are produced from alkenes and chlorine treated with alkali via chlorohydrins. This process has a high efficiency, but consumes chlorine and caustic, and produces NaCl as a by-product (eq. 1.3) [4]. Since chlorine as well as hydrochloric acid and the salt are corrosive, the construction materials must be selected very carefully and the waste should be treated before released into the environment.

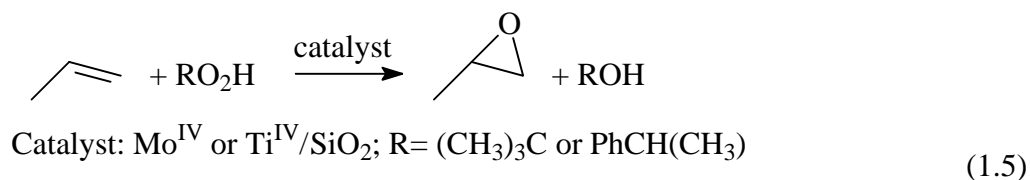


Direct oxidation with dioxygen using a silver catalyst is an alternative way for epoxidation in vapor phase (eq. 1.4). In the catalytic reaction, high temperature (250°C) and pressure (280psi) are employed to drive the transformation. Carbon dioxide is produced as a by-product due to catalytic combustion [8]. Commercially, it is viable only for forming ethylene oxide from ethylene because the reaction is limited to alkenes with lower boiling point and is not suitable for alkenes with allylic C-H

bonds due to oxidation at this position [1].

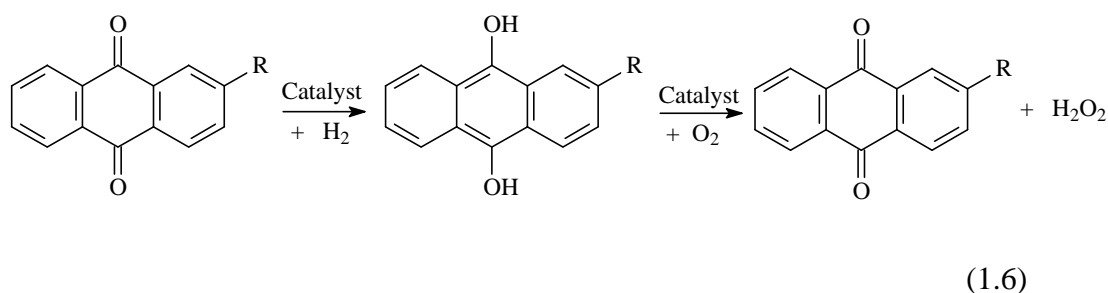


As more industrial applications use epoxides as intermediates, the demand is increasing which leads to significant development in oxidation techniques. Nowadays, epoxides are also prepared from the direct oxidation of alkenes with peroxides or peracids [9]. A key example is the epoxidation of propene with *tert*-butyl-hydroperoxide (TBHP) or ethylbenzene hydroperoxide (EBHP) (eq. 1.5), which accounts for more than one million tons of propene oxide production on an annual basis [3]. Even though this method has been widely used, it still suffers from the formation of alcohol by-products.



Many metals such as tungsten [10-16], manganese [17-20], rhenium [21-28], iron [29-33] and titanium [34-36] have been reported to be catalysts for epoxidation using

hydrogen peroxide (H_2O_2) as the terminal oxidant. H_2O_2 is an attractive option both on environmental and economic grounds. It is relatively cheap and readily available. It gives water as the only co-product and is thus considered environmentally friendly. However, there is concern on the potential hazards associated with the storage and transportation of concentrated H_2O_2 (>60%) [37, 38]. Indeed, a large proportion of the cost of H_2O_2 is due to transportation, storage and insurance. In the world, over 85% of H_2O_2 is produced by the autoxidation of 2-ethylanthrahydroquinone (the AQ process) (eq. 1.6). This process uses huge amount of toxic organic solvents (e.g. trimethyl benzene) to recycle the catalyst [39, 40], and thus the ‘green’ oxidant is ‘non-green’ in its production.



Many organic solvents commonly used as reaction media for the epoxidation of alkenes and in the separation and extraction of products are volatile organic compounds (VOCs) [21, 23, 24, 41-43]. Some of them are carcinogens, mutagens and reprotoxic substances and are harmful to human being. These volatile organics also

cause environmental problems such as ozone depletion [44]. As these solvents are used in extremely high volume, there is a strong need to replace the volatile organic solvents with 'greener' reaction media.

1.2. Some Green Approaches to Produce Epoxides

In the past decade, scientists are particularly interested in the development of environmentally benevolent methods to produce epoxides. In reality, no chemical activity is completely innocuous or totally benign to human being and the environment [45]. Therefore, the prime aim of most studies is to design processes that can reduce or eliminate the use and generation of hazardous substances.

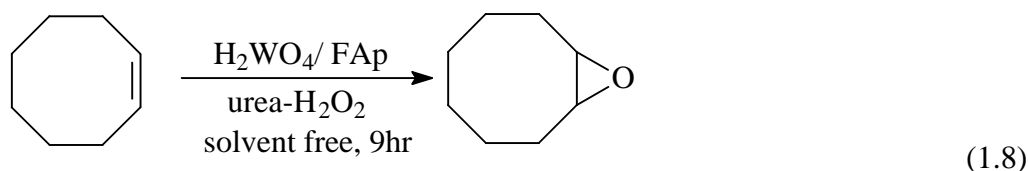
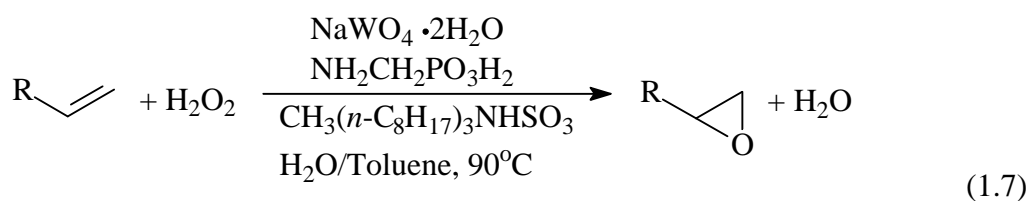
1.2.1. Green Solvents

Solventless media

Based on the principles of green chemistry [46], researchers in industry and academia are developing new solvent systems to reduce the intrinsic hazards associated with traditional organic solvents. Certainly, using no solvent at all is the ultimate solution to minimize solvent-associated hazards. In 1996, Noyori et al. [13, 14] reported a catalytic system, containing sodium tungstate, amino-methylphosphonic acid and quaternary ammonium salt hydrogen sulfate with 30% H₂O₂, to epoxidize alkenes in solvent-free conditions (eq. 1.7). The active species are formed *in-situ*, and the lipophilic ammonium salt acts as a phase transfer agent to promote the oxidation.

Under optimal conditions, terminal alkenes are transformed to epoxides in high yields with only 1.5-2 equivalents of H₂O₂. However, certain acid-sensitive epoxides are not stable under such conditions due to hydrolytic decomposition.

A similar catalytic system has been reported by Ichihara et al. [47], who embedded tungstic acid catalyst on fluoroapatite solid support and used urea-hydrogen peroxide adduct as the oxidant. Most cycloalkenes and allylic alcohols are smoothly transformed to epoxides in high yields (eq. 1.8). Products can be easily isolated by decantation and the solid-supported catalyst can be reused without any deterioration of its activity [48, 49]. The catalytic systems described by Gusevskaya et al. [50] and Schuchardt et al. [51] employed sol-gel Co/SiO₂ catalyst and Nb-MCM-41/Ti-MCM-41 catalysts respectively for this heterogeneous reaction. In the former case, dioxygen is used as the oxygen source, which is of particular interest.



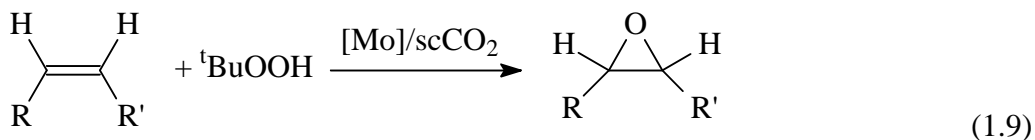
Supercritical carbon dioxide (ScCO₂)

In general, solvents act as the media for catalytic reactions, and most reactions do not proceed without them. The use of supercritical fluids especially ScCO₂ has been an extremely important area of green solvent research in the past decade [46]. ScCO₂ exhibits low surface tension and viscosity, and hence high diffusion rate for the reactants. It is completely miscible with most reaction gases and many organic/inorganic compounds. By tuning the critical point conditions, a unique set of CO₂ properties can be attained for solvent purposes [52].

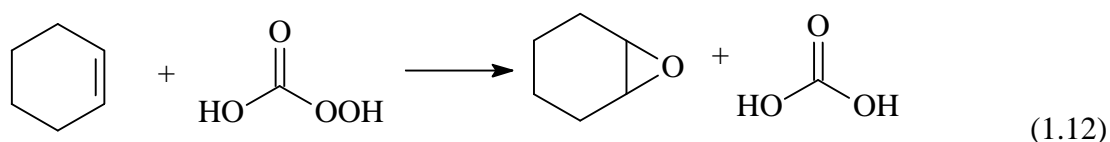
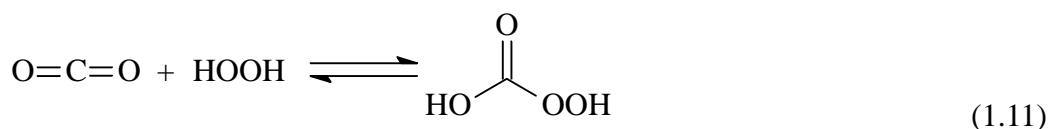
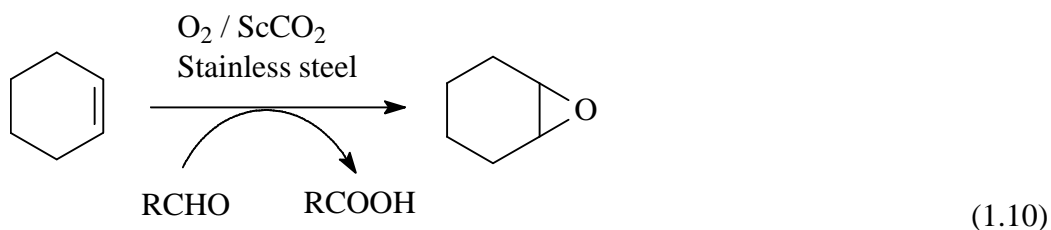
Metal-catalyzed epoxidation with organic peroxides occurs readily in ScCO₂ [53, 54]. Excellent yields of epoxides could be obtained using molybdenum hexacarbonyl [Mo(CO)₆] and oxovanadium(V) tri(isopropoxide) [VO(OPrⁱ)₃] catalysts with anhydrous ^tBuOOH (eq. 1.9). However, with aqueous ^tBuOOH, diols were formed as the major side products.

Tonellato et al. [55] have reported that manganese 5,10,15,20-tetrakis(2',6'-dichlorophenyl) porphyrin [Mn(TDCPP)Cl] can catalyze the oxidation of alkenes to epoxides with H₂O₂ and hexafluoroacetone co-catalyst. Under appropriate reaction conditions, complete conversion for cyclooctene was observed

with the formation of cyclooctene oxide as the sole product. With the catalyst embedded in polydimethylsiloxane (PDMS) and organically modified silicates (ORMOSILs), the catalyst lifetime was enhanced [56].



The use of dioxygen as the primary oxidant for epoxidation in ScCO_2 has been accomplished with iron-based catalysts, although the yields and selectivities are only moderate [57]. Recently, Locker et al. [58] have reported a simple way for epoxidation with molecular oxygen by using stainless steel reactor and an aldehyde co-oxidant (eq. 1.10). This method is particularly effective in the case of disubstituted internal alkenes and additional catalyst is not required to achieve a high reaction rate. An alternative method has been reported by Bartels et al., who used ScCO_2 as a reactant in combination with aqueous H_2O_2 in an autoclave [59, 60]. The reaction is made possible through the *in-situ* formation of peroxycarbonic acid (eq. 1.11). It was conducted without metallic catalyst or peroxy acid while high epoxide selectivities could still be maintained (eq. 1.12).

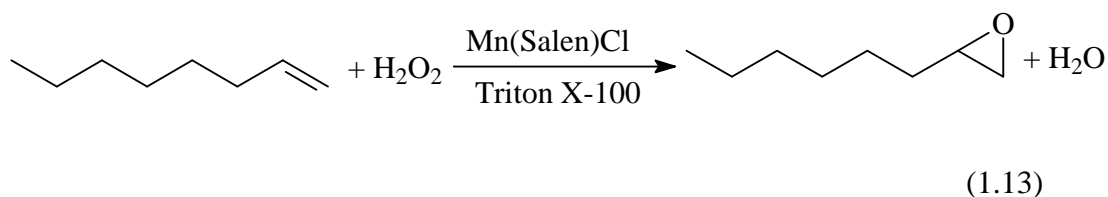


Aqueous or aqueous/organic solvent mixtures

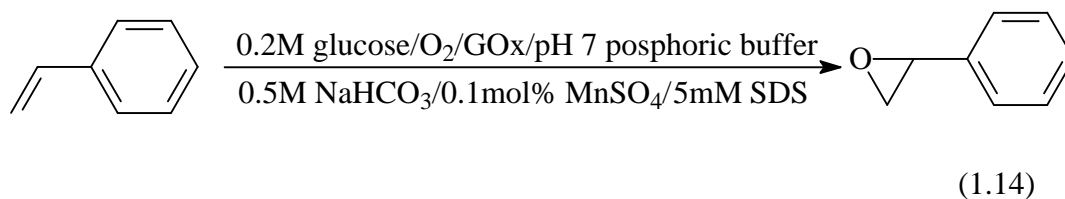
In the search for more environmentally friendly medium, there is no better-known substance nor a more widely used solvent in the world than water though in the last century, it was not considered an adequate or even possible solvent in organic reactions. The major obstacle in the development is the low solubility of lipophilic substances in water. With different techniques being discovered, advanced methods are now being developed.

An effective epoxidation making use of aqueous micelles to mediate the reaction between oxidants (e.g. H_2O_2), lipophilic alkenes (e.g. propylene) and catalysts (e.g. $\text{Mn}(\text{Salen})\text{Cl}$) has been described by Keurentjes et al. [61, 62]. In this catalytic

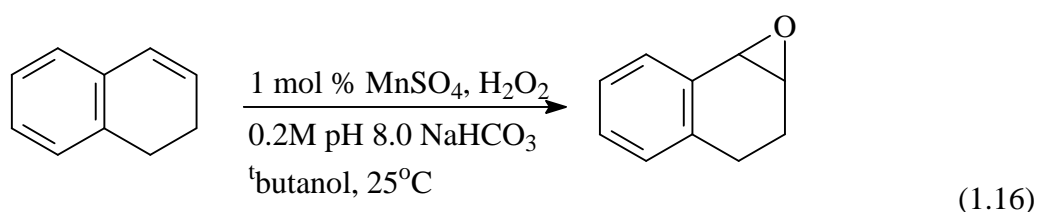
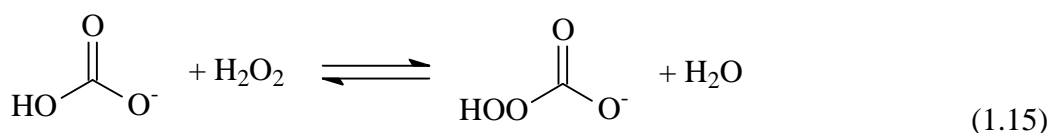
process, alkene was bubbled through the aqueous solution and at the same time, peroxy oxygen from H_2O_2 was activated and transferred through the micelle-incorporated epoxidation catalyst to the alkenes (eq. 1.13). By means of micellar-enhanced ultrafiltration, the homogeneous nonpolar catalyst could be easily separated. Similar designs have been reported by Nojima et al. [63, 64] and Plusquellec et al. [65], but the latter used amphiphilic carbohydrates rather than surfactants as the constituents of micelles.



Biochemically, glucose oxidase (GOx) is active in generating H_2O_2 , and *Mycobacterium* M156 cells are capable to epoxidize alkenes in culture media. Based on these properties, two novel approaches were developed by Chan et al. [66] (eq. 1.14) and Stuckey et al. [67] respectively to epoxidize lipophilic alkenes in aqueous medium. The major drawback of this approach is the inactivation of glucose oxidase at high concentration of H_2O_2 .



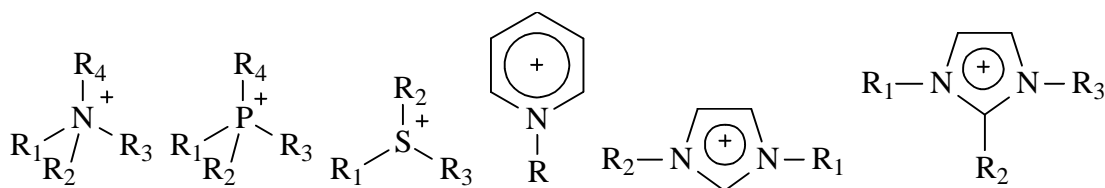
Apart from these, a simple alternative way to overcome the solubility problem is to use a mixture of organic and aqueous solvents. Recently, Richardson et al. [68] reported a bicarbonate-mediated epoxidation in which lipophilic alkenes were solubilized in acetonitrile/water mixture. The active oxidant was suggested to be a peroxymonocarbonate (HCO_4^-) species (eq. 1.15). Subsequently, Burgess et al. [69] showed that simple MnSO_4 salt could speed up the reaction in bicarbonate solutions (eq. 1.16). With the use of *tert*-butanol or DMF, most lipophilic alkenes were epoxidized within an hour. Mimura et al. [70, 71] have studied the use of dodecylamine as a surfactant to assist the solubility of aliphatic alkenes in methanol/water mixture. In their work, homogeneous catalysts were used for the oxidation by molecular oxygen in the reaction mixture.



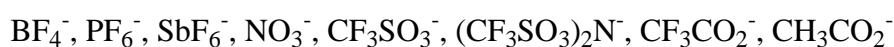
Ionic liquids (ILs)

Room temperature ionic liquids (RTILs) have generated intense interest over the last decade [72]. Most studies were centered on their possible use as “greener” alternatives to volatile organic solvents because they possess low vapor pressures and high thermal stabilities, and are good solvents for a broad spectrum of chemicals. Intrinsically, they are salts of organic cations, e.g. tetraalkylammonium, tetraalkylphosphonium, N-alkylpyridinium, 1,3-dialkylimidazolium, 1,2,3-trialkylimidazolium and trialkylsulfonium cations combined with anions such as tetrafluoroborate, hexafluorophosphate and trifluoromethanesulfonate (Scheme 1.2). By suitable choices of cation and anion, properties such as conductivity, viscosity, hydrophilicity and lipophilicity can be tuned.

Cations:

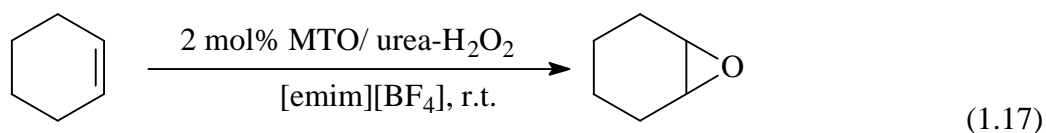


Anions:



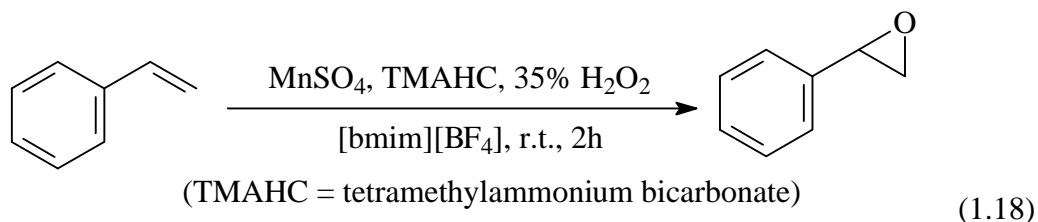
Scheme 1.2 Examples of cations and anions in ionic liquids.

The first example using ionic liquid as reaction medium for epoxidation was reported by Abu-Omar et al. [73], who employed methyltrioxorhenium (MTO) catalyst with urea- H_2O_2 (UHP) adduct to epoxidize alkenes in 1-ethyl-3-methylimidazolium tetrafluoroborate ($[\text{emim}][\text{BF}_4]$) (eq. 1.17). Both UHP and MTO are soluble in $[\text{emim}][\text{BF}_4]$, and the medium remained homogeneous throughout the reaction. When UHP was replaced with H_2O_2 , ring opening of epoxides was observed. Several olefinic substrates have been oxidized to epoxides with excellent yields. However, poor conversion was obtained with less soluble substrates (e.g. 1-dodecene) because of heterogeneity.

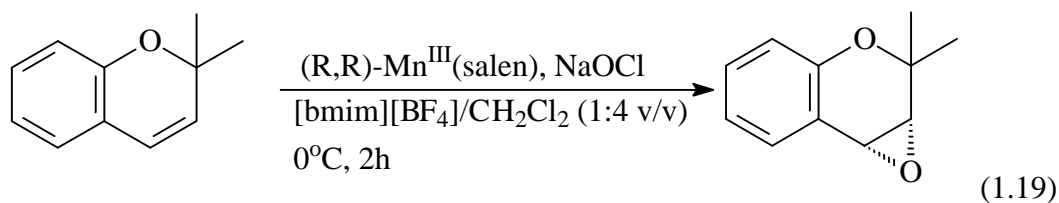


Similar studies have been presented by Romao et al. [74] and Goncalves et al. [75] using molybdenum-based catalysts, El-Hiti et al. [76] using Katsuki-type catalysts, Xia et al. [77] and Chan et al. [78] using manganese-based catalysts, and Chauhan et al. [79] using iron-based catalysts. In all cases, the ionic liquids are recoverable and reusable for subsequent cycles without any significant deterioration. Amongst these, the study of Chan et al. [78] is of particular interest, as they modified the catalytic

system of Burgess et al. [69] and found that lipophilic alkenes could also be epoxidized in ionic liquids with simple Mn^{2+} salts (eq. 1.18).



Attempt to couple Jacobsen's chiral $\text{Mn}^{\text{III}}(\text{salen})$ catalyst for asymmetric epoxidation has been conducted in ionic liquid ([bmim][PF₆]) (eq. 1.19) [80]. However, dichloromethane was required as co-solvent, as the ionic liquid solidified at the reaction temperature (0°C).



1.2.2. Green oxidants and catalysts

Hydrogen peroxide (H_2O_2) is probably the best terminal oxidant besides molecular oxygen with respect to environment and economic considerations. It can oxidize organic compounds with an atom efficiency of 47% with the generation of water as the only by-product. It is very attractive for liquid-phase reactions because of its stability and selectivity compared with molecular oxygen [81].

Direct epoxidation with dilute H_2O_2 is a long-standing goal in organic chemistry, but its polarity is the major drawback for reactions with non-polar alkenes and catalysts [82-90]. In 1983, phase transfer catalysis (PTC) for the epoxidation of alkenes using H_2O_2 was firstly reported by Ishii-Venturello et al. [82], who found that the two-component association of tungstate and phosphate ions, under acidic conditions, was a valuable catalytic system. Later on, modified procedures made from heteropolyacids (such as dodecatungstophosphoric acid) with an ammonium salt (such as cetylpyridinium bromide) was developed, that was applied to a number of biphasic epoxidation processes [11, 83, 84]. An apparent breakthrough in H_2O_2 epoxidation using phase-transfer catalyst was reported by Noyori et al [13]. They developed a totally halide and solvent-free system based on NaWO_4 catalyst with

trioctylmethyammonium hydrogen sulfate as the phase transfer agent (eq. 1.7).

Heterogeneous catalysts offer the advantages of easy catalyst separation and sometimes higher selectivity. However, most of these catalysts suffer from lower activity and instability [36]. Amongst them, titanium-containing silicates, including amorphous titania-silica materials and Ti-substituted molecular sieves, are the most efficient ones for epoxidation. A well-known solid catalyst designed by Taramasso et al. [91] is the titanium silicate-1 (TS-1) molecular sieve. However, the main drawback of TS-1 is its small pore dimension, which makes accessible to only relatively small substrates.

Heterogeneous alumina-catalyzed oxidation was first reported by Sheldon et al. [92-94]. This reaction uses chromatographic alumina as the catalyst to epoxidize a range of industrially relevant alkenes. It is cheap and easily recyclable, and shows interesting reactivity and selectivity. This economic and green method is however not applicable in industry because anhydrous H_2O_2 is required.

1.3. Electrogeneration of Hydrogen Peroxide and Its Application to the Epoxidation of Alkenes

1.3.1. Electrogeneration of hydrogen peroxide

The majority of H₂O₂ produced commercially is based on the auto-oxidation of 2-alkylanthrahydroquinones (AQ process). Environmentally, this process is not ‘green’ because volatile solvents are used and toxic wastes are produced. In industry, an alternative way to generate H₂O₂ is by electrolysis [95]. However, this technology is too energy inefficient for large-scale production. For this reason, attention is being drawn to the production of low strength H₂O₂ on small-scale plants and for on-site processes through direct O₂ reduction on the cathode (eq. 1.20):



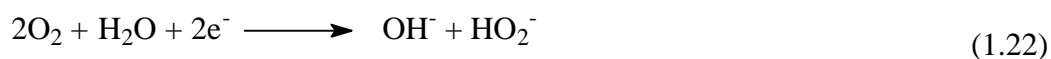
This simple and waste-free route leaves no residues in the reaction stream and employs air or oxygen as feedstock and electrons as the reducing agent.

The practical utility of this electrochemical method has been widely studied [96-108].

Electrochemical reduction of oxygen on different electrode materials is of particular interest. Mercury [96, 97], gold [98, 99], carbon [100-105], manganese oxide[106] and titanium oxide [107, 108] have been proven to give high yield and current efficiency of H₂O₂ under appropriate conditions. Amongst these electrode materials, carbon is often the choice for practical and economic considerations [101, 106, 109-112]. Studies by Taylor et al. [102] demonstrated that the reaction in acidic media should be



In alkaline media, the overall reaction is



At most other cathodes (e.g. platinum [100, 113-115] and iron [116]), 4e⁻ reduction of molecular oxygen predominates (eq. 1.23) although H₂O₂ is formed as an unstable intermediate.

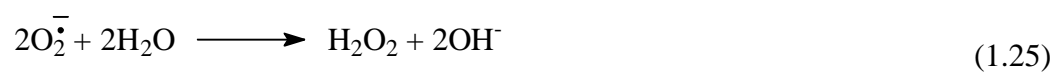


In addition to this, electrochemical processes based on three-dimensional electrodes such as beds of carbon particles or reticulated vitreous carbon [95, 117-120], and gas diffusion cathodes fabricated from carbon powders [121, 122] have also been developed. Compared with plate electrodes, these electrodes provide higher surface area to overcome the problems of oxygen solubility and mass transport limitations in the electrolyte.

Apart from aqueous medium, a two-phase (organic/aqueous) system has also been investigated for the electrogeneration of H_2O_2 [39, 123-127]. In this system, 2-ethyl-9,10-anthraquinone in organic phase is electrochemically reduced to produce the corresponding hydroquinone, which reacts with molecular oxygen to generate H_2O_2 *in-situ* in the aqueous layer. The mixture is emulsified by turbulence flow that improves the overall current efficiency of the electrosynthesis.

The electrogeneration of H_2O_2 in ionic liquids has also been investigated. Weidner et al. [128, 129] have demonstrated that stable superoxide ion could be electrogenerated from oxygen in the ionic liquid 1-butyl-3-methylimidazolium hexafluorophosphate ($[\text{bmim}][\text{PF}_6]$) (eq. 1.24). Chan and Wong have also reported that upon the addition of suitable amount of water, H_2O_2 is generated in high yield in

1-butyl-3-methylimidazolium tetrafluoroborate ([bmim][BF₄]) (eq. 1.25) [130].



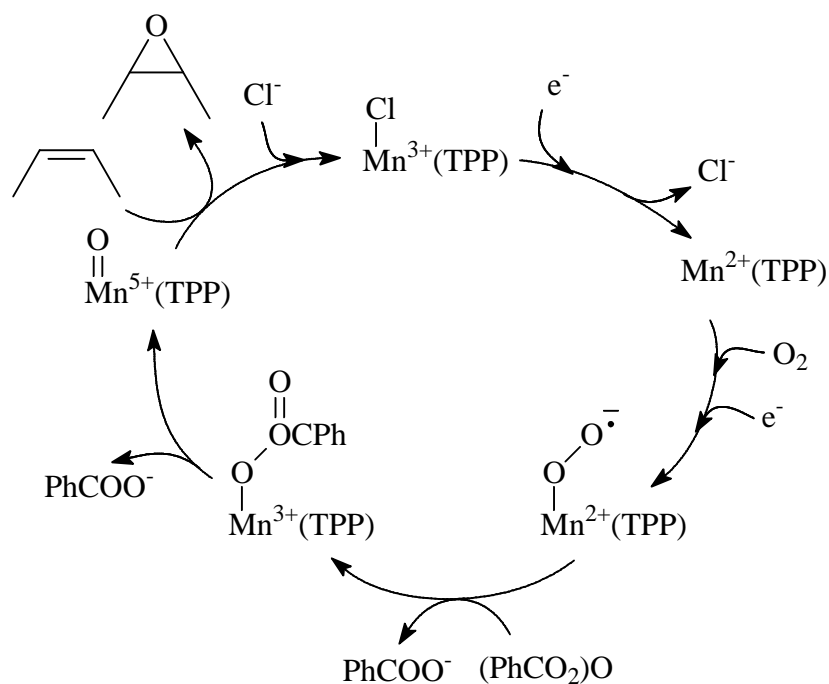
1.3.2. *In-situ* epoxidation with electrogenerated hydrogen peroxide

There has been considerable interest in using electrogenerated H_2O_2 for indirect organic oxidation [131-133], treatment of effluents [134] and destruction of organic wastes [135-137]. Although the H_2O_2 concentration prepared by this electrosynthetic method is never too high, the strength is strong enough to push most of the reactions to proceed smoothly.

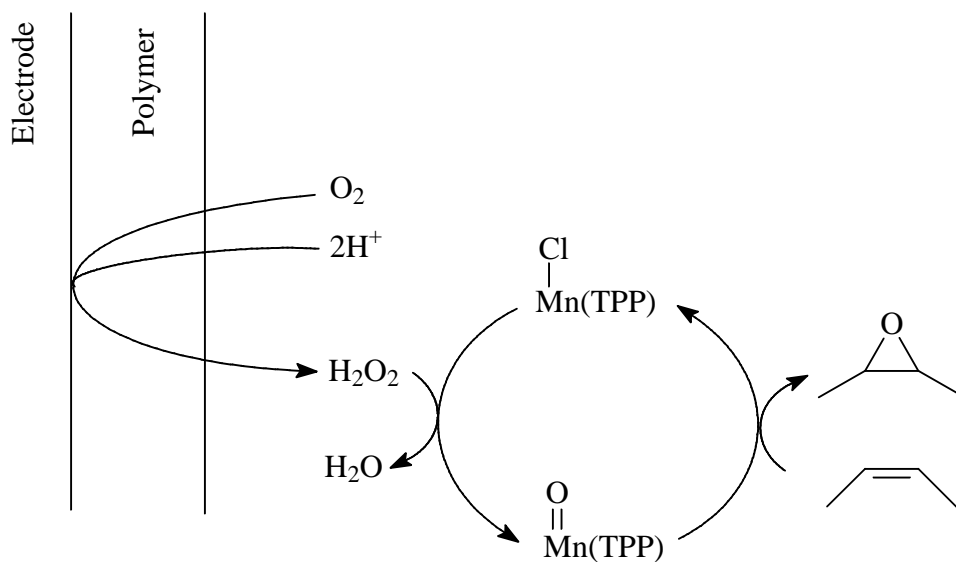
Most of the electrocatalytic epoxidation reactions in literatures are direct process, which means that the active oxidizing species were generated directly on the electrode surface. Murray et al. [138] were the first to study the electrocatalytic reduction of $[\text{Mn}(\text{TPP})\text{Cl}]$ (TPP = *meso*-tetraphenylporphyrin) at a carbon electrode in the presence of oxygen for epoxidation (Scheme 1.3). Similar studies have been carried out by Rusling et al. [139-142] using cytochrome P450(cam) and myoglobin, Steckhan et al. [143] and Colijn et al. [144] using Ag-based catalysts, Gilbert et al. [145] using Fe-porphyrin complexes, Torii et al. [146] using Mn-salen complexes and Su et al. [147] using ruthenium porphyrin complexes as catalysts. Generally, they are all effective in epoxidation, but the reactivity is limited by the catalyst concentration in the immobilized films. Later, Murray et al. [148] presented an alternative approach,

which employed modified carbon electrodes to generate H_2O_2 for *in-situ* transformation of Mn-porphyrin to Mn-oxo porphyrin complex in solutions (Scheme 1.4). Alkenes were epoxidized in the reaction mixture *in-situ* rather than inside the film. In all these systems, the reactions were carried out in organic solvents, and the catalytic life of the metal catalysts was limited.

A similar design was developed by Li et al. [149], who made use of $\text{VO}(\text{acac})_2$ [(acac) = acetylacetonate] to catalyze the epoxidation of water-soluble unsaturated carboxylic acid with H_2O_2 electrogenerated in aqueous medium. The active species was identified as $\text{VO}(\text{acac})_2\text{OOH}$, which was formed *in-situ* in the presence of H_2O_2 . Recently, Wladimir et al. [108] have reported a system using heterogeneous titanium silicate (TS-1) as catalyst. In their work, a mixture of hydrophobic carbon black and the epoxidation the catalyst was packed in the form of a trickle bed. H_2O_2 production and the following epoxidation occurred in a catalytic mixture located in the cathodic chamber of an electrolytic cell. Using molecular oxygen as reagent, it is possible to epoxidize allyl alcohol in a single step.



Scheme 1.3 Electrocatalytic epoxidation via direct approach.



Scheme 1.4 Electrocatalytic epoxidation via indirect approach using H_2O_2 electrogenerated *in-situ* in the reaction mixture.

Paired electrosynthesis for epoxidation was first reported by Chou et al. [150], who designed an electrolytic cell for propylene oxide production in both the anode and cathode compartments. This is an efficient electrochemical process because the current efficiency can reach 200% theoretically. In the anode compartment, AgNO_3 in the anolyte was used to form the redox mediator, Ag^+/AgO^+ , for indirect epoxidation of propylene. In the cathode compartment, oxygen was introduced into an acidic aqueous catholyte to form H_2O_2 , which oxidized propylene directly. Similar electrosynthesis has been developed by Nonaka et al. [151], who combined the production of epoxides and 1,2-dibromides in two concurrent oxidation processes. In the anode, a $\text{VO}(\text{acac})_2/[\text{VO}(\text{acac})_2\text{OOH}]^-$ redox mediator was used for the anodic oxidation of alkenes. On the other side, the alkenes were indirectly brominated with a Br^-/Br^+ mediator to give the corresponding 1,2-dibromides in the cathode compartment. Under optimum conditions, the total current efficiency of these paired electrosyntheses exceeded 100%.

Recently, Chan and Wong [130] have developed a ‘green’ way to epoxidize alkenes using H_2O_2 electrogenerated in an ionic liquid/ $\text{NaOH}_{(\text{aq})}$ mixture. Under alkaline conditions, the H_2O_2 electrogenerated was used successfully for the epoxidation of a number of electrophilic alkenes. After product extraction, the ionic liquid electrolyte

can be recycled for the generation of H_2O_2 and epoxidation again. While the whole process is regarded as a 'green' system because only oxygen, water and electricity are required as feedstocks, this system can only apply to the epoxidation of electrophilic alkenes such as α,β -unsaturated ketones.

1.4. Metal-assisted Epoxidations with Hydrogen Peroxide and Peracetic acid

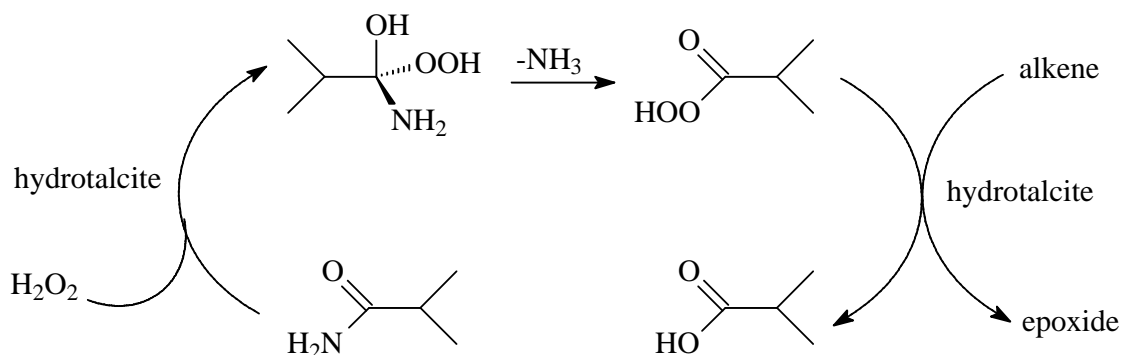
1.4.1. Hydrogen peroxide as terminal oxidant

While H_2O_2 is a unique green oxidant, its reactivity is not strong enough to push some oxidation reactions. With the assistance of catalyst, the peroxy oxygen can be transferred to the substrate with high selectivity. In general, metal-catalyzed epoxidation with H_2O_2 can be classified as either heterogeneous or homogeneous catalysis depending on whether the metal catalyst is soluble in the reaction medium.

Heterogeneous catalysts

Heterogeneous systems for the epoxidation with H_2O_2 typically employ mineral-type catalysts, including zeolites [152-154] and hydrotalcites [155-158]. The latter is more widely used as they can be applied to a greater variety of substrates. Hydrotalcites are polynuclear-alumina clays, which promote epoxidation through nucleophilic attack [159]. In 1998, Kaneda et al. [156] reported that $\text{Mg}_{10}\text{Al}_2(\text{OH})_{24}\text{CO}_3$ effectively catalyzes the epoxidation of many alkenes with high conversion and selectivity. This system works for acid-sensitive epoxides. However, amide or nitrile is inevitably

charged as additives in the synthetic process (Scheme 1.5).

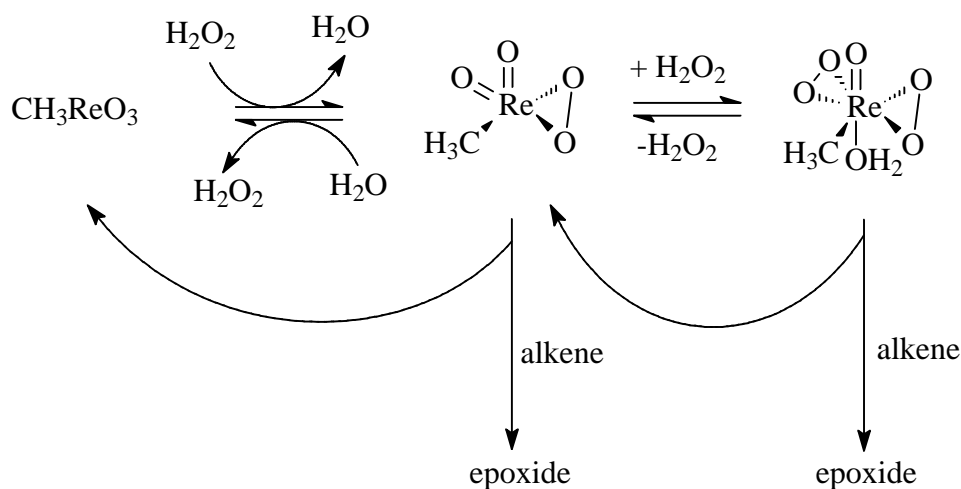


Scheme 1.5 Heterogeneous epoxidation of alkenes with H_2O_2 catalyzed by hydrotalcites.

Homogeneous catalysts

Polyoxometalates are anionic salts incorporated with two or more metal centres, which can act as homogeneous epoxidation catalysts [160]. Herrmann and co-workers [161, 162] used methyltrioxorhenium (MTO) as a simple and soluble catalyst for epoxidation (Scheme 1.6). MTO activates H_2O_2 through the formation of η^2 -peroxo species, which transfers the peroxy oxygen to alkenes [163, 164]. Inherently, this system is acidic, and hence ring opening of sensitive epoxides to diol is inevitable. Procedural modification reported by Sharpless et al. [22, 42] indicates that alkaline additives (e.g. pyridine and 3-cyanopyridine) can alleviate the problem through neutralization. However, these additives are difficult to be separated from the product.

Other than MTO, polyoxotungstates [82, 165-171] and peroxomolybdates [172-177] are also effective catalysts, but application of these systems in large-scale reactions tends to be restricted by the toxicity related to the catalysts themselves and the solvents used (chlorinated solvents).



Scheme 1.6 Homogeneous epoxidation of alkenes with H_2O_2 catalyzed by methyltrioxorhenium (MTO).

Porphyrins-, salen- and 1,4,7-tacn-derived catalysts [salen = salicylideneiminato and tacn = triazacyclononane] have been widely investigated as ligands to stabilize metals (e.g. manganese or iron) with respect to undesirable decomposition and to tune their reactivities. By modification of the ligand, catalytic ability and stereospecificity may be systematically tuned.

In 1985, Mansuy and co-workers [178, 179] reported that Mn-porphyrin complexes are effective catalysts in epoxidation with H_2O_2 (Figure 1.3). They reported that chlorinated porphyrins are robust oxidation catalysts, and additives, such as imidazole and carboxylic acids, can ensure high catalytic reactivities [180, 181]. A series of reports presented by Taylor et al. [182-184] have demonstrated that Fe-porphyrin complexes are active enough to promote the epoxidation reaction smoothly. Most alkenes are readily transformed to epoxides under mild conditions. However, the conversion and selectivity tend to be inferior to their Mn counterparts.

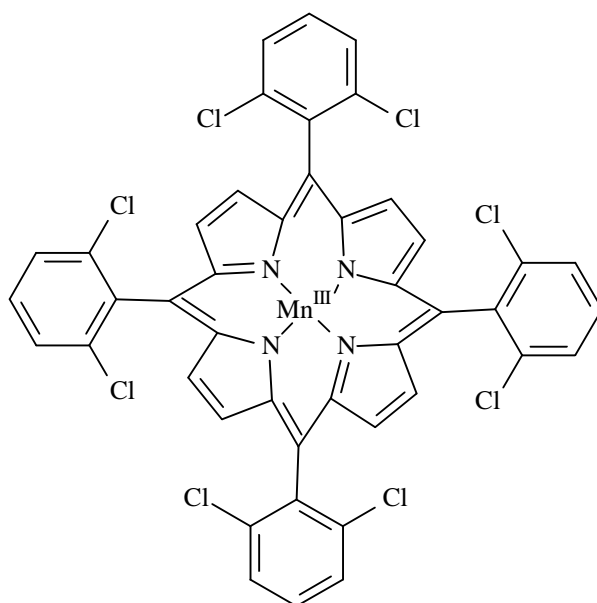


Figure 1.3 Molecular structure of chlorinated Mn-porphyrin designed by Mansuy et al.

Manganese-salen complexes have been extensively investigated in alkene

epoxidations with H_2O_2 , largely from the perspective of asymmetric catalysis with Jacobsen's catalyst (Figure 1.4). Berkessel et al. [185, 186] were the first to report the application of Mn-salen in epoxidation with H_2O_2 , and noticed that most of these Mn complexes required additives such as imidazole to generate the Mn-oxo intermediates via heterolytic cleavage of H_2O_2 . They found that a salen ligand with tethered imidazole groups can enhance the epoxidation rate and enantioselectivities relative to unmodified salen system. On the other hand, Katsuki et al. [187] reported that unfunctionalized Mn-salen complex together with imidazole in solution would give high ee's but low yield of epoxides. Pietikainen et al. [188, 189] have also studied the effect of imidazoles in salen-mediated epoxidation with H_2O_2 , and found that high yields and ee's can be obtained using carboxylates and simple soluble salts (acetates, formates, benzoates) as additives.

Generally, Mn-salen mediated epoxidation alkenes with H_2O_2 is an effective system in asymmetric synthesis. However, catalyst deactivation caused by radicals from homolytic cleavage of peroxide unfortunately exists in the catalytic process [190]. Comparatively, Mn-tacn complexes [191-194] are more stable catalysts for epoxidation, though the ligands are difficult to prepare in large-scale. Attempts to mediate asymmetric epoxidation with H_2O_2 using manganese complexes of chiral tacn

derivatives has also been reported by Bothe et al. [195, 196] and Sherrington et al. [197], but these systems gave only low to moderate enantioselectivities.

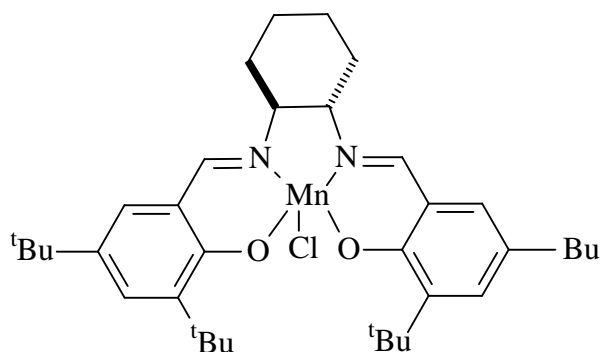


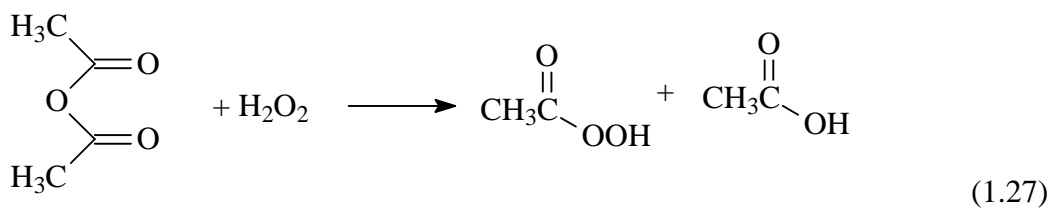
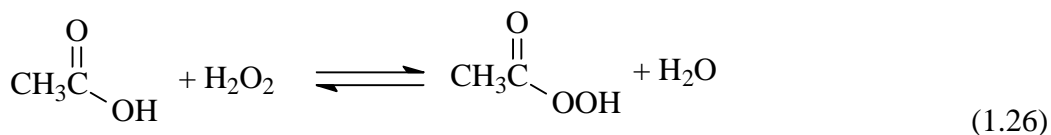
Figure 1.4 Molecular structure of Jacobsen's catalyst.

The generation of metal oxo species from selenium [198-201] and arsenic [202, 203] compounds as well as from some simple metal salts [204] are alternative means to activate H_2O_2 . The former systems are surprisingly active and selective on epoxidation, but there are environmental concerns regarding the fluorinated media used and the high concentration of H_2O_2 (>60%) required in the reactions. The method developed by Burgess et al. [204] in which epoxidation is promoted by catalytic amount of simple manganese(2+) salts with 30% H_2O_2 in bicarbonate solutions (eq. 1.16) deserves special attention. The manganese catalyst is relatively inexpensive, far less toxic and more environmentally compatible solvents such as *tert*-butanol and DMF (as opposed to halogenated hydrocarbons) are used.

Furthermore, a variety of aryl-substituted, cyclic and trialkyl-substituted alkenes can be readily epoxidized.

1.4.2. Peracetic acid as terminal oxidant

The active oxygen in H_2O_2 is sometimes not ‘active’ enough for certain epoxidation reactions, but this oxygen can be transformed to give the more active peracetic acid (eq. 1.26 and 1.27). Peracetic acid behaves as strong electrophilic oxidant, which transfers its peroxy oxygen preferentially to electron-rich alkenes (e.g. di- tri- or tetra-substituted alkyl alkenes). For those electron-deficient and terminal aliphatic alkenes, it is reactive only at elevated reaction temperatures and with extended reaction times, but significantly amounts of epoxide ring-opened products are often formed.



Metal-assisted epoxidation potentially overcome these limitations by enhancing the reaction rates and lowering the reaction temperatures. In literature, the first account on the use of manganese complexes in catalytic epoxidation of alkenes with peracetic acid was reported by Banfi et al. [205], who used metallo-porphyrins, phthalocyanines and tetraazaporphyrins as catalysts. Amongst them, manganese-porphyrins showed the highest reactivities on aryl- and alkyl- substituted alkenes with moderate turnovers [206-208]. Reports on mechanistic and kinetic studies are also available [209-211]. These studies suggested that the first step of the reaction involves an adduct formation, followed by an irreversible formation of Mn^V -oxo species. The higher catalytic oxidative activity of these active species is related to the existence of electronegative substitution in the macrocycles.

Recently, investigations made by Murphy et al. [212] on $Mn(mep)$ or $Mn(R,R-mep)$ as catalysts [(*mep*) = *N,N'*-dimethyl-*N,N'*-bis(2-pyridylmethyl)-ethane-1,2-diamine, (*R,R-mep*)=*N,N'*-dimethyl-*N,N'*-bis(2-pyridylmethyl)-(R,R)-(+)-cyclohexane-1,2-diamine] indicated that these systems can epoxidize a wide scope of alkenes with low catalyst loadings rapidly (< 5 mins), albeit short lifetime. A large number of *Mn*-complexes have been screened for their ability to catalyze terminal alkenes [213]. It was found that most manganese complexes bearing neutral polyamine or

polypyridyl ligands show a significant increase in epoxidation reactivity under less acidic conditions with peracetic acid. $\text{Mn}^{\text{II}}(\text{bipy})_2^{2+}$ [(bipy) = 4,4'-bipyridine] proved to be the most active species based on the relative rates toward electronically and sterically distinct alkenes.

Catalytic epoxidation using iron complexes has been reported by Kotani et al. [214], who employed iron(III) picolinate catalyst generated *in-situ* from a mixture of $\text{Fe}(\text{ClO}_4)_3$ and picolinic acid in pyridine/acetonitrile. Cholesteryl acetate was transformed to the corresponding 5,6-epoxide without the formation of any hydroxy compounds. The active species is suggested to be a monomeric Fe(V)-oxo intermediates. Similar catalyst has also been prepared by Murphy et al. [215], who synthesized dimeric complexes by simply mixing $\text{Fe}(\text{ClO}_4)_3$ or $\text{Fe}(\text{NO}_3)_3$ with phenanthroline ligands in acetonitrile/water. It was found that the catalytic mixture in combination with peracetic acid drives epoxidation of a wide range of electron-rich and electron-poor alkenes efficiently and rapidly (< 5 mins) at 0°C.

1.5. Aims and Objectives of this Project

Epoxidation of alkenes is an industrially important reaction because epoxy compounds are widely used in the preparation of a wide variety of commodity chemicals. Although many literatures reported on catalytic epoxidation are available, most of them are limited to the use of volatile organic solvents and/or toxic catalysts. Some of these catalytic systems are only applicable to a particular class of alkenes. There is a need to develop environmentally benign, inexpensive, scalable and simple catalytic systems for alkene epoxidation that are applicable to a wide varieties of alkene substrates.

Hydrogen peroxide (H_2O_2) is considered to be a green oxidant because it gives water as the sole co-product. However, its preparation is 'non-green' as the anthraquinone process (AQ process) requires volatile and toxic solvents. In this project, H_2O_2 is electrochemically generated in aqueous solutions (Chapter 2) and ionic liquids (Chapter 3). The electrogeneration of hydrogen peroxide is coupled with the manganese/bicarbonate system, which has been considered to be a green catalytic system for epoxidation. The whole system uses oxygen as feedstock and electricity as reducing agent. Moreover, manganese and bicarbonate salts are inexpensive and

relative non-toxic. The results will be discussed in chapters 2 and 3 of this thesis.

Terminal aliphatic alkenes are a challenging class of substrates to be epoxidized because they lack nucleophilicity. Most of the reported catalytic systems in literatures are not strong enough to transform them effectively or require carefully controlled conditions (e.g. subzero temperature) to keep the catalyst stable. In this work, we aim at developing a simple system based on manganese salt to catalyze the epoxidation of terminal aliphatic alkenes by peracetic acid. This system leaves only acetic acid as the by-product and selectively epoxidizes most terminal aliphatic alkenes within 30 mins at ambient temperature. The results will be discussed in chapter 4 of this thesis.

Chapter 2

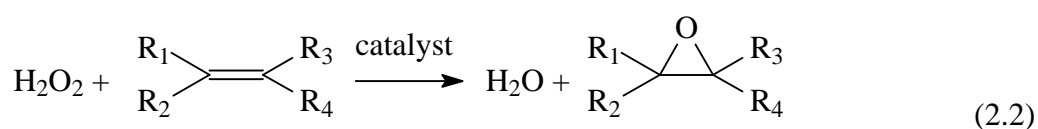
Manganese-mediated Epoxidation of Alkenes with Hydrogen

Peroxide Electrogenenerated *in-situ* in Bicarbonate Solutions

2.1. Introduction

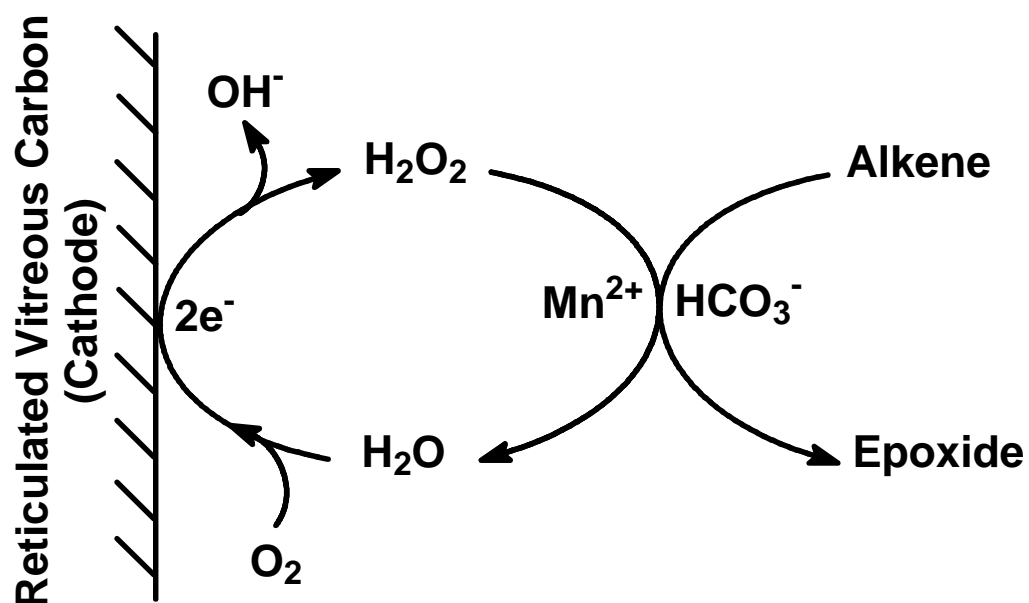
Catalytic epoxidation with hydrogen peroxide (H_2O_2) electrogenerated *in-situ* is of particular interest due to a number of reasons. Firstly, H_2O_2 is produced at the cathode under mild condition by the reduction of oxygen. Air can be used as the source of oxygen which is inexpensive. Secondly, its usage as a dilute solution greatly reduces the hazards associated with the explosive nature of H_2O_2 . Thirdly, this simple and waste-free route leaves no residues in the reaction. With the suitable choice of catalysts, high selectivity can be achieved.

The success of catalytic epoxidation with electrogenerated H_2O_2 depends on whether we can couple H_2O_2 electrogeneration (eq. 2.1) with the oxygen transfer reaction (eq. 2.2) together:



Murray et al. [148] were the first to describe this electrocatalytic approach for

epoxidation with electrogenerated H_2O_2 . A manganese meso-tetraphenylporphyrin was used as catalyst in dichloromethane electrolyte. This is a simple route for epoxidation, but undesirable elements such as the requirement for external proton sources, instability of catalyst and involvement of hazardous organic solvents make this method impractical. Recently, similar approaches were reported by Atobe et al. [151] and Zimmer et al. [108] using heterogeneous titanium silicate (TS-1) and homogeneous bis(acetyl-acetonato)oxovanadium(IV) ($\text{VO}(\text{acac})_2$) as catalysts. However, the alkenes epoxidized were only limited to water-soluble alkenes as water was used as the solvent. To improve the scope of substrates and to increase the electrocatalytic efficiency, there is a need to improve these systems so that lipophilic alkenes can be epoxidized efficiently. In this chapter, the coupling of the manganese/bicarbonate catalytic system for epoxidation [69, 204] with the electrogeneration of H_2O_2 in *tert*-butanol/water mixture (Scheme 2.1) will be described. *tert*-Butanol was chosen because it is relatively non-toxic and it can dissolve most lipophilic alkenes.



Scheme 2.1 H_2O_2 electrogenerated *in-situ* in bicarbonate solutions for alkene epoxidation.

2.2. Experimental Section

2.2.1. Materials

All chemicals and solvents used were of analytical reagent (A.R.) grade. Double deionized water was purified by passing through an ion-exchange resin purification train (Millipore). Pure oxygen (>99.7%) and argon (>99.995%) were provided by Hong Kong Oxygen Co. Manganese(II) sulfate monohydrate (>99%), sodium bicarbonate (>99%), H₂O₂ (35 wt. % solution in water) and *tert*-butanol (99%) were purchased from Aldrich Co. All alkenes and epoxides were obtained from commercial sources either from Aldrich Co. or Acros Organic, and were used as received unless otherwise noted. Sodium 4-oxirane benzenesulfonate [216] and sodium 4-oxirane benzoic acid [204] were synthesized by literature reported methods with minor modifications.

2.2.2. Synthesis of epoxides

Sodium 4-oxirane benzenesulfonate [216]

3-Chloroperoxybenzoic acid (0.7 g, 0.003 mol) and sodium 4-styrenesulfonate (0.0005 mol) were dissolved in a mixture of ethanol (4.5 ml) and water (0.5 ml). After

stirring at room temperature for 8 hours, the solvent was removed by a rotary evaporator. Acetone (10 ml) was added to dissolve the unreacted starting materials and byproducts, i.e. 3-chloroperoxybenzoic acid and 3-chlorobenzoic acid, and the product (sodium 4-oxirane benzenesulfonate) was filtered off. The purity was >95% as observed by ^1H NMR spectrum. Yield: 0.078 g (73%). ^1H NMR (D_2O , δ ppm): 3.05 (d, 1H), 3.30 (d, 1H), 4.11 (t, 1H), 7.72 (dd, 4H).

4-Oxirane benzoic acid [204]

A round-bottomed flask was charged with 4-vinylbenzoic acid (0.1 g, 0.67 mmol) and *tert*-butanol (5 ml). A mixture composed of 0.1 M $\text{MnSO}_{4(\text{aq})}$ (100 μl), 35% H_2O_2 (700 μl) and 1 M $\text{NaHCO}_{3(\text{aq})}$ (1 ml) was added drop by drop to the flask with stirring over one hour. After removal of the solvents by distillation under reduced pressure, 10 ml of ethanol was added to dissolve the product and to precipitate the NaHCO_3 . The product 4-oxirane benzoic acid was isolated as a white powder by removing the ethanol under reduced pressure. The purity was >97% as observed by ^1H NMR spectrum. Yield: 0.067 g (61%). ^1H NMR (D_2O , δ ppm): 3.09 (d, 1H), 3.30 (d, 1H), 4.10 (t, 1H), 7.63 (dd, 4H).

2.2.3. Instrumentation

The flow of electrolyte (Figure 2.1) was achieved with peristaltic pumps obtained from Cole-Parmer Instrumental Company. Gas and electrolyte flow rates were monitored by flowmeters obtained from Gilmont Instruments. Electrolyses were conducted using an EG&G Princeton Applied Research model 273A Potentiostat.

Voltammetric measurements

Glassy carbon (0.2 cm^2) and platinum (0.02 cm^2) electrodes were polished with $0.05\text{ }\mu\text{m}$ α -alumina (Buehler) on a microcloth, rinsed with double deionized water and then sonicated for 5 minutes in water before used. Cyclic voltammetry (CV) and differential pulse voltammetry (DPV) were carried out by a Bioanalytical Systems (BAS) model 100W electrochemical analyzer in a conventional two-compartment cell with a sintered glass separating the two compartments. A platinum wire was used as the counter electrode, whereas the reference electrode was a saturated calomel electrode (SCE).

Microflow cell (MFC)

The microflow cell used for electrolysis (Figure 2.2) was purchased from ElectroCell

AB, Sweden. The cathode was a 33 mm x 27 mm x 5 mm reticulated vitreous carbon (Electrosynthesis Co., 60 pores per inch (ppi)) mounted onto a graphite plate by conducting glue of epoxy resin (Araldite) and graphite power (Merck). The anode was a platinum-coated titanium plate. The two compartments were separated by a Nafion 424 cation permeable membrane. The reference electrode was a saturated calomel electrode (SCE) located close to the cathode.

Identification and quantification of products

A Waters HPLC system (model 486) with LC-18 Column (Supelco) was used for monitoring the product yields of reactions with water-soluble substrates. The eluent (1 ml/min) was a water/methanol mixture of various volume ratios depending on the compounds to be analyzed. For ionizable compounds, tetrabutylammonium acetate (1 g/L) was added into the eluent to enhance the resolving power.

A Hewlett-Packard model 8900 GC-MS equipped with ECTM-1 or ECTM-WAX columns (Alltech Associate, Inc.) was used for yield determination and chemical analysis of the epoxidized products. Benzoic acid and tetradecane were used as internal standards for HPLC and GC-MS quantitative measurements respectively. ¹H and ¹³C NMR spectra were recorded on a Bruker DPX-400MHz NMR spectrometer.

2.2.4. Hydrogen peroxide electrogeneration

The two reservoirs shown in Figure 2.1 were filled with 50 ml of electrolyte solutions. Electrolysis was carried out in the microflow cell at a flow rate of 500 ml/min. Oxygen was supplied to the catholyte by continuous bubbling at a flow rate of 80 ml/min. H_2O_2 was electrogenerated by constant potential electrolysis.

The concentration of H_2O_2 generated was monitored by differential pulse voltammetry. The measurement was performed *in-situ* in the catholyte at regular time intervals.

2.2.5. Epoxidation of alkenes with hydrogen peroxide electrogenerated *in-situ*

The experimental conditions were similar to those above except that a fixed volume of oxygen was fed into the system using a balloon, and 2.5 mmol of alkene and catalytic amount of MnSO_4 were added into the NaHCO_3 electrolyte solution. For the water-soluble alkenes, a 1 M NaHCO_3 solution was used as electrolyte. At regular intervals, 0.1 ml of the reaction mixture was withdrawn by a micropipette and diluted to 10 ml. The product yield was determined by HPLC with benzoic acid as internal standard.

For the lipophilic alkenes, the catholyte was replaced by 50 ml of a water/*tert*-butanol mixture (1.5:1 v/v) containing 0.24 M NaHCO₃ and 0.1 M NaCl. The anolyte was a mixture of water and *tert*-butanol (1.5:1 v/v) with 2 M H₂SO₄. The products were extracted by pentane and the product yields were determined by GC-MS with tetradecane as internal standard.

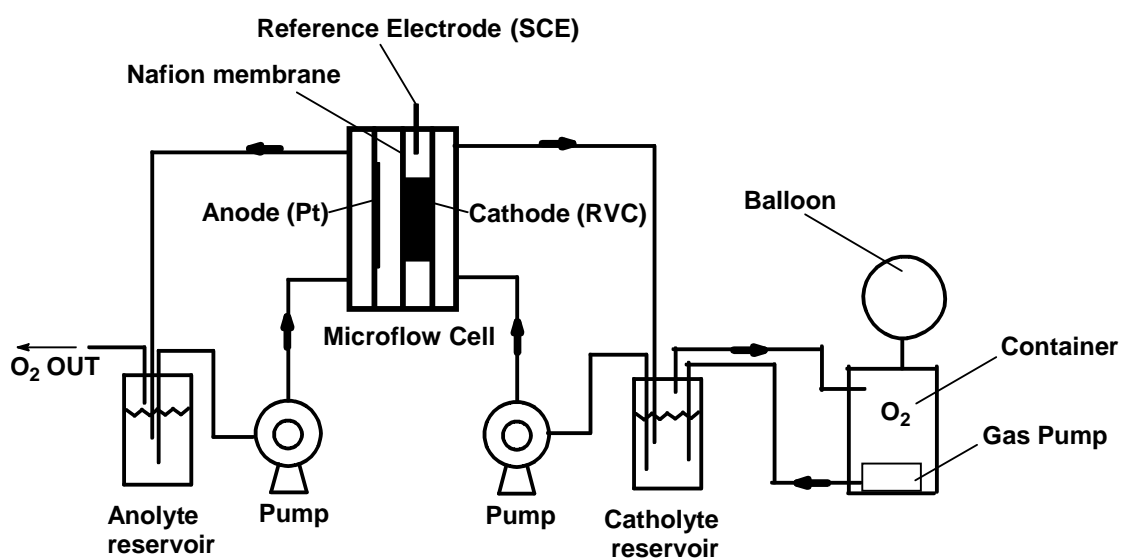


Figure 2.1 Schematic diagram showing the flow of electrolyte and gas in the epoxidation of alkenes with H_2O_2 electrogenerated *in-situ*.

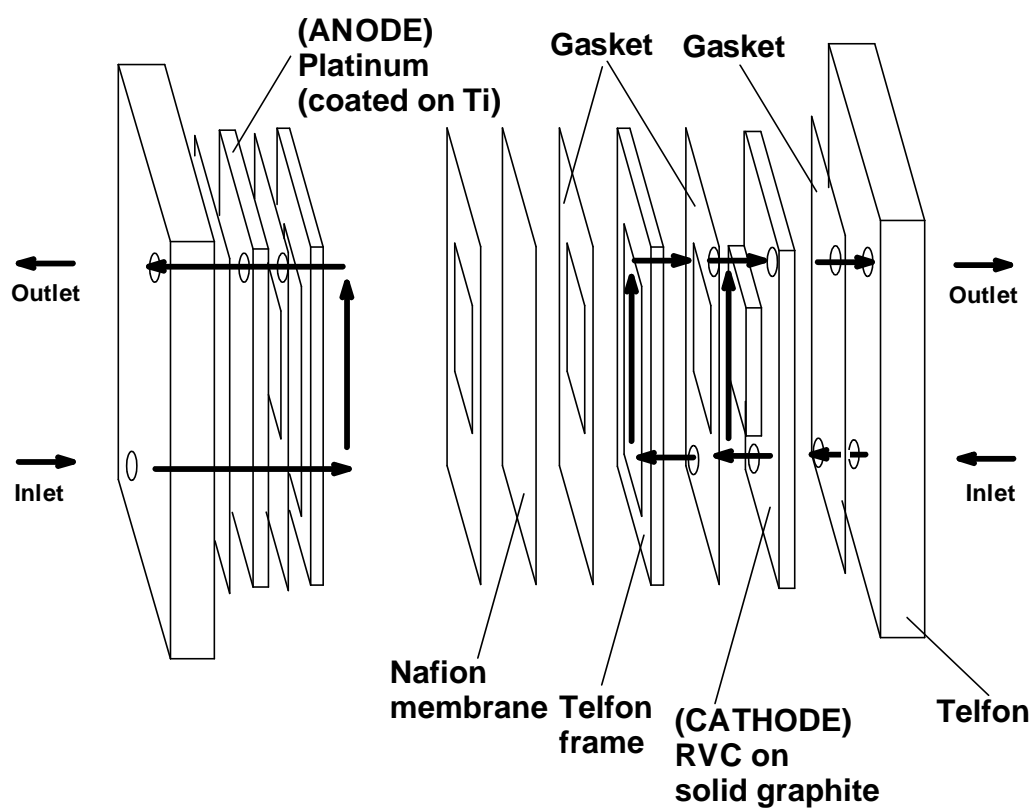
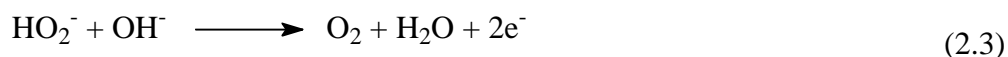


Figure 2.2 The construction of the microflow cell (MFC).

2.3. Results and Discussion

2.3.1. Preparation of calibration curves for the determination of hydrogen peroxide concentration

In this work, the concentration of electrogenerated H_2O_2 was monitored by differential pulse voltammetry (DPV) [217]. At a given potential, H_2O_2 is oxidized to oxygen at a platinum electrode (eq. 2.3).



The calibration curve was constructed by adding known amounts of H_2O_2 to the electrolyte and the voltammograms were recorded. The peak currents were formed to be proportional to the concentrations of H_2O_2 in $\text{NaHCO}_{3(\text{aq})}$ (Figure 2.3) and $\text{NaOH}_{(\text{aq})}$ (Figure 2.5) solutions. The plots of peak current versus concentration of H_2O_2 are shown in Figure 2.4 and Figure 2.6 for the $\text{NaHCO}_{3(\text{aq})}$ and $\text{NaOH}_{(\text{aq})}$ electrolytes respectively.

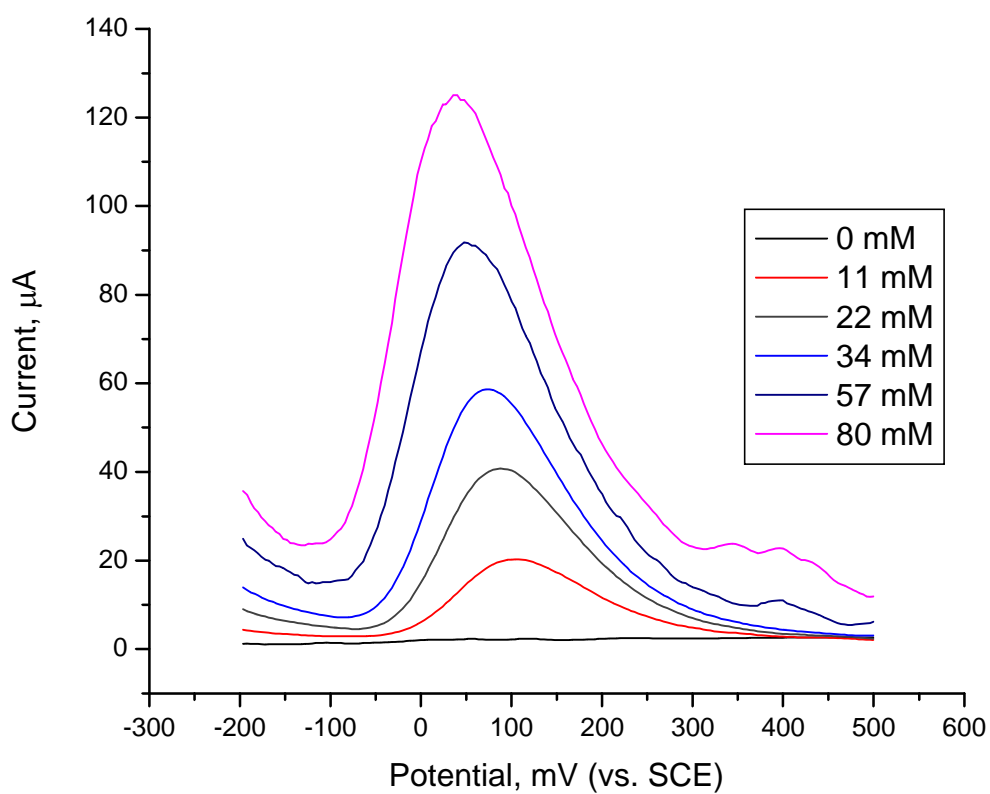


Figure 2.3 Differential pulse voltammograms for different concentration of H_2O_2 in 1 M $\text{NaHCO}_{3(\text{aq})}$ solution. Working electrode: 0.02 cm^2 platinum. Scan rate: 20 mVs^{-1} . Pulse amplitude: 50 mV. Pulse width: 50 ms. Sample width: 17 ms.

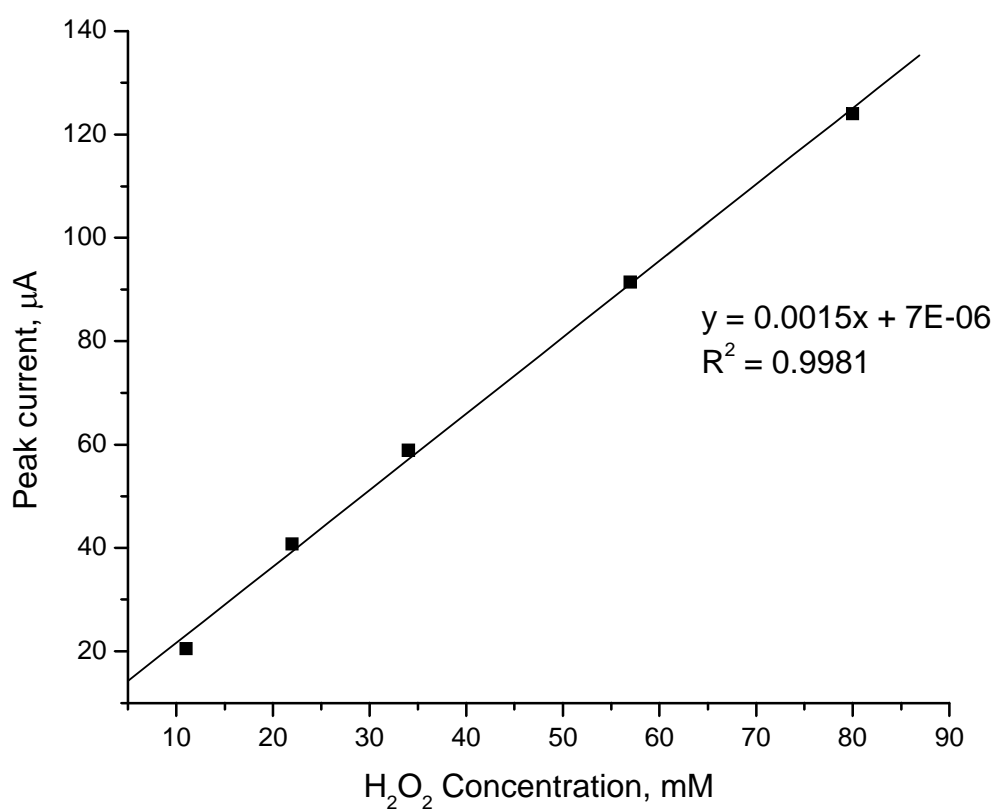


Figure 2.4 Calibration curve showing the plot of peak current versus H_2O_2 concentration in 1 M $\text{NaHCO}_{3(\text{aq})}$ solution.

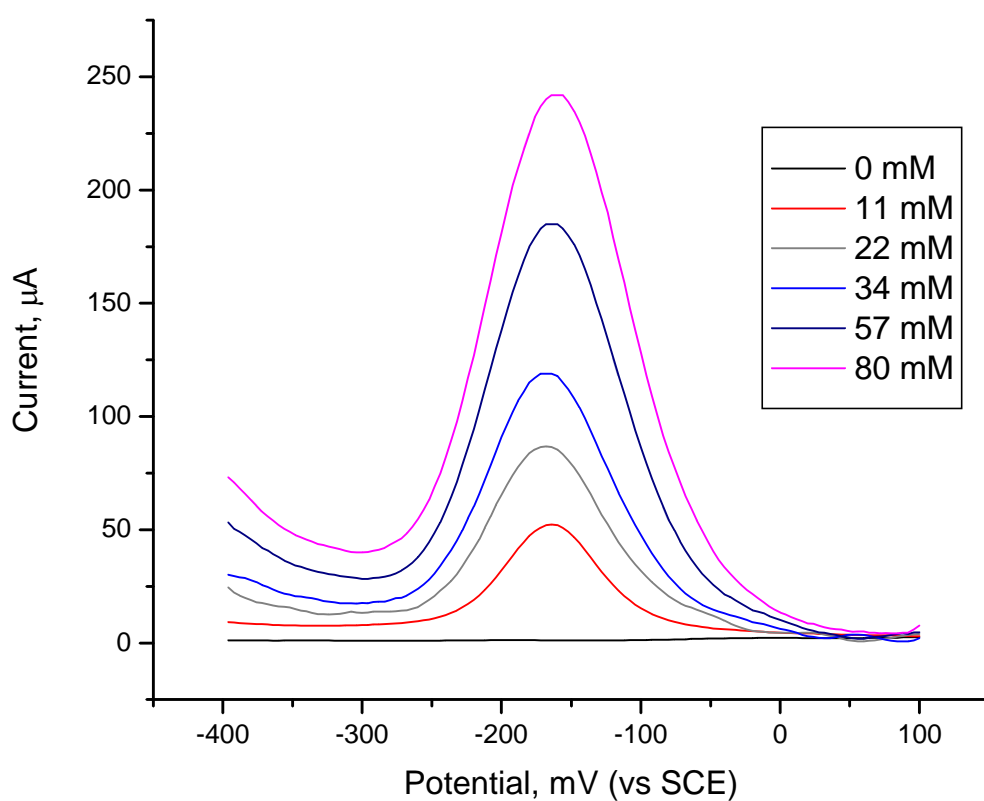


Figure 2.5 Differential pulse voltammograms for different concentration of H_2O_2 in 1 M $\text{NaOH}_{(\text{aq})}$ solution. Working electrode: 0.02 cm^2 platinum. Scan rate: 20 mVs^{-1} . Pulse amplitude: 50 mV. Pulse width: 50 ms. Sample width: 17 ms.

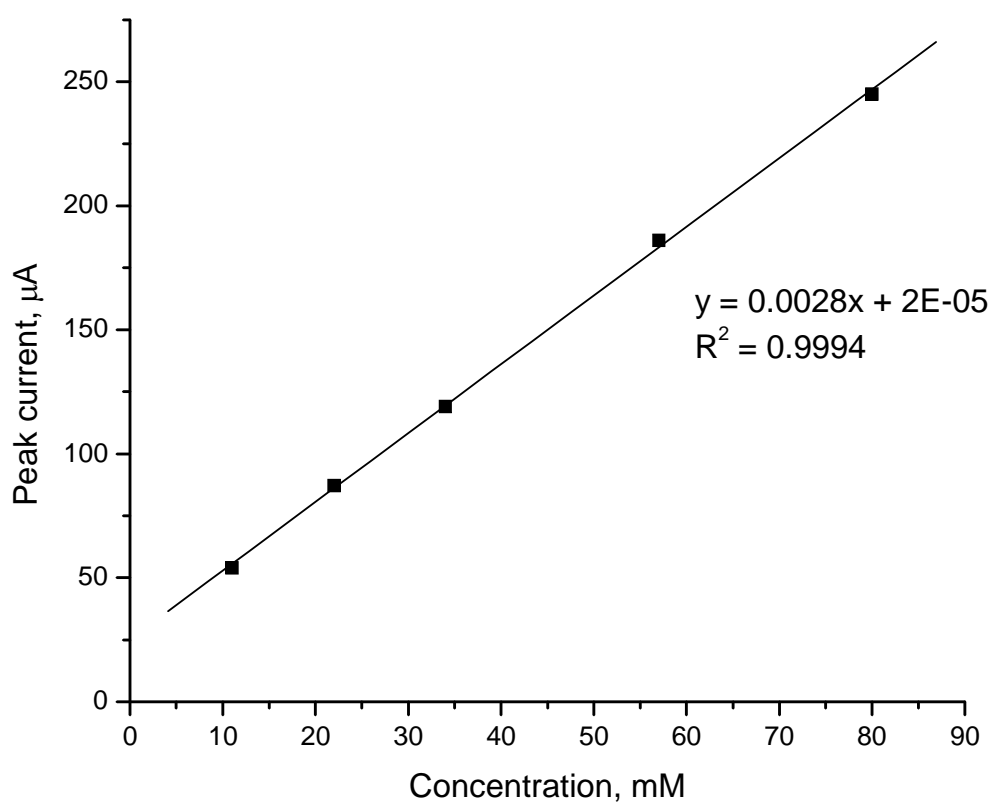
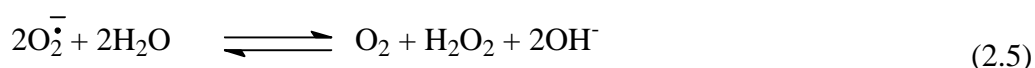


Figure 2.6 Calibration curve showing the plot of peak current versus H₂O₂ concentration in 1 M NaOH_(aq) solution.

2.3.2. Voltammetric studies for the electrochemical reduction of dioxygen to hydrogen peroxide

The cyclic voltammogram of dioxygen (O_2) reduction at a glassy carbon electrode in 1 M $NaHCO_{3(aq)}$ is shown in Figure 2.7. Two irreversible reduction peaks at -352 mV (I) and -613 mV (II) vs. SCE are observed. Sawyer et al. and Yeager et al. [111, 125, 218] proposed that the first peak (I) is the 1-electron reduction of O_2 to $O_2^{\cdot-}$ (eq. 2.4), which is followed by a dismutation reaction to generate H_2O_2 in alkaline medium (eq. 2.5).



The second peak (II) is assigned as the overall 2-electron reduction to generate H_2O_2 directly from O_2 (eq. 2.1) [103, 105]. Comparing the peak height and area, the latter is the dominant process where the potential should be held in H_2O_2 electrogeneration.

The cyclic voltammograms of O_2 reduction in *tert*-butanol/water mixtures are shown

in Figure 2.8. For those containing *tert*-butanol, the two irreversible reduction peaks are observed, indicating that the electrochemical processes are similar to those in aqueous bicarbonate solutions. However, it is noted that the size of II' is much greater than II with increasing the amount of *tert*-butanol. This can be attributed to the higher solubility of O₂ in *tert*-butanol than in water [219, 220]. Besides, on comparing with the peak potential, the peaks I' and II' all shift cathodically. This is probably due to the higher resistance of the *tert*-butanol/water electrolyte.

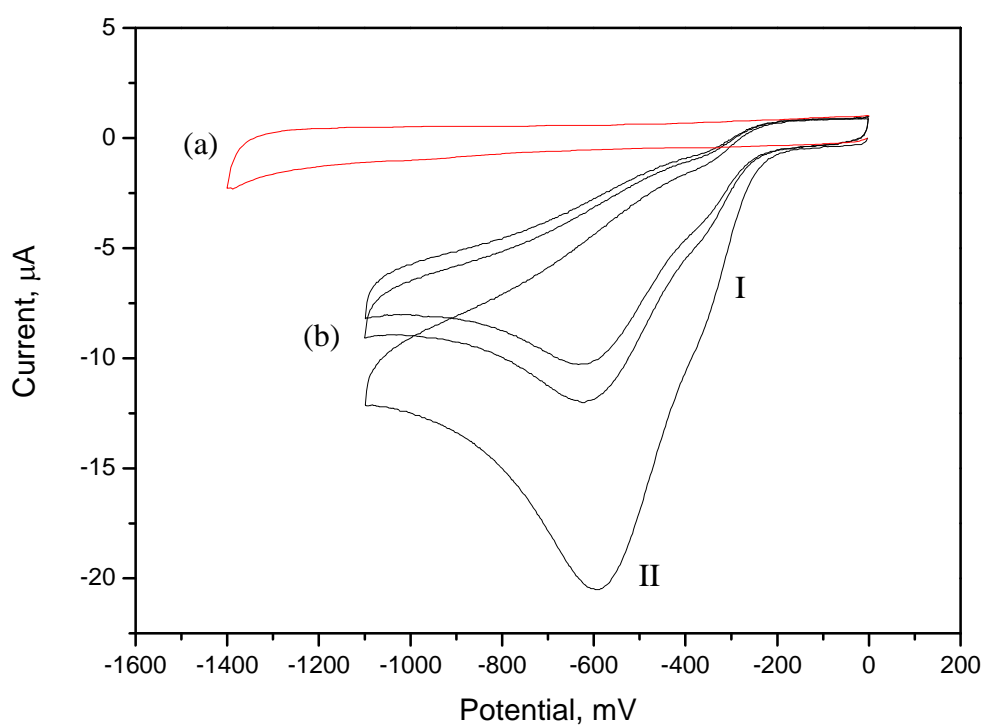


Figure 2.7 Cyclic voltammograms of O_2 reduction in 1 M $\text{NaHCO}_3(\text{aq})$ solution.

Working electrode: 0.2 cm^2 glassy carbon. Scan rate: 100 mVs^{-1} .

Saturated with (a) argon and (b) oxygen.

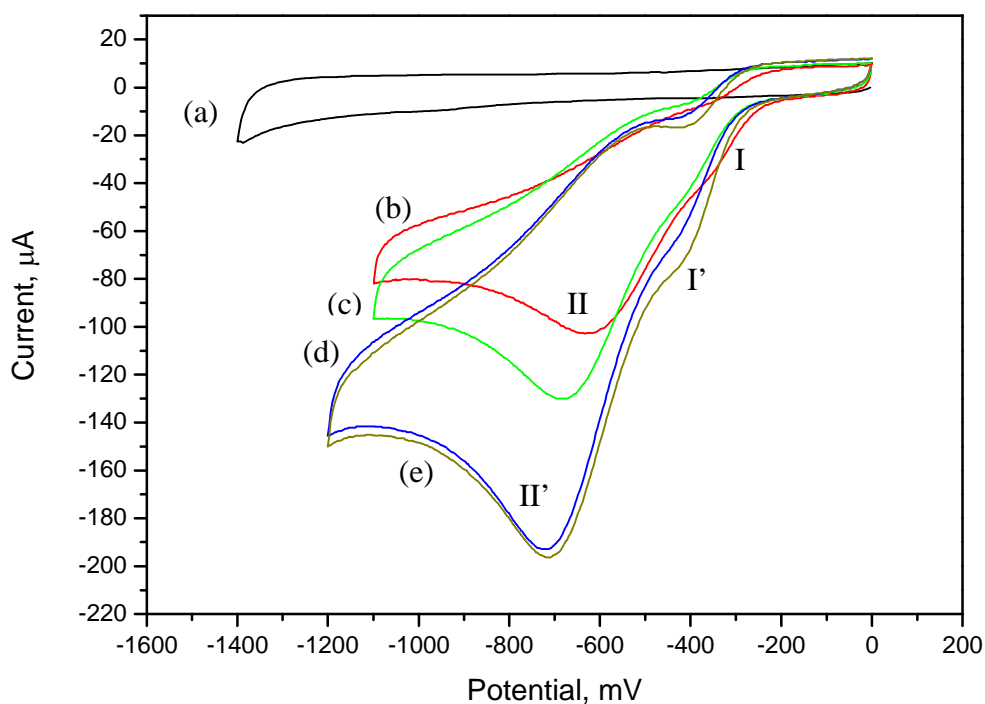


Figure 2.8 Cyclic voltammograms of O_2 reduction in (a) 1 M $NaHCO_{3(aq)}$ solution (saturated with Ar), (b) 1 M $NaHCO_{3(aq)}$ solution, (c) a mixture of *tert*-butanol/water (1:4 v/v) and $NaHCO_3$ (0.24 M), (d) a mixture of *tert*-butanol/water (2:3 v/v) and $NaHCO_3$ (0.24M) and (e) a mixture of *tert*-butanol/water (2:3 v/v), $NaHCO_3$ (0.24M) and $NaCl$ (0.1M). Working electrode: 0.2 cm^2 glassy carbon. Scan rate: 100 mVs^{-1} . All voltammograms were recorded under oxygen-saturated condition except (a).

2.3.3. Electrogeneration of hydrogen peroxide in bicarbonate solution

2.3.3.1. The effect of applied potential on the electrogeneration of hydrogen peroxide

The effect of applied potential on the electrogeneration of H_2O_2 in 1 M $\text{NaHCO}_{3(\text{aq})}$ is shown in Figure 2.9. The H_2O_2 concentration increases with time when a fixed potential is applied to the cathode. However, the current efficiency for H_2O_2 production varies with the applied potential. A great improvement on current efficiency was observed when the potential was made more negative from -400 to -600 mV (Figure 2.10 and Table 2.1), which corresponds to the second reduction peak II in the cyclic voltammogram.

When the potential is further lowered to beyond -600 mV, the current efficiency drops as a result of side reactions such as the 4-electron reduction of oxygen to generate hydroxyl ion (OH^-) (eq. 2.6). Obviously, the optimum potential for H_2O_2 electrogeneration in 1M $\text{NaHCO}_{3(\text{aq})}$ solution is about -600 mV vs. SCE.



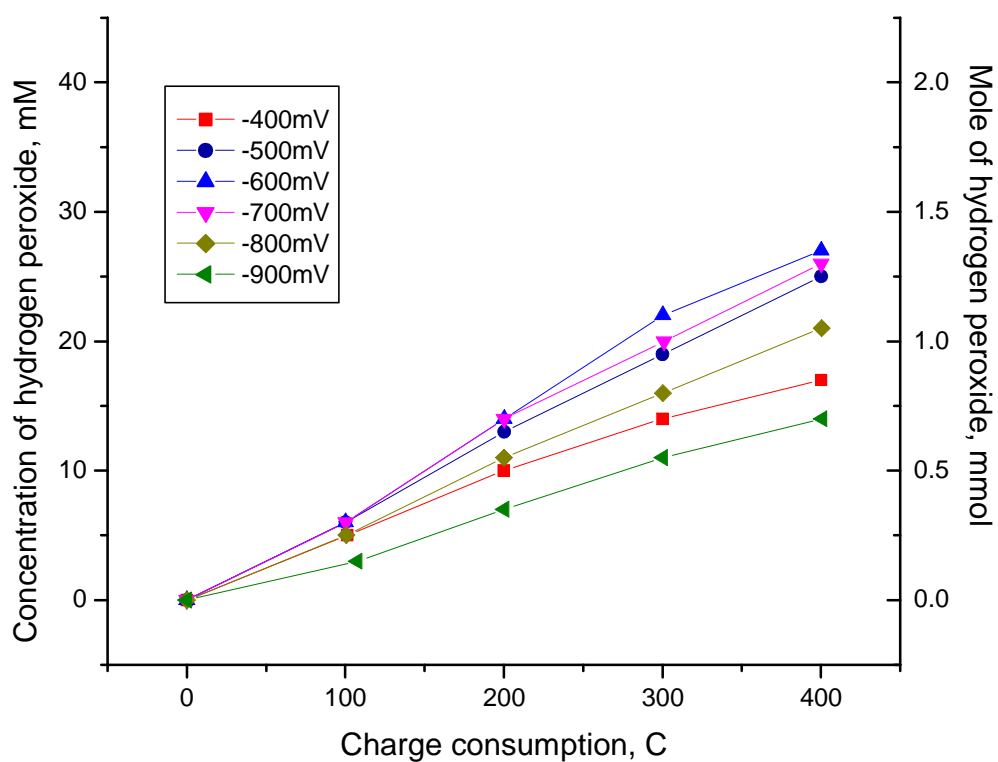


Figure 2.9 Plots of concentration of H_2O_2 electrogenerated in 1 M $\text{NaHCO}_{3(\text{aq})}$ at various applied potentials versus the charge consumed in the electrolysis. All potentials are referred to the standard calomel electrode (SCE). Catholyte: 1 M $\text{NaHCO}_{3(\text{aq})}$. Anolyte: 2 M $\text{H}_2\text{SO}_{4(\text{aq})}$.

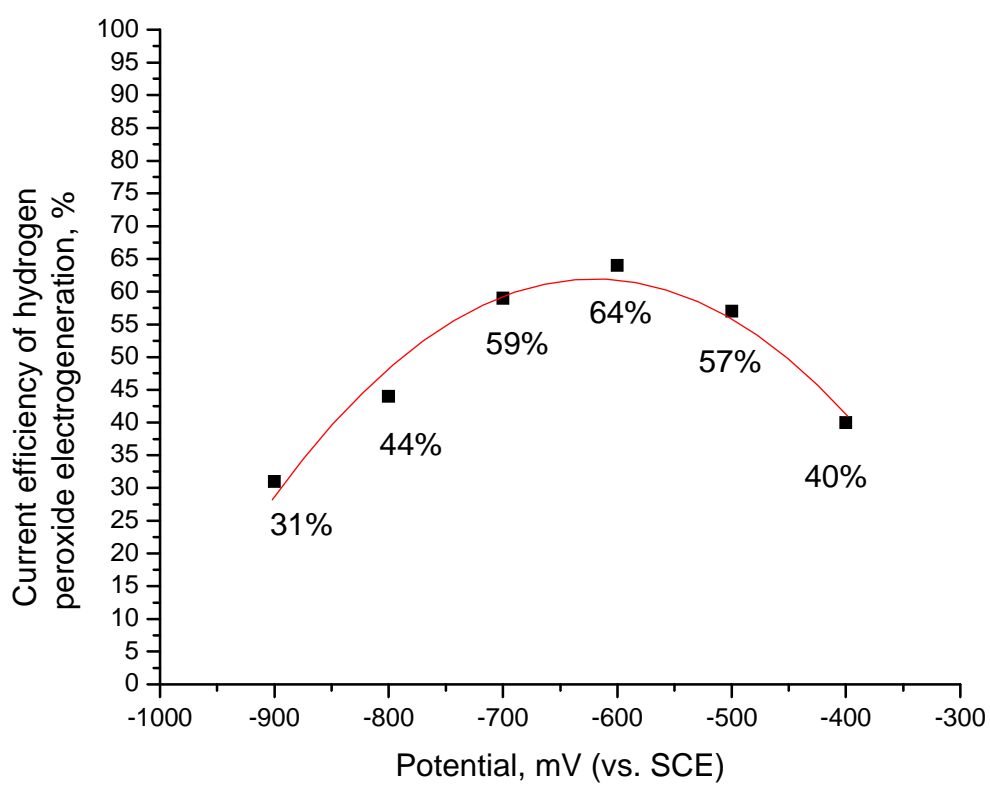


Figure 2.10 Effect of applied potential on the current efficiency of H_2O_2 electrogenerated in 1 M $\text{NaHCO}_{3(\text{aq})}$. Catholyte: 1M $\text{NaHCO}_{3(\text{aq})}$. Anolyte: 2 M $\text{H}_2\text{SO}_{4(\text{aq})}$.

Table 2.1 Electrogeneration of H₂O₂ at different applied potentials.

Potential, mV (vs. SCE)	Current density, mAcm ⁻²	Current efficiency, %
-400	0.21	40
-500	0.58	57
-600	1.03	64
-700	1.35	59
-800	2.18	44
-900	2.89	31

Catholyte: 1 M NaHCO_{3(aq)}. Anolyte: 2 M H₂SO_{4(aq)}. Cathode: 33 mm x 27 mm x 5 mm 60ppi RVC.

Cathode surface area: 156 cm².

2.3.3.2. The effect of catholyte alkalinity on the current efficiency of hydrogen peroxide electrogeneration

A comparison of the current efficiency for H_2O_2 electrogeneration in 1 M $\text{NaHCO}_{3(\text{aq})}$ with that in 1 M $\text{NaOH}_{(\text{aq})}$ is shown in Figure 2.11 and Table 2.2. In 1 M $\text{NaOH}_{(\text{aq})}$, H_2O_2 is electrogenerated in the form of hydroperoxy anion (HO_2^- , $\text{pK}_{\text{a},\text{H}_2\text{O}_2} = 11.62$ at 25°C) (eq. 2.7) [136]. Because of its repulsion to the cathode, the chance of further reduction of HO_2^- to OH^- (eq. 2.8) is minimized. Furthermore, the retainment of HO_2^- in the cathode compartment by the nafion membrane also prevents its loss through diffusion to the anode compartment. As a result, the current efficiency for H_2O_2 generation in 1 M NaOH is always higher than that in NaHCO_3 .



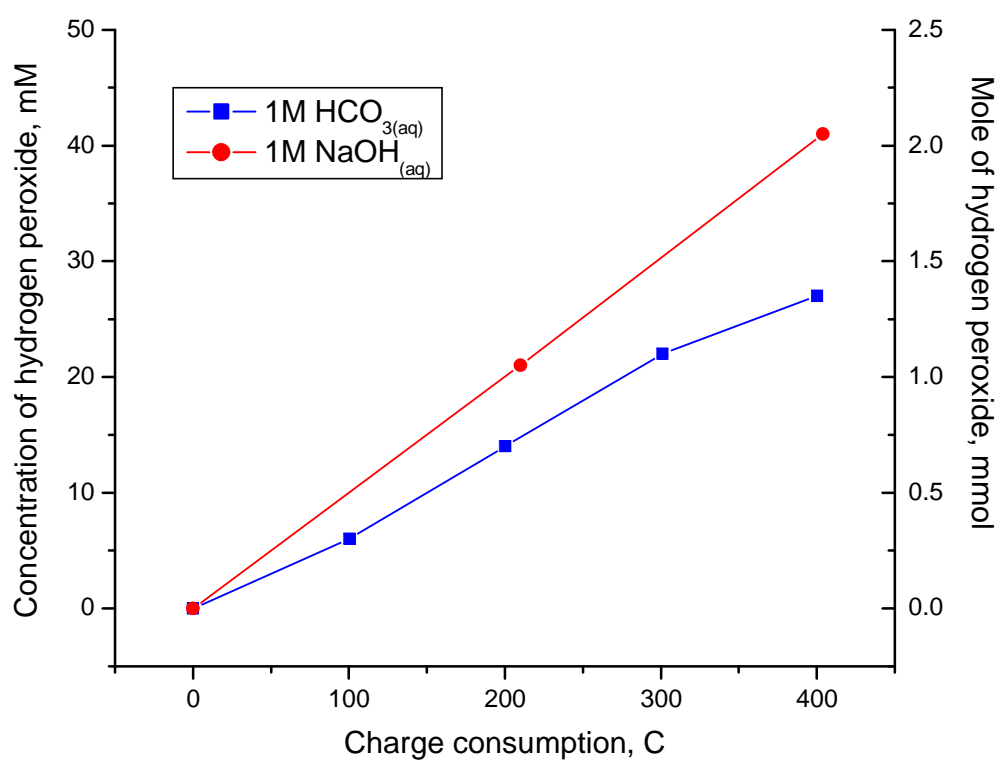


Figure 2.11 Plots of the H_2O_2 electrogenerated in 1 M $\text{NaHCO}_{3(\text{aq})}$ and 1 M $\text{NaOH}_{(\text{aq})}$ catholyte solutions against charge consumed in the electrolysis. Potential: -600 mV (vs. SCE). Anolyte: 2 M $\text{H}_2\text{SO}_{4(\text{aq})}$.

Table 2.2 Electrogeneration of H₂O₂ in different catholytes.

Catholyte	Potential, mV (vs. SCE)	Current density,	Current efficiency,
		mAcm ⁻²	%
1M NaOH	-600	1.44	91
1M NaHCO ₃	-600	1.03	64

Anolyte: 2 M H₂SO_{4(aq)}. Cathode: 33 mm x 27 mm x 5 mm 60ppi RVC. Cathode surface area: 156 cm².

2.3.4. Electrogeneration of hydrogen peroxide in *tert*-butanol/H₂O/NaHCO₃ mixture

2.3.4.1. Optimal amount of *tert*-butanol in bicarbonate solution for hydrogen peroxide electrogeneration

tert-Butanol is a tertiary alcohol which is stable against oxidation. In combination with an appropriate catalytic system, it provides a suitable medium for epoxidation. In our work, electrolyses were carried out in oxygen-saturated *tert*-butanol/NaHCO_{3(aq)} mixtures. The amount of *tert*-butanol used was always less than 40 vol.% because of ohmic resistance and NaHCO₃ solubility (Table 2.3). In all cases, the electrolyte was always saturated with NaHCO₃.

The effect of *tert*-butanol content on the H₂O₂ electrogenerated in NaHCO_{3(aq)} solution is shown in Figures 2.12 and 2.13. The presence of *tert*-butanol greatly improves the current efficiency of the H₂O₂ production. As noted in Section 2.3.2., the solubility of O₂ in *tert*-butanol is much higher than that in water. As can be seen in Table 2.3, further improvement in current efficiency is obtained upon the addition of 0.1 M NaCl. This shows that conductivity is another crucial factor in affecting the

current efficiency of H_2O_2 production.

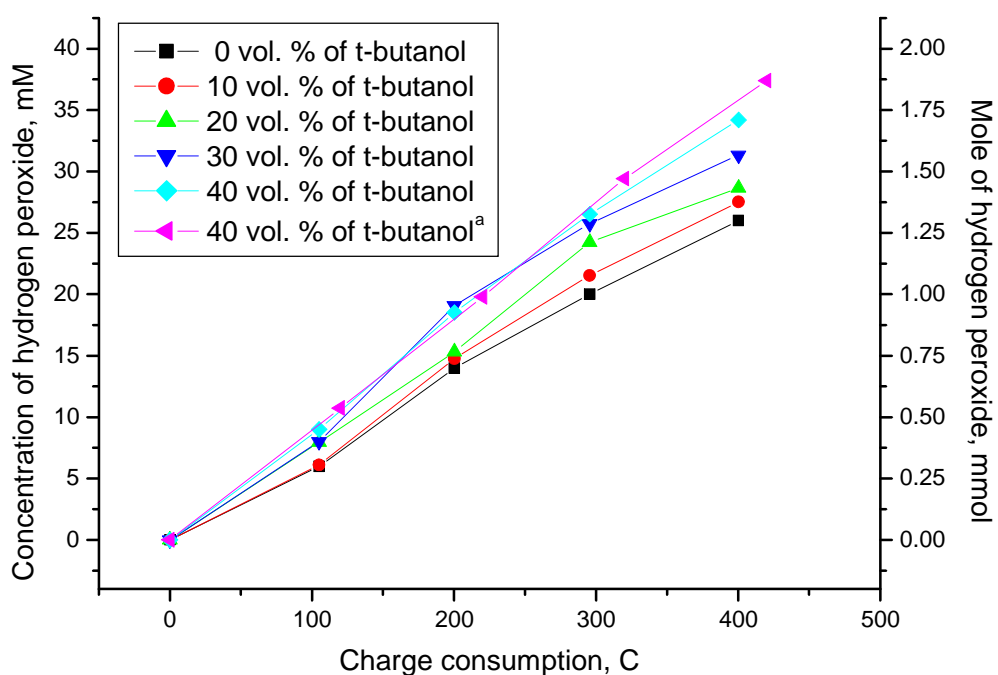


Figure 2.12 Plots of the H₂O₂ electrogenerated in NaHCO_{3(aq)} solutions with different *tert*-butanol content versus charge consumed in the electrolysis. Anolyte: *tert*-butanol/water (1:1.5 v/v) mixture with 2 M H₂SO₄. Potential: -600 mV. ^a0.1 M NaCl was added.

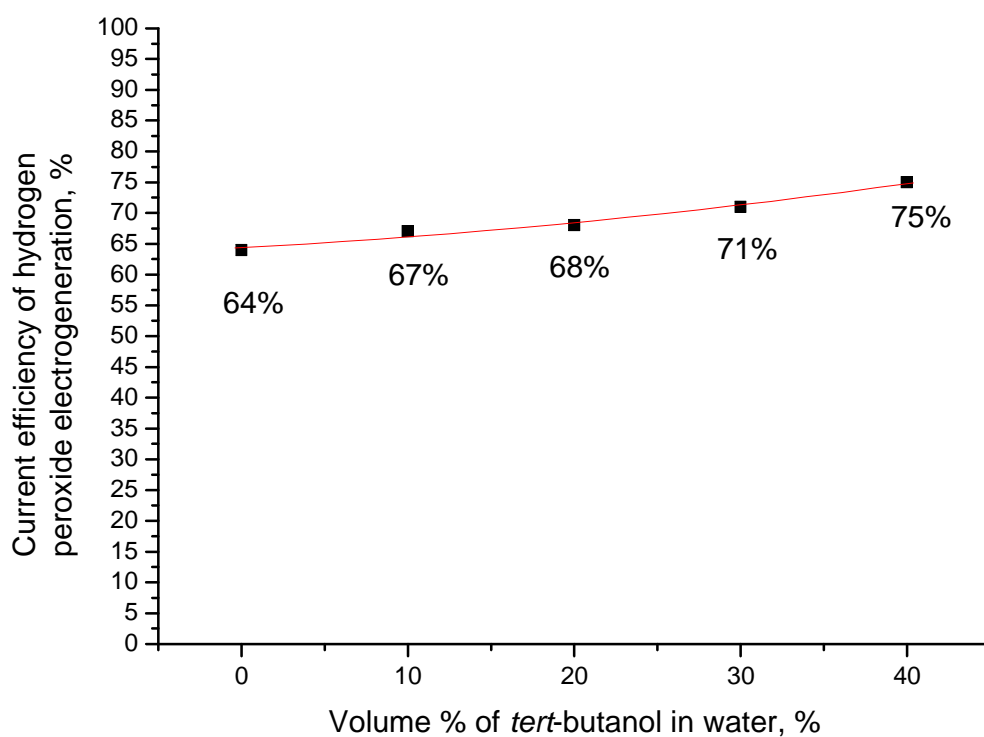


Figure 2.13 Effect of the *tert*-butanol content on the current efficiency of H_2O_2 electrogenerated in $\text{NaHCO}_{3(\text{aq})}$ solutions. Anolyte: *tert*-butanol/water (1:1.5 v/v) mixture containing 2 M H_2SO_4 . Potential: -600 mV.

Table 2.3 Electrogeneration of H_2O_2 in $\text{NaHCO}_{3(\text{aq})}$ solutions with different *tert*-butanol content.

Volume of <i>tert</i> -butanol in water, % (v/v)	Saturated concentration of NaHCO_3 , M	Conductivity, mScm^{-1}	Current density, mAcm^{-2}	Current efficiency, %
0	1	>20	1.03	64
10	0.72	>20	1.09	67
20	0.48	13.75	1.28	68
30	0.35	8.69	1.41	71
40	0.24	5.19	1.47	75
^a 40	0.24	7.79	1.60	79

Anolyte: 2 M $\text{H}_2\text{SO}_{4(\text{aq})}$. Cathode: 33 mm x 27 mm x 5 mm 60ppi RVC. Cathode surface area: 156 cm^2 .

Potential: -600 mV. ^a0.1 M NaCl was added.

2.3.4.2. Optimal applied potential for the electrogeneration of hydrogen peroxide in *tert*-butanol/H₂O/NaHCO₃ mixture

The effect of applied potential on the H₂O₂ electrogenerated in *tert*-butanol/H₂O/NaHCO₃ mixture is shown in Figures 2.14 and 2.15. The optimal applied potential is about -700 mV vs. SCE, which is 100 mV more negative than the optimal potential in 1 M NaHCO_{3(aq)} solution. This is consistent with the cyclic voltammogram shown in Figure 2.8, which indicates that peak potential shifts towards the negative side upon the addition of *tert*-butanol.

A high concentration of H₂O₂ can be easily attained when the potential is lowered from -400 to -700 mV. Beyond -700 mV, a sharp decline in H₂O₂ production was observed because of side reactions such as the generation of hydroxyl ion (eq. 2.6). On comparison of Table 2.4 with Table 2.1, it is noted that the current efficiencies of H₂O₂ electrogeneration in *tert*-butanol/water mixture are always higher than that in aqueous solution alone.

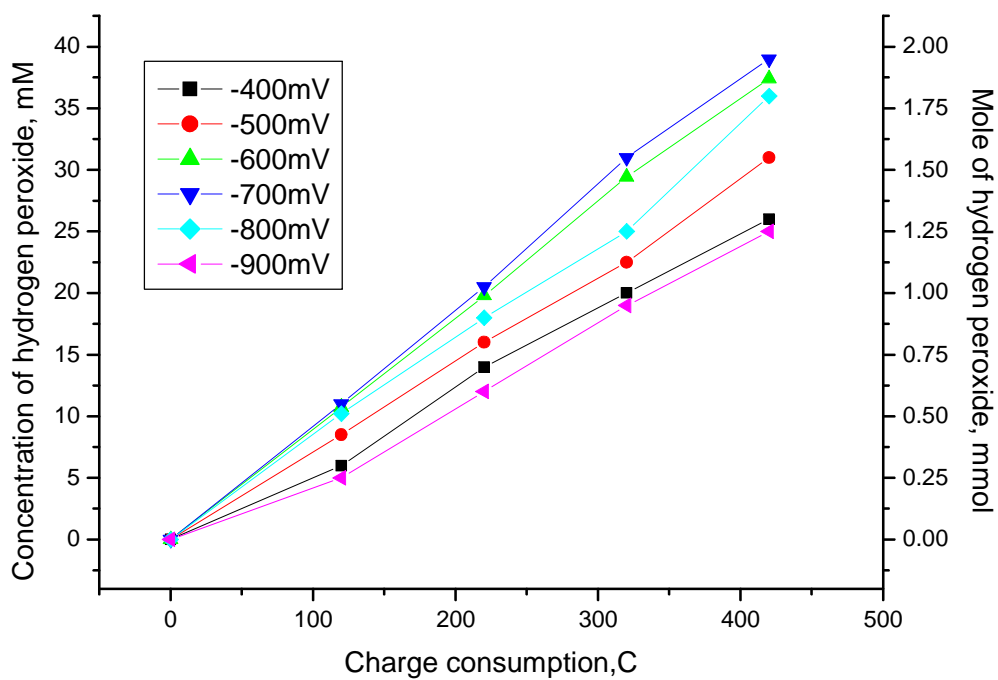


Figure 2.14 Plots of the H_2O_2 electrogenerated in *tert*-butanol/water (1:1.5 v/v) mixture with 0.24 M NaHCO_3 and 0.1 M NaCl at different applied potentials versus charge consumed in the electrolysis. All potentials are referred to the standard calomel electrode (SCE). Anolyte: *tert*-butanol/water (1:1.5 v/v) with 2 M H_2SO_4 .

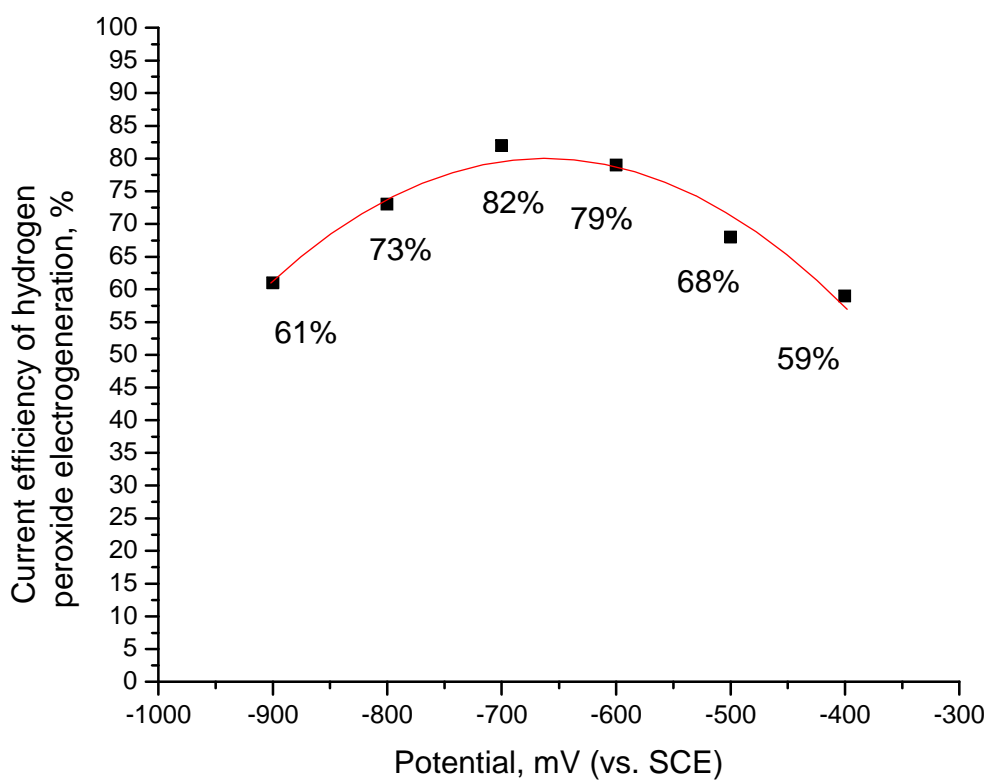


Figure 2.15 Effect of applied potential on the current efficiency of H_2O_2 electrogenerated in *tert*-butanol/water (1:1.5 v/v) with 0.24 M NaHCO_3 and 0.1 M NaCl . All potentials are referred to the standard calomel electrode (SCE). Anolyte: *tert*-butanol/water (1:1.5 v/v) with 2 M H_2SO_4 .

Table 2.4 Electrogeneration of H₂O₂ at various potentials.

Potential, mV (vs. SCE)	Current density, mAcm ⁻²	Current efficiency, %
-400	0.58	58
-500	0.96	68
-600	1.47	79
-700	1.86	82
-800	2.44	73
-900	3.08	61

Anolyte: *tert*-butanol/4 M H₂SO_{4(aq)} (v/v 2:3) mixture. Catholyte: *tert*-butanol/H₂O (v/v 2:3), [NaHCO₃]

= 0.24M and [NaCl] = 0.1M. Cathode: 33 mm x 27 mm x 5 mm 60ppi RVC. Cathode surface area: 156

cm².

2.3.5. The role of anolyte in controlling the catholyte alkalinity

During electrolysis, hydroxyl ion is formed as a by-product in H_2O_2 generation. The rise in pH is, of course, not favorable for the subsequent epoxidation in the catalytic mixture. A comparison of the epoxidation reactivity using 1 M $\text{NaHCO}_{3(\text{aq})}$ and 1 M $\text{H}_2\text{SO}_{4(\text{aq})}$ solutions as anolytes is shown in Figure 2.16. At the beginning, there was no significant difference but the epoxide yield dropped sharply in the former case as the electrolysis continued. This can be partly attributed to the conversion of HCO_3^- to CO_3^{2-} as the pH was increased, as CO_3^{2-} is not efficiency in the generation of HCO_4^- with H_2O_2 (Figure 2.17). On the other hand, base hydrolysis of epoxides also occurred as the pH was raised.

When 1 M $\text{H}_2\text{SO}_{4(\text{aq})}$ was used as the anolyte, protons were formed in the anode by water oxidation (eq. 2.9). Due to the charge difference between the cathode and anode compartments, the protons would move from the anolyte to the catholyte through the cation selective nafion membrane. The excess hydroxyl ions generated in the cathode were thus neutralized and the pH could be kept more or less constant to avoid the conversion of HCO_3^- to CO_3^{2-} and the base hydrolysis of the epoxide products.



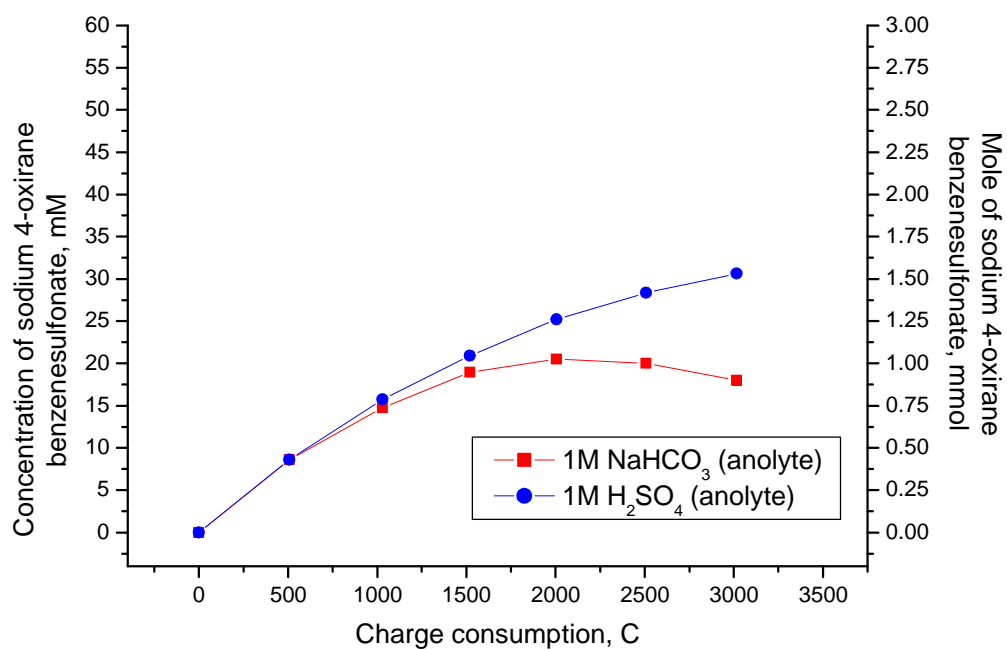


Figure 2.16 Effect of anolyte on the epoxide yield. Catholyte: 1 M NaHCO_{3(aq)}.

Substrate: sodium 4-styrenesulfonate. Potential: -600 mV (vs. SCE).

MnSO₄: 0.001 mol % of the substrate.

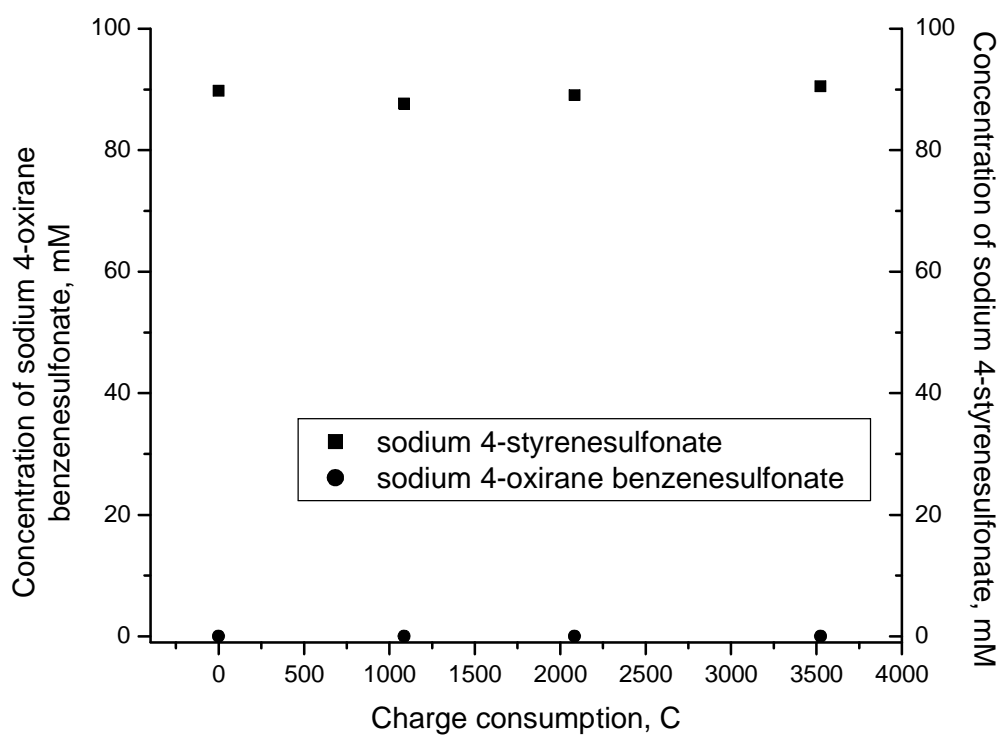
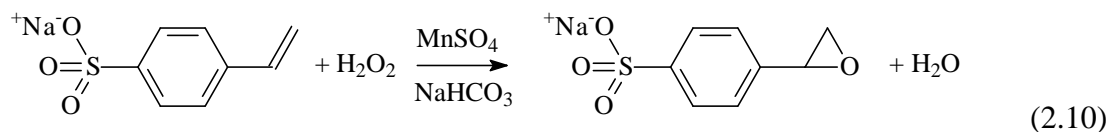


Figure 2.17 Effect of replacing 1 M $\text{NaHCO}_{3(\text{aq})}$ with 1 M $\text{Na}_2\text{CO}_{3(\text{aq})}$ as the catholyte in the electrolysis. Substrate: sodium 4-styrenesulfonate. Potential: -600 mV (vs. SCE). MnSO_4 : 0.06 mol % of the substrate.

2.3.6. Epoxidation of water-soluble alkenes with hydrogen peroxide electrogenerated *in-situ* in bicarbonate solutions

2.3.6.1. The effect of applied potential on the current efficiency of epoxide production

Sodium 4-styrenesulfonate was used as the standard substrate to test the effect of applied potential on the product yield (eq. 2.10).



The effect of applied potential on the current efficiency of electrosynthesis of epoxide is shown in Figures 2.18 and 2.19. A decrease in potential from -400 mV to -600 mV caused insignificant change on the product yield. The H_2O_2 electrogenerated is effectively consumed for the subsequent epoxidation reaction. By applying the potential in this optimal range, the current efficiency of the electrolysis can reach 97%. When the potential is lower than -600 mV, the current efficiency declines sharply because of energy wastes on the generation of hydroxyl ion.

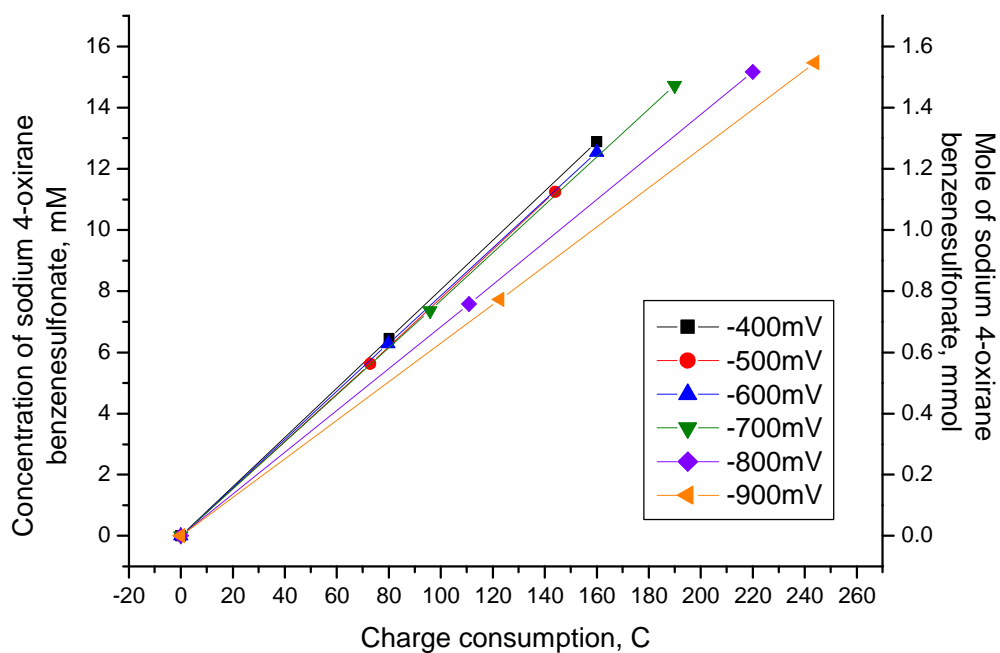


Figure 2.18 Plots of sodium 4-oxirane benzenesulfonate concentration in 1 M $\text{NaHCO}_{3(\text{aq})}$ solution at different applied potentials versus charge consumed in the electrolysis. All potentials are referred to the standard calomel electrode (SCE). Catholyte: 1 M $\text{NaHCO}_{3(\text{aq})}$. Anolyte: 2 M $\text{H}_2\text{SO}_{4(\text{aq})}$. Substrate: sodium 4-styrenesulfonate. MnSO_4 : 0.06 mol % of the substrate.

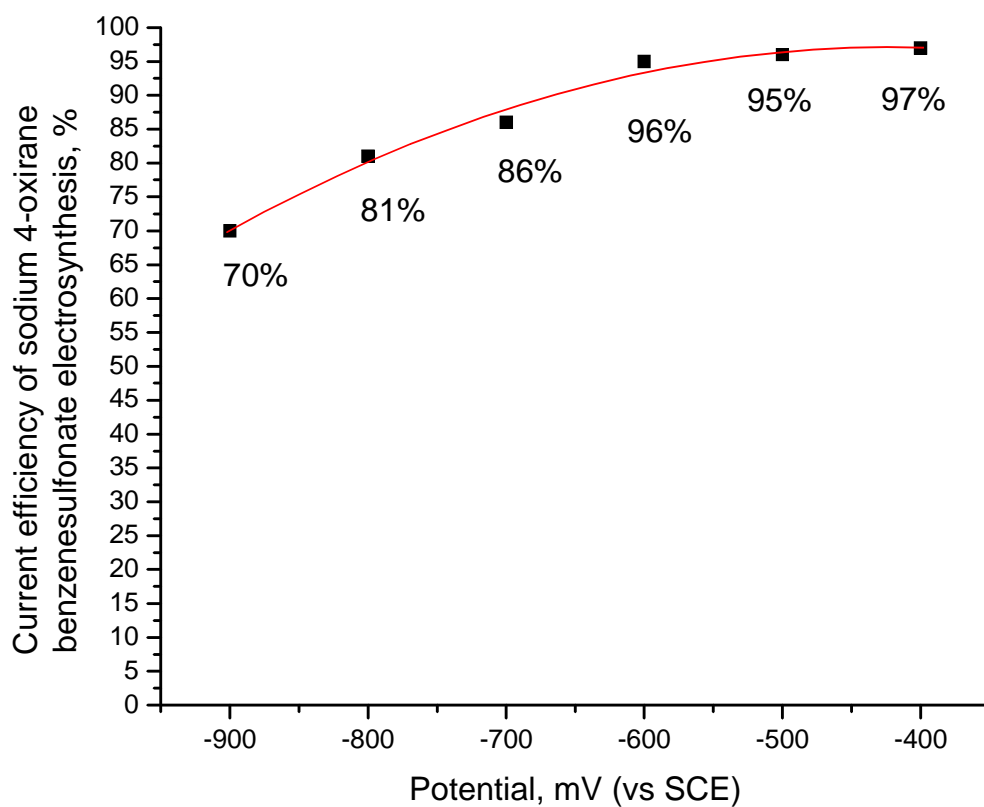


Figure 2.19 The effect of applied potential on the current efficiency of sodium 4-oxirane benzenesulfonate production in 1 M $\text{NaHCO}_{3(\text{aq})}$ solution. All potentials are referred to the standard calomel electrode (SCE). Catholyte: 1 M $\text{NaHCO}_{3(\text{aq})}$. Anolyte: 2 M $\text{H}_2\text{SO}_{4(\text{aq})}$. Substrate: sodium 4-styrenesulfonate. MnSO_4 : 0.06 mol % of the substrate.

2.3.6.2. The effect of catalyst loading on the current efficiency of epoxide production

MnSO₄ was used as the catalyst to epoxidize alkene with H₂O₂. The effect of the amount of Mn²⁺ catalyst on epoxide yield and current efficiency of epoxide production are shown in Figure 2.20 and Figure 2.21 respectively.

The best yield of epoxide was obtained when the Mn²⁺ concentration is higher than 0.03mM (0.06 mol %) (Table 2.5). The epoxide yield is lower when the concentration of MnSO₄ is below 0.002 mM. At this catalyst level, the H₂O₂ generated at the cathode was not consumed fast enough by the epoxidation reaction. As a result, some of the H₂O₂ may be wasted through decomposition (e.g. by Mn²⁺).

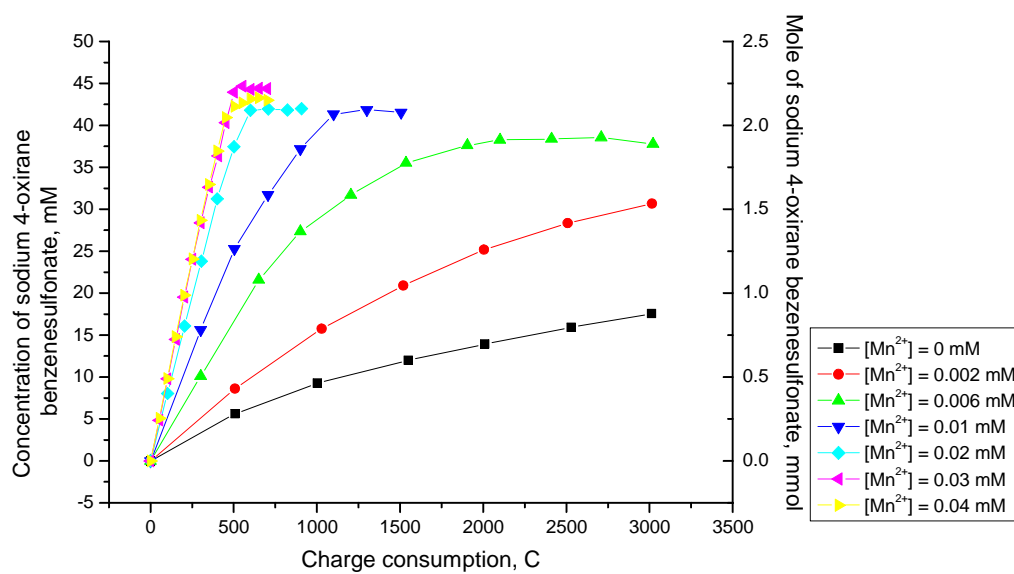


Figure 2.20 Plots of sodium 4-oxirane benzenesulfonate concentration in 1 M $\text{NaHCO}_{3(\text{aq})}$ solution at different $\text{MnSO}_{4(\text{aq})}$ concentrations versus the charge consumed in the electrosynthesis. Catholyte: 1 M $\text{NaHCO}_{3(\text{aq})}$. Anolyte: 2 M $\text{H}_2\text{SO}_{4(\text{aq})}$. Substrate: sodium 4-styrenesulfonate. Potential: -600 mV (vs. SCE).

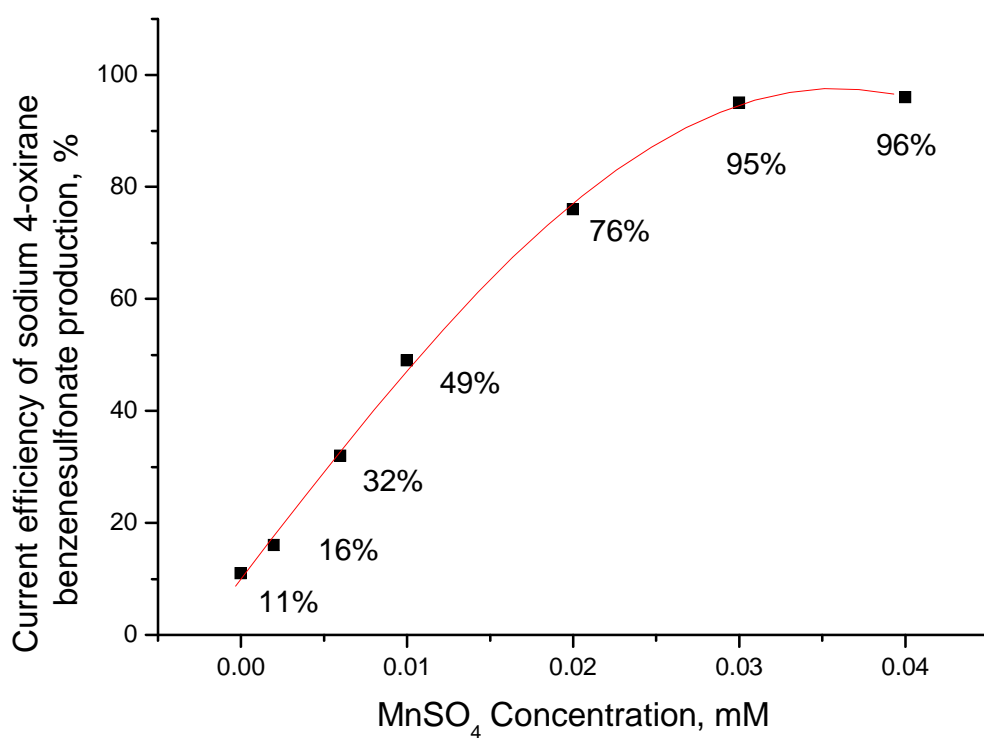


Figure 2.21 The effect of $\text{MnSO}_{4(\text{aq})}$ concentration on the current efficiency of sodium 4-oxirane benzenesulfonate production in 1 M $\text{NaHCO}_{3(\text{aq})}$. Catholyte: 1 M $\text{NaHCO}_{3(\text{aq})}$. Anolyte: 2 M $\text{H}_2\text{SO}_{4(\text{aq})}$. Substrate: sodium 4-styrenesulfonate. Potential: -600 mV (vs. SCE).

Table 2.5 The production of sodium 4-oxirane benzenesulfonate at different MnSO_4 concentrations.

Current efficiency of sodium 4-oxirane	
$[\text{Mn}^{2+}]$, mM	benzenesulfonate production, %
0	11
0.002	16
0.006	32
0.01	49
0.02	76
0.03	95
0.04	96

Catholyte: 1 M $\text{NaHCO}_{3(\text{aq})}$. Anolyte: 2 M $\text{H}_2\text{SO}_{4(\text{aq})}$. Substrate: sodium 4-styrenesulfonate. Potential:

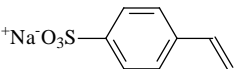
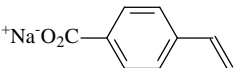
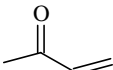
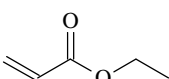
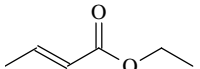
-600 mV (*vs.* SCE).

2.3.6.3. Epoxidation of various water-soluble alkenes

The optimal applied potential and $\text{MnSO}_{4(\text{aq})}$ concentration used for the electrosynthesis of epoxides were chosen to be -600 mV and 0.03 mM (0.06 mol %) respectively. Under these conditions, H_2O_2 was electrogenerated effectively and the subsequent epoxidation also occurred at a reasonable rate.

Table 2.6 summarizes the water-soluble alkenes that were tested for epoxidation in this study. The water-soluble styrenes (entries 1 and 2) were converted to the corresponding epoxides at high yields and current efficiencies. This can be attributed to the activation of the carbon-carbon double bond by the phenyl ring. For the other water-soluble alkenes (entries 3-5), the yields are comparatively lower, which is accord with the lower reactivity of the carbon-carbon double bond in these alkenes.

Table 2.6 Manganese-mediated epoxidation of water-soluble alkenes in bicarbonate solutions.

Entry	Substrate	Electrolysis	Epoxide yield,	Current
		Time, min	%	Efficiency, %
1	Sodium 4-styrenesulfonate 	45	97	95
2	Sodium 4-vinyl benzoate 	50	96	81
3	Methyl vinyl ketone 	80	44	32
4	Ethyl acrylate 	90	51	17
5	Ethyl <i>trans</i> -crotonate 	90	58	21

Catholyte: 1 M NaHCO_{3(aq)}. Anolyte: 2 M H₂SO_{4(aq)}. Substrate: 2.5 mmol. MnSO₄: 0.06 mol % of substrate. Potential: -600 mV (vs. SCE).

2.3.7. Epoxidation of lipophilic alkenes with hydrogen peroxide electrogenerated in *tert*-butanol/H₂O/NaHCO₃ mixture

The lipophilic alkenes are soluble in *tert*-butanol/H₂O/NaHCO₃ mixture. In this study, the catholyte used was *tert*-butanol/water (v/v 1:1.5) containing 0.24 M NaHCO₃. This mixture provides a medium to solubilize both the lipophilic alkenes and the NaHCO₃ salt at relatively high concentration. When NaCl (0.1 M) was added to the electrolyte, the conductivity of the electrolyte can be further improved.

The optimal potential for H₂O₂ electrogeneration in *tert*-butanol/H₂O/NaHCO₃ mixture has been shown to be about -700 mV (vs. SCE) (Table 2.4). However, only moderate current efficiency was obtained when this potential was applied for β -methyl styrene oxide production (Figure 2.22). This could be caused by the relatively slow rate of epoxidation (H₂O₂ consumption) as compared to the H₂O₂ generation rate.

Raising the potential to -400 mV (vs. SCE) greatly improved the current yield from 45 to 60%. At this potential, the H₂O₂ generation is slow enough to keep pace with the subsequent epoxidation reaction. Its loss due to self-decomposition is minimized.

When the potential is higher than -400mV , the electrochemical driving force is not large enough to reduce O_2 to H_2O_2 . No epoxide products could be detected at this potential (Table 2.7).

The lipophilic alkenes epoxidized by this system are summarized in Table 2.8. Entries 6-10 illustrate that the epoxidation of styryl alkenes proceeded efficiently with reasonable yields of 45-78%. The oxidation of cyclooctene (entry 11) gives only a fair yield (42%) probably because of angle strain in the cyclic alkene. α -Pinene oxide (entry 12) is unreactive due to its sterically hindered carbon-carbon double bond.

For volatile alkenes, such as styrene (entry 10), the oxidation gave fair yields only compared with the literature [69]. This can be partly attributed to the loss of the volatile substrate into headspace from the reaction mixture during electrolysis (Figure 2.1). This could be a drawback of this electrogenerated H_2O_2 -epoxidation system as the purging of oxygen gas will inevitably vaporize the volatile substrates from the electrolyte.

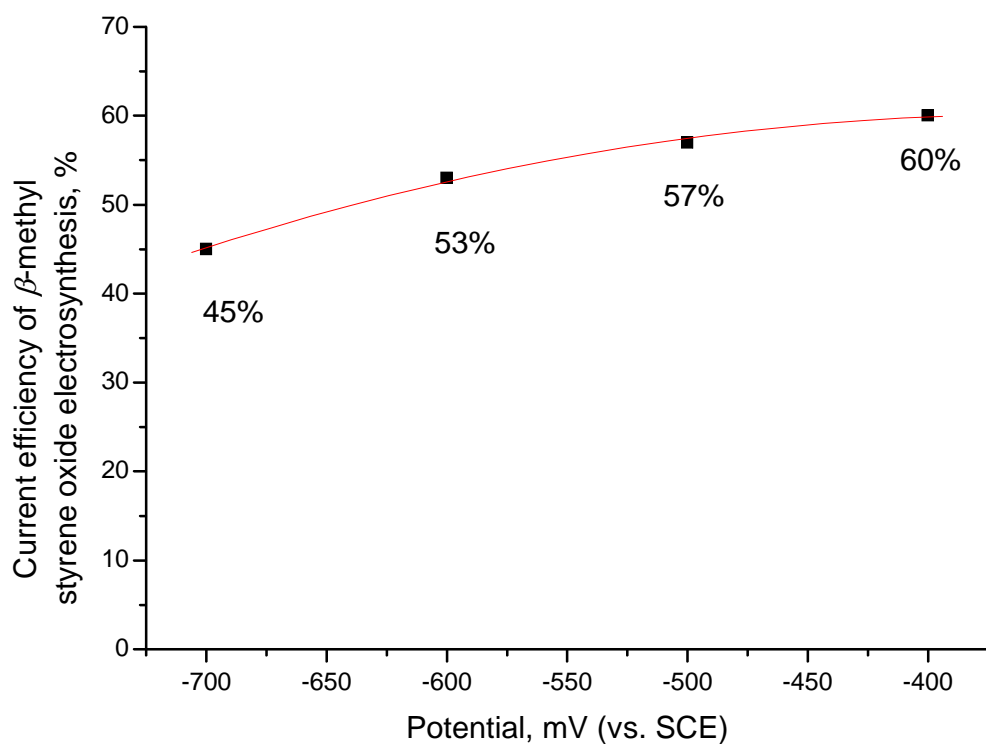


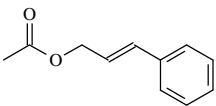
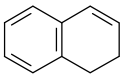
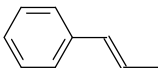
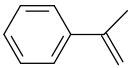
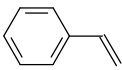
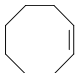

Figure 2.22 Effect of applied potential on the current efficiency of β -methyl styrene oxide production in *tert*-butanol/water (v/v 1:1.5) mixture containing 0.24 M NaHCO_3 and 0.1M NaCl . All potentials are referred to the standard calomel electrode (SCE). Anolyte: *tert*-butanol/4 M $\text{H}_2\text{SO}_{4(\text{aq})}$ (v/v 2:3) mixture. Substrate: β -methyl styrene (2.5 mmol). MnSO_4 : 0.06 mol %.

Table 2.7 Epoxidation of β -methyl styrene in *tert*-butanol/H₂O/NaHCO₃ mixture with electrogenerated H₂O₂ at different applied potentials.

Potential, mV (vs. SCE)	Electrolysis	Epoxide yield,	Current
	Time, min	%	Efficiency, %
-700	90	45	12
-600	90	53	15
-500	90	57	23
-400	90	60	29
-300	180	16	5

All potentials are referred to standard calomel electrode (SCE). Anolyte: *tert*-butanol/4 M H₂SO_{4(aq)} (v/v 2:3) mixture. Catholyte: *tert*-butanol/H₂O (v/v 2:3), [NaHCO₃] = 0.24M, [NaCl] = 0.1M. Substrate: β -methyl styrene (2.5 mmol). MnSO₄: 0.06 mol % of the substrate.

Table 2.8 Manganese-mediated epoxidation of lipophilic alkenes in *tert*-butanol/H₂O/NaHCO₃ mixture with electrogenerated H₂O₂.

Entry	Substrate	Electrolysis	Epoxide yield,	Current
		Time, min	%	Efficiency, %
6	Cinnamyl acetate 	90	78	23
7	1,2-Dihydronaphthalene 	90	73	43
8	β -methyl styrene 	90	60	29
9	α -methyl styrene 	80	43	32
10	Styrene 	70	50	40
11	Cyclooctene 	80	42	29
12	α -pinene 	90	23	8

Catholyte: *tert*-butanol/water (v/v 2:3) mixture containing 0.24 M NaHCO₃ and 0.1 M NaCl. Anolyte:

tert-butanol/4 M H₂SO_{4(aq)} (v/v 2:3) mixture. Substrate: β -methyl styrene (2.5 mmol, 0.05 M). MnSO₄:

0.06 mol %. Potential: -400 mV (vs. SCE).

2.4. Conclusion

Using dioxygen as the oxygen source, the electrogeneration of H_2O_2 for *in-situ* epoxidation has been achieved. *tert*-Butanol assists both the solubility of O_2 and the lipophilic alkenes in the $\text{Mn}^{2+}/\text{H}_2\text{O}_2/\text{HCO}_3^-$ epoxidation system. In literature [69], epoxidation with the $\text{Mn}^{2+}/\text{HCO}_3^-$ catalytic system was achieved by adding H_2O_2 solution dropwisely to the reaction mixture. If all the H_2O_2 was added in a single batch during the course of reaction, catalytic decomposition of H_2O_2 caused by Mn^{2+} became dominant and the reaction would become very exothermic. In the system described in this chapter, H_2O_2 was generated continuously at relatively low concentration and the problem of H_2O_2 wastage through Mn^{2+} decomposition was minimized. On comparison of our results with those in literature (Table 2.9), it is obvious that a smaller amount of H_2O_2 was required for the electrogenerated H_2O_2 -epoxidation reaction. This appears to be a major advantage of the electrochemical method.

Table 2.9 Comparison of this study with the literature method [69] on the amount of H₂O₂ used.

Substrate	This method, Equivalent of H ₂ O ₂	Literature method, Equivalent of H ₂ O ₂
Sodium 4-styrenesulfonate	1.1	10
Sodium 4-vinyl benzoate	1.2	10
1,2-dihydronaphthalene	2.3	5
Cinnamyl acetate	4.3	10

Chapter 3

Indirect Catalytic Epoxidation with Hydrogen Peroxide

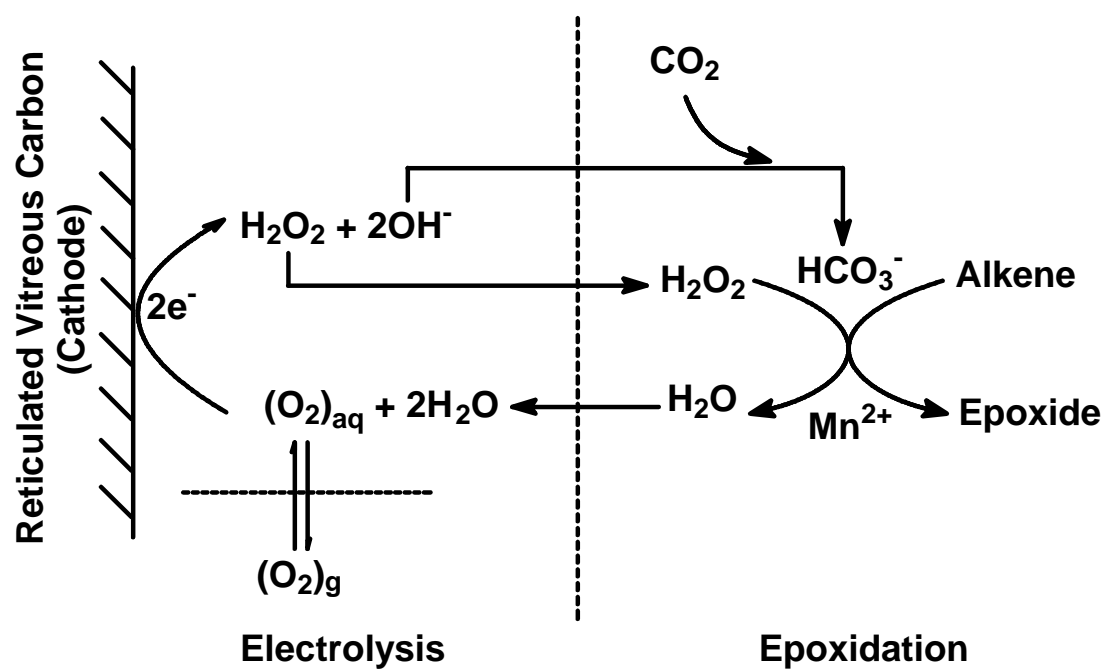
Electrogenerated in Ionic Liquids

3.1. Introduction

Ionic liquids (ILs) possess many unique and interesting chemical and physical properties. They have been proposed as ‘green’ alternatives to volatile organic solvents in extraction processes [221, 222], as the electrolyte in solar cell applications[223, 224] and as media for selective catalytic processes[225-227]. However, there are relatively few studies on the application of ILs in electro-organic synthesis [228, 229]. In principle, ionic liquids are ideal solvent/electrolyte for electro-organic synthesis because no supporting electrolyte is required, and they can be recovered and reused.

Electrogeneration of hydrogen peroxide (H_2O_2) in aqueous [118, 119, 121, 230] and biphasic systems [126, 127, 231] has been extensively reported in literatures. Recently, Chan and co-workers [130] reported the electrochemical generation of H_2O_2 in the ionic liquid 3-butyl-1-methyl imidazolium tetrafluoroborate and demonstrated that the H_2O_2 can be used *in-situ* for the epoxidation of electrophilic alkenes in alkaline medium. As this system is only applicable to the epoxidation of electrophilic alkenes such as α,β -unsaturated ketones, it is of particular interest to couple the electrogeneration of H_2O_2 with other catalytic epoxidation systems to broaden its

applications. As shown in Chapter 2, the $\text{Mn}^{2+}/\text{HCO}_3^-$ system is a particularly promising ‘green’ catalytic system for epoxidation. It is thus of interest to design an IL-based analogue of the electrogenerated $\text{H}_2\text{O}_2/\text{Mn}^{2+}/\text{HCO}_3^-$ epoxidation system. In this chapter, the electrogeneration of H_2O_2 in ILs, the *in-situ* generation of the active peroxymonocarbonate species (HCO_4^-), and the epoxidation of alkenes using this system will be reported (Scheme 3.1). The active oxidant peroxymonocarbonate was generated *in-situ* by mixing CO_2 gas with the electrogenerated H_2O_2 in IL. The recovery and reuse of the ILs for H_2O_2 electrogeneration/epoxidation have also been studied.



Scheme 3.1 Electrogeneration of H_2O_2 for the epoxidation of lipophilic alkenes with active species generated *in-situ* in ionic liquid/ $\text{NaOH}_{(\text{aq})}$ mixtures.

3.2. Experimental Section

3.2.1. Materials

All chemicals and solvents used were of analytical reagent (A.R.) grade. Alkenes and epoxides were obtained from commercial sources (Aldrich Co. or Acros Organic), and were used as received unless otherwise noted. Manganese(II) sulfate monohydrate (>99%), sodium hydroxide (98%) and H₂O₂ (35 wt. % solution in water) were purchased from Aldrich Co. Oxygen (>99.7%) and argon (>99.995%) were obtained from Hong Kong Oxygen Co. Double deionized water was purified by passing through an ion-exchange resin purification train (Millipore).

3.2.2. Synthesis of ionic liquids

1-Butyl-3-methylimidazolium tetrafluoroborate ([bmim][BF₄]) [232, 233]

A solution of 1-bromobutane (119 ml, 1.1 equiv.) was added slowly to 1-methylimidazole (78 ml, 1 mol) in acetone (500 ml) in a 1 L round bottle flask (*1-methylimidazole was first distilled under vacuum to give a clear colourless oil*).

The mixture was gently refluxed under argon for 24 hours. After cooling to room

temperature, the solvent was removed and the 1-butyl-2-methylimidazolium bromide ([bmim]Br) was washed thoroughly with ether (3x300 ml). A 2 L round bottle flask was charged with 1.5 L acetonitrile, [bmim]Br and sodium tetrafluoroborate (120 g, 1.1 eq.), and the mixture was allowed to stand at room temperature for 3 days with stirring. The precipitate (NaBr) was then filtered off and the filtrate was concentrated by rotary evaporator. More NaBr was precipitated by adding dichloromethane (1 L). The crude IL was further purified on a silica column using dichloromethane as eluent to give a pale yellow liquid. Yield: 167.2 g (74%). ¹H NMR (CDCl₃, δ ppm): 8.72 (s, 1H), 7.51 (dd, 2H), 4.23 (t, 2H), 3.97 (s, 3H), 1.88 (m, 2H), 1.36 (m, 2H), 0.94 (t, 3H).

1-Butyl-2,3-dimethylimidazolium tetrafluoroborate ([bdmim][BF₄]) [234]

A solution of 1-bromobutane (119 ml, 1.1 eq.) was added slowly and cautiously to 1,2-dimethylimidazole (96.1 g, 1 mol) in 500 ml acetone. The mixture was gently heated at reflux under argon for 24 hours. After cooling to room temperature, a white solid precipitated out and the yellowish solvent was decanted. The white solid (1-butyl-2,3-dimethylimidazolium bromide, [bdmim]Br) was washed thoroughly with acetone (2x300 ml) and ether (2x300 ml). A 2 L round bottle flask was then charged with 1.5 L acetonitrile, [bdmim]Br and sodium tetrafluoroborate (120 g, 1.1 eq.). The

mixture was allowed to stand at room temperature for 3 days with stirring. The precipitate (NaBr) that appeared was filtered off and the filtrate was concentrated under vacuum to give a colorless liquid. Further precipitation of NaBr was achieved upon the addition of dichloromethane (1 L). The crude IL was purified on a silica column using dichloromethane as eluent to give a colorless liquid. Yield: 201.6 g (84%). ^1H NMR (CDCl_3 , δ ppm): 7.32 (dd, 2H), 4.07 (t, 2H), 3.80 (s, 3H), 2.61 (s, 3H), 1.76 (m, 2H), 1.37 (m, 2H), 0.93 (t, 3H).

3-Octyl-1,2-dimethylimidazolium tetrafluoroborate ([odmim][BF₄]) [234]

The preparation was similar to that of [bdmim][BF₄] except that 1-bromooctane (190 ml, 1.1 eq.) was used. Yield: 228.0 g (77%). ^1H NMR (CDCl_3 , δ ppm): 7.33 (dd, 2H), 4.07 (t, 2H), 3.80 (s, 3H), 2.61 (s, 3H), 1.76 (m, 2H), 1.77 (m, 10H), 0.86 (t, 3H).

3.2.3. Instrumentation

The microflow cell (MFC) described in Chapter 2 was used in this study. It was connected to the peristaltic pumps and teflon tubings obtained from Cole-Parmer Instrumental Company (Figure 3.1). The gas and electrolyte flow rates were monitored by flowmeters purchased from Gilmont Instruments. An EG&G Princeton

Applied Research Model 273A Potentiostat/Galvanostat was used for electrolysis. A 33mm x 27mm x 5mm reticulated vitreous carbon (60 pores per inch (ppi)) was used as the cathode. The anode was a platinum-coated titanium plate. A Nafion 424 cation permeable membrane was used to separate the cathode and anode compartments.

For voltammetric measurements, glassy carbon and platinum electrodes were polished with 0.05 μm α -alumina (Buehler) on a microcloth, rinsed with double deionized water and then sonicated for 5 minutes in water before used. Cyclic voltammetry (CV) was measured by a Bioanalytical Systems (BAS) model 100W electrochemical analyzer and carried out in a conventional two-compartment cell with a sintered glass separated the two compartments. A platinum wire was used as the counter electrode, whereas the reference electrode was a saturated calomel electrode (SCE).

^1H and ^{13}C NMR spectra were recorded on a Bruker DPX-400MHz NMR spectrometer. A Hewlett-Packard 8900 GC-MS equipped with ECTM-1 or ECTM-WAX columns (Alltech Associate, Inc.) was used for analyzing volatile chemicals. DMSO and tetradecane were used as internal standards for ^1H NMR and GC-MS quantitative measurements respectively.

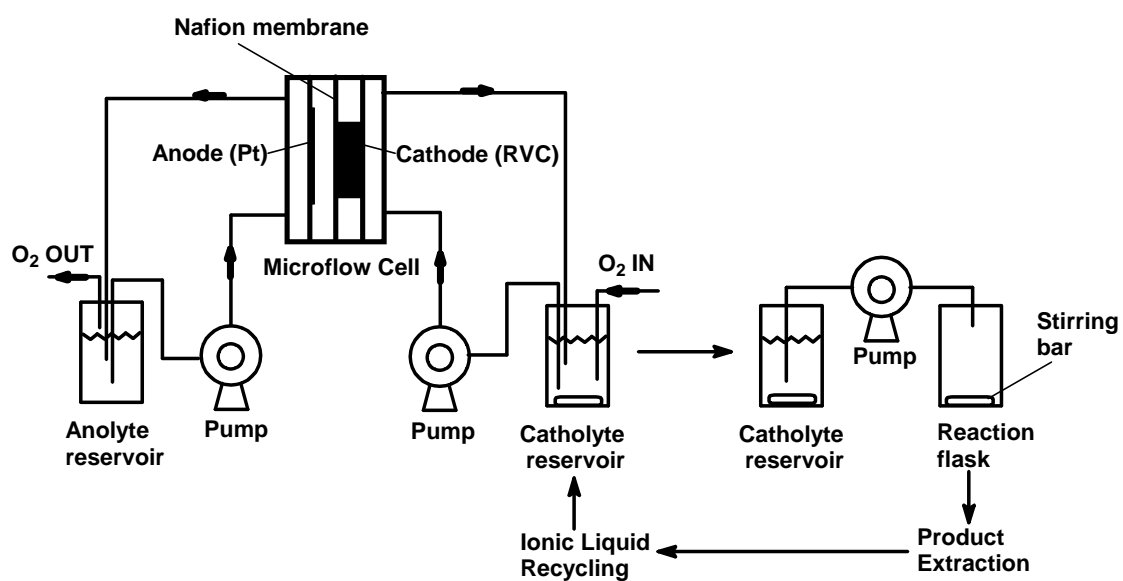


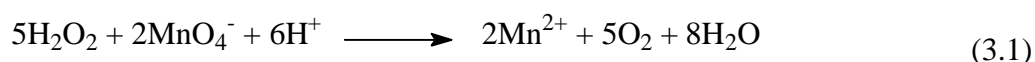
Figure 3.1 Schematic diagram of H_2O_2 electrogeneration in ionic liquid for catalytic epoxidation.

3.2.4. Electrogeneration of hydrogen peroxide in ionic liquid/NaOH_(aq) mixture

The two reservoirs were charged with 25 ml solutions of anolyte (IL/H₂SO_{4(aq)} mixture) and catholyte (IL/NaOH_(aq) mixture) respectively as shown in Figure 3.1. Electrolysis was carried out under circulation mode at a flow rate of 135 ml/min. Oxygen was continuously purged into the catholyte throughout the process at 45 ml/min for the electrogeneration of H₂O₂.

The H₂O₂ concentration was determined using permanganate titration (eq. 3.1) [235].

At regular time intervals during electrolysis, 0.1 ml catholyte was withdrawn and diluted with 0.5 M H₂SO_{4(aq)} (5 ml) for the titration.



3.2.5. Epoxidation of lipophilic alkenes with hydrogen peroxide electrogenerated in ionic liquid

Epoxidation of alkenes was achieved by using the H₂O₂ electrogenerated in IL/NaOH_(aq) mixture (Figure 3.1). This mixture was added dropwise into a flask

pre-charged with alkene substrate and MnSO_4 at 2 ml/min. Meanwhile, $\text{CO}_{2(g)}$ was continuously purging at 10 ml/min. Alternatively, dry ice (solid CO_2) was added in small portions. Throughout the mixing process, the flask was kept at 5°C to reduce the loss of volatile alkene. It was sealed afterwards and allowed to stand at room temperature for another 3-5 hours. The product was then extracted by pentane (3x20 ml), and the organic layer was washed with brine (2x10 ml) and dried over sodium sulfate. A portion of the mixture (10 ml) was mixed with the internal standard tetradecane (100 μl of a 0.156 M solution) and analysed by GC-MS. The other portion was analysed by ^1H NMR after the solvent had been removed under reduced pressure.

3.2.6. Recovery and reuse of ionic liquid

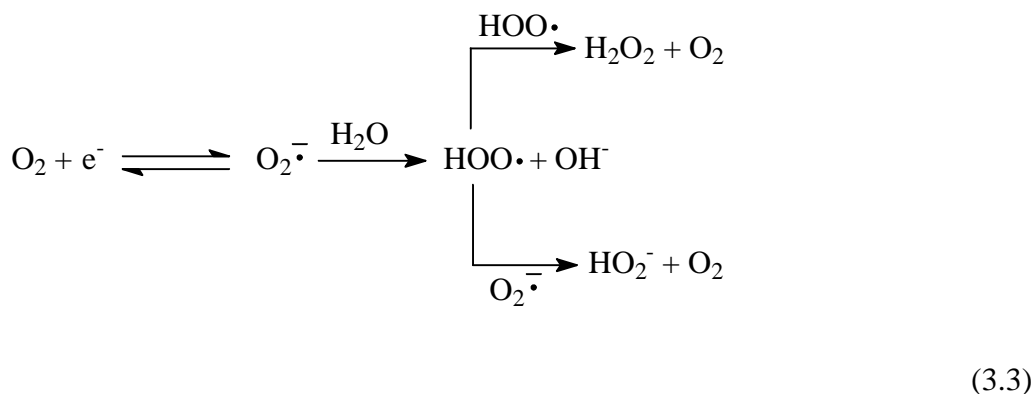
Prior to the reuse of ILs for the next H_2O_2 electrogeneration/catalytic epoxidation cycle, removal of Mn^{2+} is necessary to avoid any adverse effects on the electrogeneration of H_2O_2 . 1M $\text{Na}_2\text{CO}_{3(aq)}$ (2x15 ml) was used to extract the manganese salt for the electrolyte. After extraction, the mixture separated into two phases. The IL phase was a mixture of IL/ H_2O / NaOH / Na_2CO_3 in which the water content [130], sodium carbonate and NaOH concentrations were measured and adjusted before reused for H_2O_2 electrogeneration. Around 10-15% of ILs remained in

the aqueous phase which was recovered by evaporating the water and then extracting with dichloromethane.

3.3. Results and discussion

3.3.1. Voltammetric studies on the reduction of oxygen in [bdmim][BF₄]

The cyclic voltammograms of oxygen reduction in [bdmim][BF₄] are shown in Figure 3.2. A reduction peak appears at approximately -879 mV vs. SCE and the corresponding oxidation peak appears at -622 mV vs. SCE. This is consistent with the results reported by AlNashef and coworkers [128, 129], who assigned the couple to the reduction of oxygen to superoxide ion ($O_2^{\cdot-}$) according to eq. 3.2. In our case, the ratio of i_{pc}/i_{pa} is larger than 1 (where i_{pc} and i_{pa} stand for cathodic and anodic peak currents respectively). This is likely to be caused by the presence of small amount of water in the IL.





In [bdmim][BF₄], the addition of 10% (v/v) of water enhances the magnitude of i_{pc} and diminishes that of i_{pa} ($i_{\text{pc}} > i_{\text{pa}}$) (Figure 3.3). This can be attributed to the activation of $\text{O}_2^{\cdot -}$ by water leading to the further reduction to H_2O_2 or HO_2^- (eq. 3.3) [236]. In the presence of water, the reduction of dioxygen in [bdmim][BF₄] shifts to a more positive potential (-668 mV vs. SCE). This can be attributed to the improvement of solvating properties of the reduced forms of dioxygen upon the addition of water [129]. Increasing the water content to 10% (v/v) causes the reduction wave to further shift towards the anodic side (Figure 3.4).

H_2O_2 is thermodynamically unstable with respect to the further electroreduction to water or hydroxyl ions. Nevertheless, while the 2-electron reduction of O_2 to H_2O_2 or HO_2^- is reasonably fast (eq. 3.4), the over-potential for the further 2-electron reduction to OH^- or H_2O is high on carbon electrode (eq. 3.5). Hence, the loss due to the 4e^- reduction of O_2 to H_2O is minimized [120].

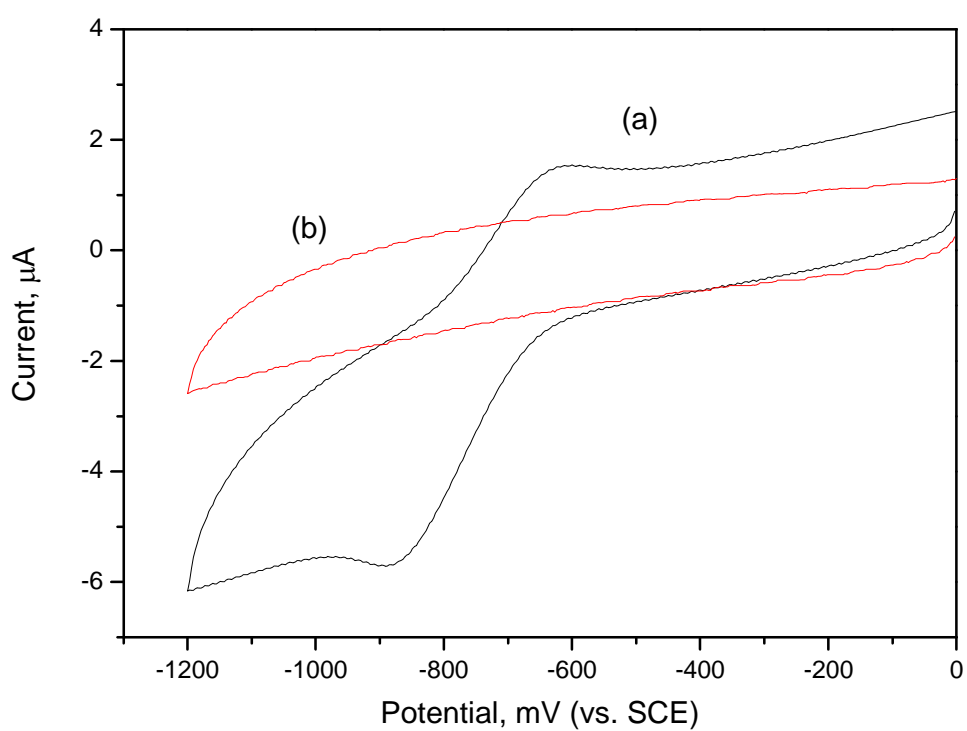


Figure 3.2 Cyclic voltammograms of oxygen reduction in [bdmim][BF₄].

Working electrode: 0.2 cm² glassy carbon. Scan rate: 100 mVs⁻¹.

Saturated with (a) oxygen and (b) argon.

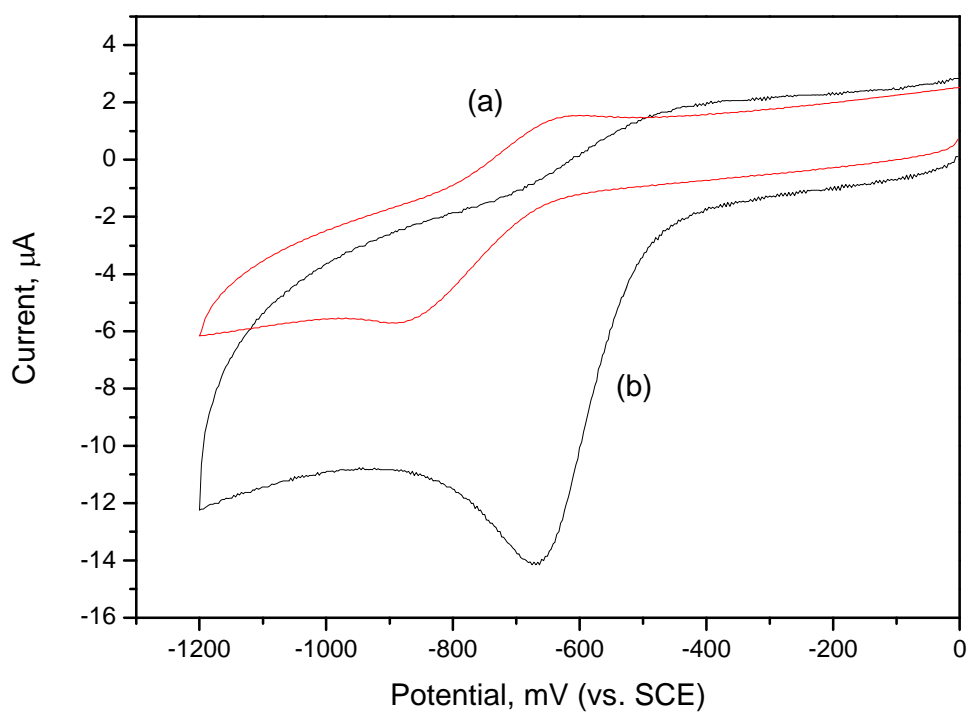


Figure 3.3 Cyclic voltammograms of oxygen reduction in [bdmim][BF₄]/water mixture. Working electrode: 0.2 cm² glassy carbon. Scan rate: 100 mVs⁻¹. (a) [bdmim][BF₄] only and (b) [bdmim][BF₄]/water (9:1 v/v) mixture.

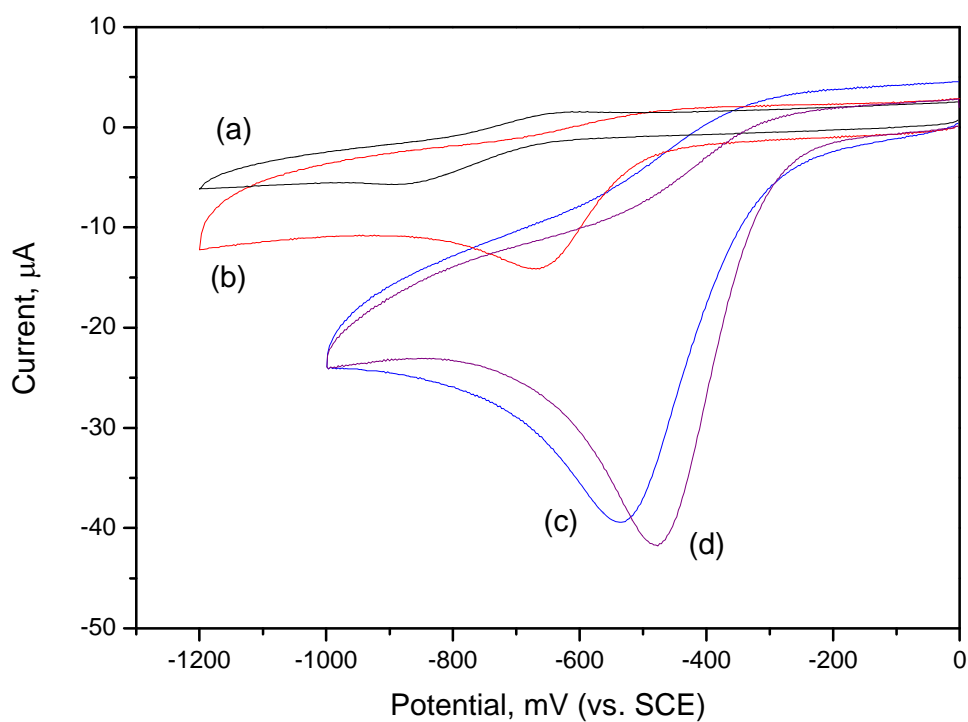
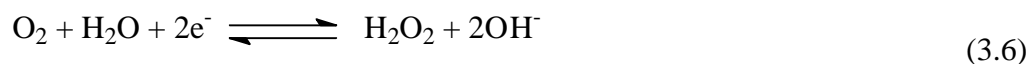


Figure 3.4 Cyclic voltammograms of oxygen reduction in [bdmim][BF₄]/water mixture. Working electrode: 0.2 cm² glassy carbon. Scan rate: 100 mVs⁻¹. (a) [bdmim][BF₄] only, (b) [bdmim][BF₄]/water (9:1 v/v) mixture, (c) [bdmim][BF₄]/water (4:1 v/v) mixture and (d) ([bdmim][BF₄]/water (4:1 v/v))/0.006M NaOH mixture.

3.3.2. The effect of water content in [bdmim][BF₄] on the current efficiency of hydrogen peroxide electrogeneration

The main limitation in O₂ reduction is its low solubility in most electrolytes [120]. As the solubility of O₂ in ILs are 2-10 fold higher than water and organic solvents [237], using ILs as the electrolyte can partly alleviate this problem. As mentioned above, O₂ is reduced reversibly to superoxide ion in water-free IL. The addition of water produces H₂O₂ through a two-electron reduction pathway (eq. 3.6). Because of its non-polar character, the increase in water content in ILs reduces the O₂ solubility in the resulting mixture, which will affect the H₂O₂ production process accordingly [238]. On the other hand, ILs are viscous solvents and slow diffusion of O₂ is expected [239, 240]. When the water content in ILs increases, O₂ mass transport also becomes faster.



When a constant current was applied to the electrochemical cell, H₂O₂ was electrogenerated at a steady rate and its concentration in the electrolyte increased with time (Figure 3.5). The current efficiency, however, shows a clear correlation with the

water content in the IL (Figure 3.6). When the water concentration is less than 20% (v/v), H_2O_2 production is relatively slow and a higher cell potential is required to drive the reaction at fixed current density (Table 3.1). When the water content is increased to 20% (v/v) or above, the production of H_2O_2 occurs at a relatively fast rate. However, too high a water content will lead to a drop in the current efficiency of H_2O_2 production due to the lower solubility of O_2 as well as side reactions such as the electrolysis of water. In general, 20 % (v/v) of water is the optimal amount to drive the production of H_2O_2 effectively in the [bdmim][BF_4]/ $\text{NaOH}_{(\text{aq})}$ mixture.

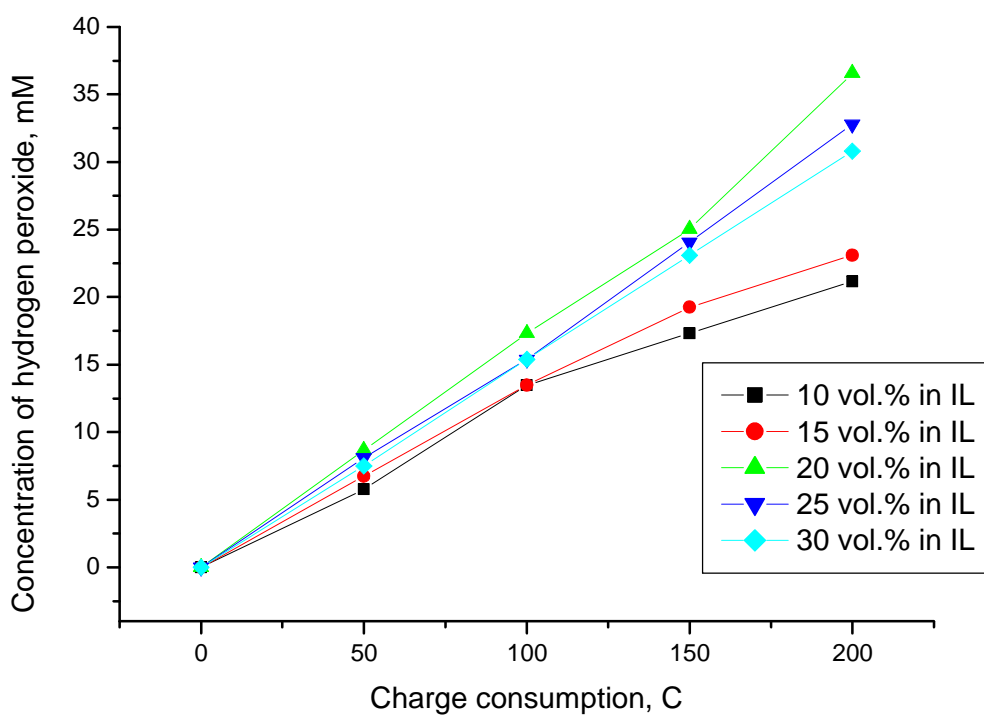


Figure 3.5 Plots of H_2O_2 electrogenerated in $[\text{bdmim}][\text{BF}_4]/\text{NaOH}_{(\text{aq})}$ mixture with different water content versus the charge consumption. Current density: 0.38 mAcm^{-2} . Catholyte: $[\text{bdmim}][\text{BF}_4]/0.006\text{M NaOH}_{(\text{aq})}$ mixture. Anolyte: $[\text{bdmim}][\text{BF}_4]/4\text{M H}_2\text{SO}_{4(\text{aq})}$ mixture.

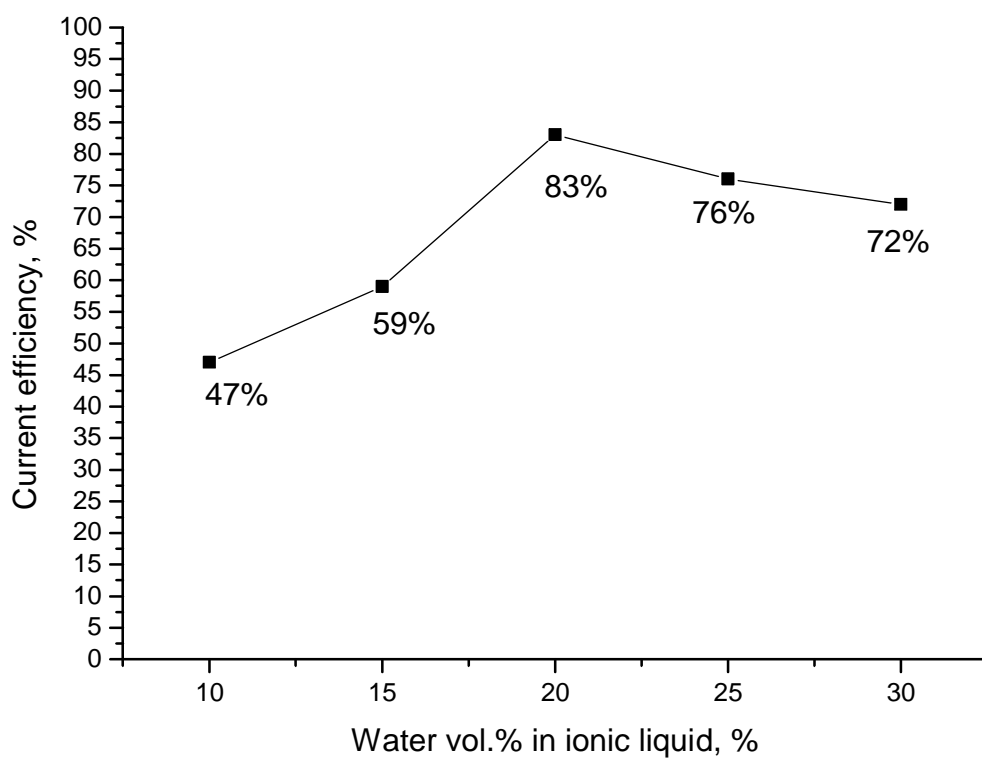


Figure 3.6 The effect of water content on the current efficiency of H_2O_2 electrogeneration in $[\text{bdmim}][\text{BF}_4]/\text{NaOH}_{(\text{aq})}$ mixture. Current density: 0.38mAcm^{-2} . Catholyte: $[\text{bdmim}][\text{BF}_4]/0.006\text{M NaOH}_{(\text{aq})}$ mixture. Anolyte: $[\text{bdmim}][\text{BF}_4]/4\text{M H}_2\text{SO}_{4(\text{aq})}$ mixture.

Table 3.1 Electrogeneration of H_2O_2 in $[\text{bdmim}][\text{BF}_4]/\text{NaOH}_{(\text{aq})}$ mixture with different water contents.

Water content, vol.% in		Concentration of		Current
$[\text{bdmim}][\text{BF}_4]$	Cell potential, V	H_2O_2 , mM		efficiency, %
10	3.53	21		47
15	3.37	23		59
20	2.94	37		83
25	3.02	33		76
30	3.17	31		72

Current density: 0.38 mAcm^{-2} . Catholyte: $[\text{bdmim}][\text{BF}_4]/0.006\text{M NaOH}_{(\text{aq})}$ mixture. Cathode: 60ppi

RVC. Cathode surface area: 156cm^2 . Anolyte: $[\text{bdmim}][\text{BF}_4]/4\text{M H}_2\text{SO}_{4(\text{aq})}$ mixture. Volumes of

catholyte and anolyte: 25 ml. Electrolysis time: 1 hr.

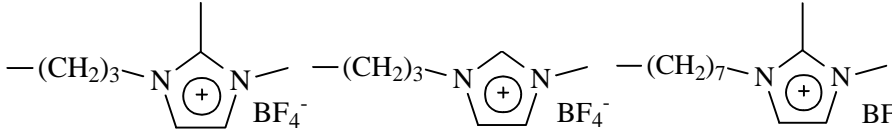
3.3.3. The effect of catholyte and anolyte composition in hydrogen peroxide electrogeneration

Different imidazolium-based ILs, i.e. [bdmim][BF₄], [bmim][BF₄] and [odmim][BF₄], were tested as the media for H₂O₂ electrogeneration. In terms of current efficiency, there is no significant difference amongst them (Table 3.2). [bdmim][BF₄] was chosen because of its ease of preparation and purification, and its high chemical stability [241-243].

In the H₂O₂ electrogeneration, O₂ is electrochemically reduced to H₂O₂ in the form of HO₂⁻ with OH⁻ produced concurrently (eq. 3.4) in the [bdmim][BF₄]/NaOH_(aq) (4:1 v/v) mixture. When the same electrolyte was used as the anolyte, precipitates appeared in the catholyte upon continuous electrolysis and the cell potential increased with the charge consumption. When the anolyte was replaced with [bdmim][BF₄]/4M H₂SO_{4(aq)} mixture (4:1 v/v) mixture, no such problem arose throughout the whole electrolysis. Experimentally, the precipitate that appeared in the catholytes when [bdmim][BF₄]/NaOH_(aq) was used as the anolyte was found to be NaOH. The solubility of NaOH in [bdmim][BF₄]/water (4:1 v/v) mixture was found to be ~0.044M. When the concentration exceeds this value, it precipitates out quickly.

In the electrochemical cell, the cation-selective nafion membrane allows cations to move between the anode and cathode compartments. The permeation selectivity depends on the size ($H^+ < Na^+ < bdmim$ ion) and concentration of cations. When an acidic mixture was used as the anolyte, H^+ diffused to the cathodic side through the nafion during electrolysis to balance the charge consumption. Those OH^- generated at the cathode were simply neutralized and the alkalinity was maintained. On the contrary, when $[bdmim][BF_4]/NaOH_{(aq)}$ was used as the anolyte, the build-up of NaOH in the catholyte would cause its precipitation and hence a rise in the cell resistance (Table 3.3).

Table 3.2 The current efficiency of H₂O₂ electrogeneration in different ionic liquids.

Ionic Liquid			
	Current efficiency, %	Current efficiency, %	Current efficiency, %
	83	78	85

Catholyte: IL/NaOH_(aq) (4:1 v/v) mixture. Anolyte: IL/4M H₂SO_{4(aq)} (4:1 v/v) mixture. Cathode surface area: 156 cm². Current density: 0.38 mAcm⁻². Volumes of catholyte and anolyte: 25 ml.

Table 3.3 Effect of anolyte composition on the current efficiency of H₂O₂ electrogeneration. .

Anolyte	Cell potential, V	Concentration of	Current
		H ₂ O ₂ , mM	efficiency, %
[bdmim][BF ₄]/4M H ₂ SO _{4(aq)}			
(4:1 v/v)	2.94	37	83
[bdmim][BF ₄]/0.06M NaOH _(aq)			
(4:1 v/v)	3.12-3.57	32	71

Catholyte: [bdmim][BF₄]/NaOH_(aq) (4:1 v/v) mixture. Cathode surface area: 156 cm². Current density: 0.38 mAcm⁻². Volumes of catholyte and anolyte: 25 ml. Electrolysis time: 1 hr.

3.3.4. The effect of current density on the current efficiency of hydrogen peroxide electrogeneration

In chapter 2, a fixed potential was applied in the electrochemical cell for the electrogeneration of H_2O_2 in aqueous or aqueous/*tert*-butanol solutions. At optimal conditions, high current efficiency of the production was attained. However, when similar approach was used in the IL/water mixture, relatively slow electrolysis (low cathode current density) was observed. This is probably due to the high viscosity of IL which retards the O_2 diffusion in the reaction mixture. When a fixed current density was applied instead, the reduction of oxygen was driven at the expense of higher overpotential and a relatively fast electrolysis rate was attained.

The H_2O_2 concentration-charge consumption curves at different current densities are shown in Figure 3.7. The favourable current density range for H_2O_2 production lies from 0.27 to 0.38 mAcm^{-2} (Figure 3.8). There is only a small change in cell potential at this current density range (Table 3.4). At a current density of 0.38 mAcm^{-2} , the current efficiency reaches 83%. The current efficiency drops at current density higher than 0.45 mAcm^{-2} . Side reaction such as the reduction of O_2 to H_2O or the formation of H_2 may occur at such high current densities [111].

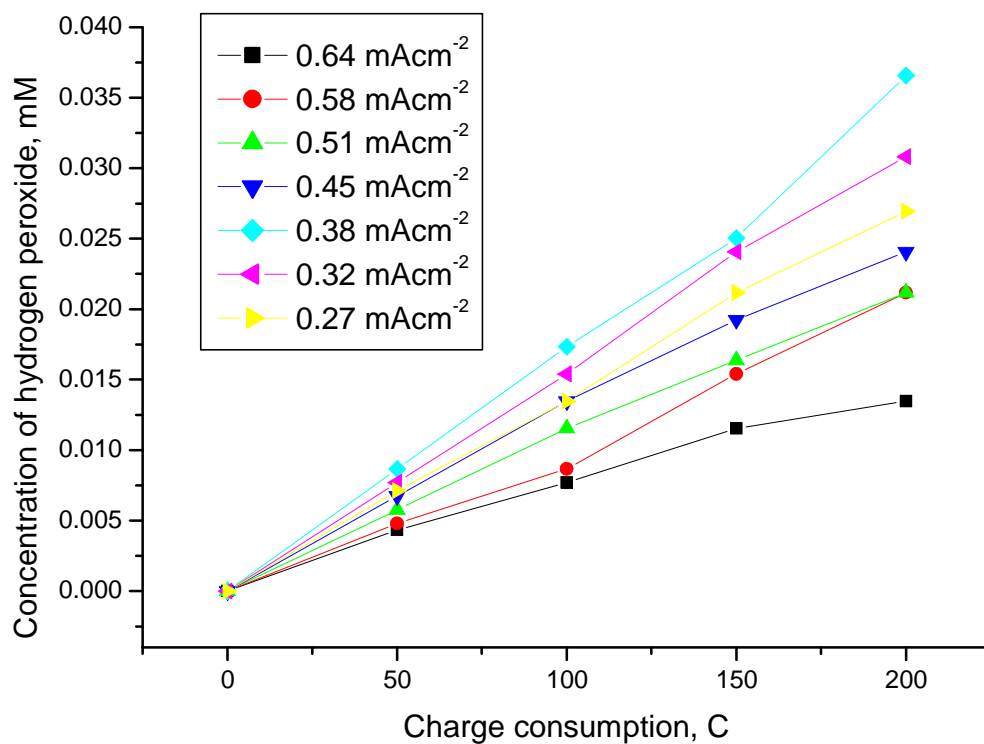


Figure 3.7 Plots of H₂O₂ electrogenerated in [bdmim][BF₄]/NaOH_(aq) mixture at different current density versus the charge consumption. Catholyte: [bdmim][BF₄]/0.006M NaOH_(aq) (4:1 v/v) mixture. Anolyte: [bdmim][BF₄]/4M H₂SO_{4(aq)} (4:1 v/v) mixture.

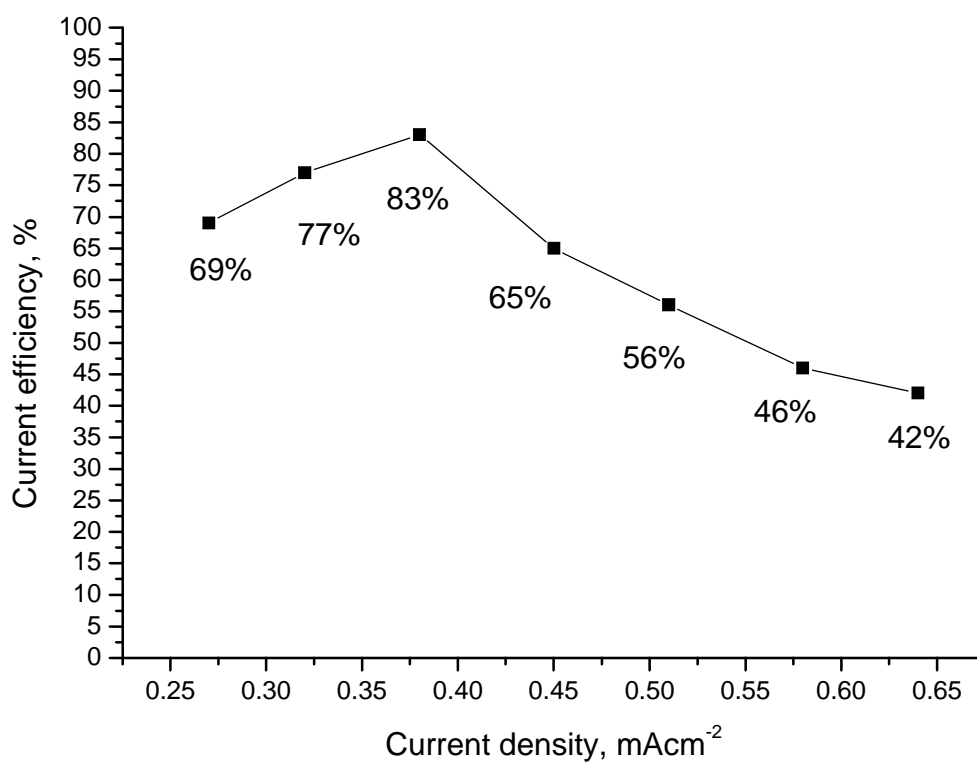


Figure 3.8 The effect of current density on the current efficiency of H₂O₂ electrogeneration in [bdmim][BF₄]/NaOH_(aq) mixture. Catholyte: [bdmim][BF₄]/0.006M NaOH_(aq) mixture. Anolyte: [bdmim][BF₄]/4M H₂SO_{4(aq)} mixture. Cathode surface area: 156 cm².

Table 3.4 Electrogeneration of H_2O_2 in $[\text{bdmim}][\text{BF}_4]/\text{NaOH}_{(\text{aq})}$ mixture at different current densities.

Current density,			
Current, mA	mAcm^{-2}	Cell potential, V	Current efficiency, %
100	0.64	4.83	42
90	0.58	4.27	46
80	0.51	3.75	56
70	0.45	3.31	65
60	0.38	2.94	83
50	0.32	2.69	77
40	0.27	2.55	69

Catholyte: $[\text{bdmim}][\text{BF}_4]/0.006\text{M NaOH}_{(\text{aq})}$ (4:1 v/v). Anolyte: $[\text{bdmim}][\text{BF}_4]/4\text{M H}_2\text{SO}_{4(\text{aq})}$ (4:1 v/v).

Cathode surface area: 156 cm^2 . Volumes of catholyte and anolyte: 25 ml.

3.3.5. Epoxidation of alkenes with hydrogen peroxide electrogenerated in the

[bdmim][BF₄]/NaOH_(aq) mixture

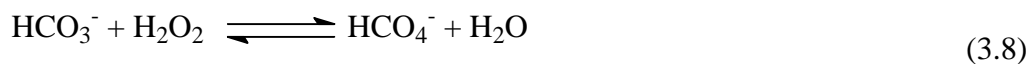
3.3.5.1. *In-situ* generation of peroxymonocarbonate by purging CO_{2(g)} into the

[bdmim][BF₄]/NaOH_(aq)/HO₂⁻ mixture

CO₂ gas is inexpensive and commercially available chemical. In this study, epoxidation of alkenes was achieved by mixing the electrogenerated H₂O₂ in [bdmim][BF₄]/NaOH_(aq) mixture with alkenes and catalytic amount of MnSO₄ (Figure 3.1). The active species (HCO₄⁻) was formed *in-situ* by purging with CO_{2(g)}. Previous investigations have shown that CO₂ is remarkably soluble in imidazolium-based ILs [238, 244]. The high solubility can be attributed to a weak Lewis acid-base interaction between the CO₂ and the anions. CO₂ is an acidic gas that reacts directly with OH⁻ (eq. 3.7) and HO₂⁻ (eq. 3.9) to form HCO₃⁻ and HCO₄⁻. This provides a convenient means to generate HCO₃⁻ and HCO₄⁻ in the IL/NaOH_(aq)/H₂O₂ mixture.

The active species corresponding to the epoxidation is believed to be a peroxymonocarbonate anion, HCO₄⁻, which is generated *in-situ* by the reaction of H₂O₂ with HCO₃⁻ (eq. 3.8) or HO₂⁻ with the CO₂ gas (eq. 3.9) [69]. In our study, we

were able to demonstrate that HCO_4^- existed in equilibrium with HCO_3^- by ^{13}C NMR at the reaction mixture (Figure 3.9). In the absence of CO_2 , no ^{13}C NMR signal was observed in the range from 150 to 170 ppm. When CO_2 was continuously purged into the mixture for 5 minutes, two ^{13}C NMR signals were observed at 158.3 ppm and 160.3 ppm, which correspond to HCO_4^- and HCO_3^- respectively.



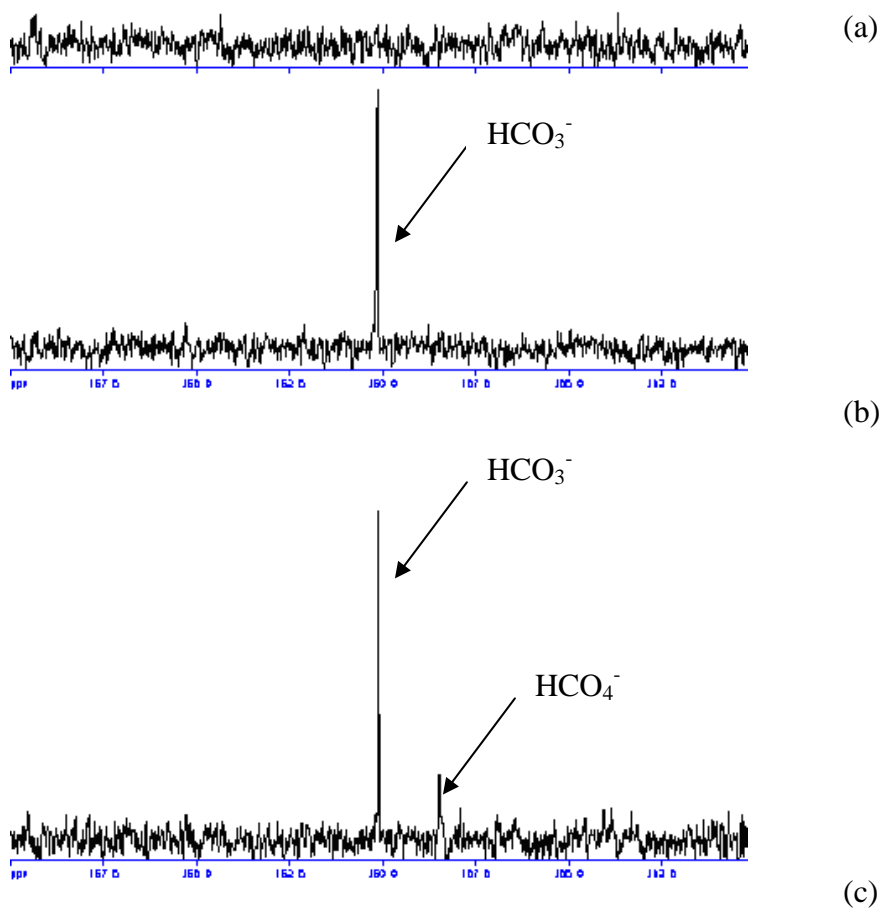
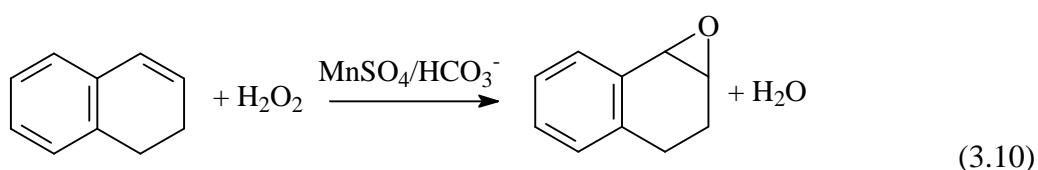


Figure 3.9 ^{13}C NMR spectra. (a) $[\text{bdmim}][\text{BF}_4]/\text{NaOH}_{(\text{aq})}/0.1\text{M HO}_2^-$ mixture, (b) $[\text{bdmim}][\text{BF}_4]/\text{NaOH}_{(\text{aq})}/\text{CO}_{2(\text{g})}$ mixture and (c) $[\text{bdmim}][\text{BF}_4]/\text{NaOH}_{(\text{aq})}/0.1\text{M HO}_2^-/\text{CO}_{2(\text{g})}$ mixture.

3.3.5.2. The effect of catalyst loading and CO₂ sources on the efficiency of alkene epoxidation

In this study, the H₂O₂ electrogeneration in IL was used for on-site epoxidation of alkenes, which is different from the coupling reaction as described in chapter 2. This is because the electrogeneration of H₂O₂ in IL is slower than in water/*tert*-butanol due to the slower mass transfer of O₂. If H₂O₂ is generated in a IL/NaHCO_{3(aq)} mixture, the low pH (<10) and long electrolysis time would cause significant loss of H₂O₂ through diffusion across the nafion membrane to the anode compartment. As a result, H₂O₂ was generated in a IL/NaOH_(aq) mixture (pH>12) in the form of HO₂⁻. In our study, epoxidation was carried out in a separate step with the HCO₄⁻ *in-situ* generated by purging the IL/NaOH_(aq)/HO₂⁻ mixture with CO₂ gas.

1,2-Dihydronaphthalene was used as the standard substrate for optimizing the reaction conditions because of its high solubility and reactivity in the IL/H₂O₂/Mn²⁺/HCO₃⁻ mixture (eq. 3.10) [78].



MnSO₄ is the catalyst for the epoxidation of alkenes with H₂O₂ in the presence of bicarbonate ion. A set of experiments was carried out to test for the optimal loading of Mn²⁺ salt in the IL system. Figure 3.10 indicates that the extent of conversion of the alkene to epoxide was comparable when 0.41-0.74 mol% of MnSO₄ (relative to that of the alkene substrate) was used. When the amount of MnSO₄ was less than 0.08 mol%, the conversion efficiency dropped significantly (Table 3.5).

A comparison of conversion efficiency using different CO₂ sources is shown in Table 3.6. When the reaction temperature was maintained at 5°C, there was no significant difference on the product yield whether dry ice (solid CO₂) (entry 4) or CO₂ gas (entry 2) was used to generate HCO₃⁻ and HCO₄⁻, and good yields of epoxide (>80%) were obtained [245]. By comparison, when the temperature was controlled at 22°C, only moderate yields were obtained in both cases (entries 1 and 3). The use of air (0.04% CO₂) as control indicates that no epoxide product could be obtained (entries 5 and 6).

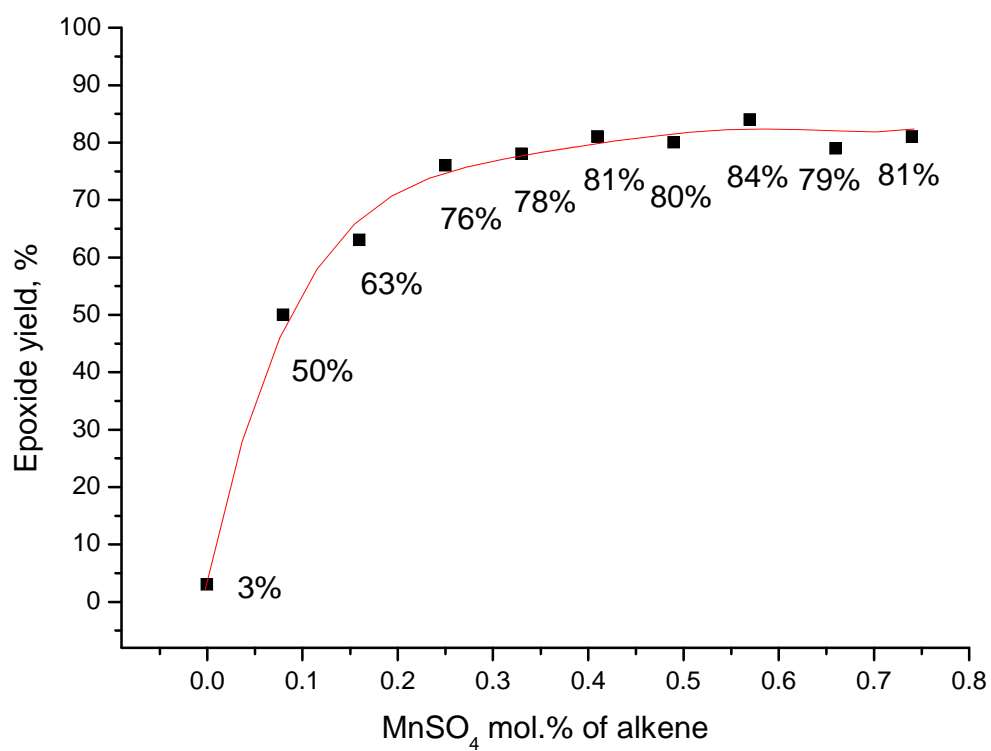


Figure 3.10 The effect of MnSO_4 concentration on the efficiency of epoxide formation. Substrate: 1,2-dihydronaphthalene (0.13 mmol). $[\text{H}_2\text{O}_2]$: 0.08M (electrogenerated in 25 ml $[\text{bdmim}][\text{BF}_4]/\text{NaOH}_{(\text{aq})}$ mixture).

Table 3.5 Optimization of the catalyst/alkene stoichiometry in the epoxidation reaction.

MnSO₄ mol% of alkene	Epoxide yield, %
0	3
0.08	50
0.16	63
0.25	76
0.33	78
0.41	81
0.49	80
0.57	84
0.66	79
0.74	81

Substrate: 1,2-dihydronaphthalene (0.13 mmol). [H₂O₂]: 0.08M (electrogenerated in 25 ml [bdmim][BF₄]/NaOH_(aq) mixture).

Table 3.6 The effect of CO₂ sources and temperature on the epoxide yield.

Entry	CO ₂ source	Reaction temperature, °C	Epoxide yield, %
1	CO ₂ (g)	22	61
2	CO ₂ (g)	5	80
3	CO ₂ (s) (<i>Dry ice</i>)	22	70
4	CO ₂ (s) (<i>Dry ice</i>)	5	83
5	CO ₂ (g) (<i>Air</i>)	22	0
6	CO ₂ (g) (<i>Air</i>)	5	0

Substrate: 1,2-dihydronaphthalene (0.13 mmol). [H₂O₂]: 0.08M (electrogenerated in 25 ml

[bdmim][BF₄]/NaOH_(aq) mixture).

3.3.6. Catalytic epoxidation of alkenes

The alkene was mixed with a solution of MnSO_4 in the reaction flask prior to charge with $\text{CO}_{2(\text{s})}$. When 0.08 M H_2O_2 (15 equiv.) in $[\text{bdmim}][\text{BF}_4]/\text{NaOH}_{(\text{aq})}$ mixture was added all at once, gas bubble was observed and only moderate yield of the epoxide (36%) was obtained. This showed that H_2O_2 decomposition had occurred in the presence of Mn^{2+} [115, 246]. On the other hand, if the mixture was added dropwise over a period of 1 hr at 5°C to minimize the catalytic decomposition of H_2O_2 , the epoxidation reaction proceeded smoothly to give the epoxides in good yield.

The optimal amount of electrogenerated H_2O_2 in the $[\text{bdmim}][\text{BF}_4]/\text{NaOH}_{(\text{aq})}$ mixture was tested. Figure 3.11 indicates that the epoxide yield was the highest when 15-16 equivalents of H_2O_2 were used. This value is comparable to that reported by Chan and co-workers [78] who used 10 equivalents of H_2O_2 for epoxidation with the $\text{HCO}_3^-/\text{Mn}^{2+}/[\text{bmim}][\text{BF}_4]$ system. It should be noted that the concentration of H_2O_2 in that report (11.7 M) is much higher than the concentration of H_2O_2 (~0.08M) prepared by electrogeneration in this study.

After optimizing the catalytic process, a number of lipophilic alkenes were epoxidized

under similar conditions (Table 3.7). In general, good to excellent yields of the epoxides could be obtained. The styryl and cyclic alkenes (entries 1-8) were easily oxidized to give epoxides in good yields. For trans-stilbene (entry 9), 3-octyl-1,2-dimethylimidazolium tetrafluoroborate ([odmim][BF₄]) was used to enhance its solubility of trans-stilbene in the IL mixture and moderate yield was obtained. 1-Octene (entry 10) was not epoxidized, which is in agreement with the fact that the Mn²⁺/HCO₃⁻/H₂O₂ system is not effective in the epoxidation of aliphatic terminal alkenes [160].

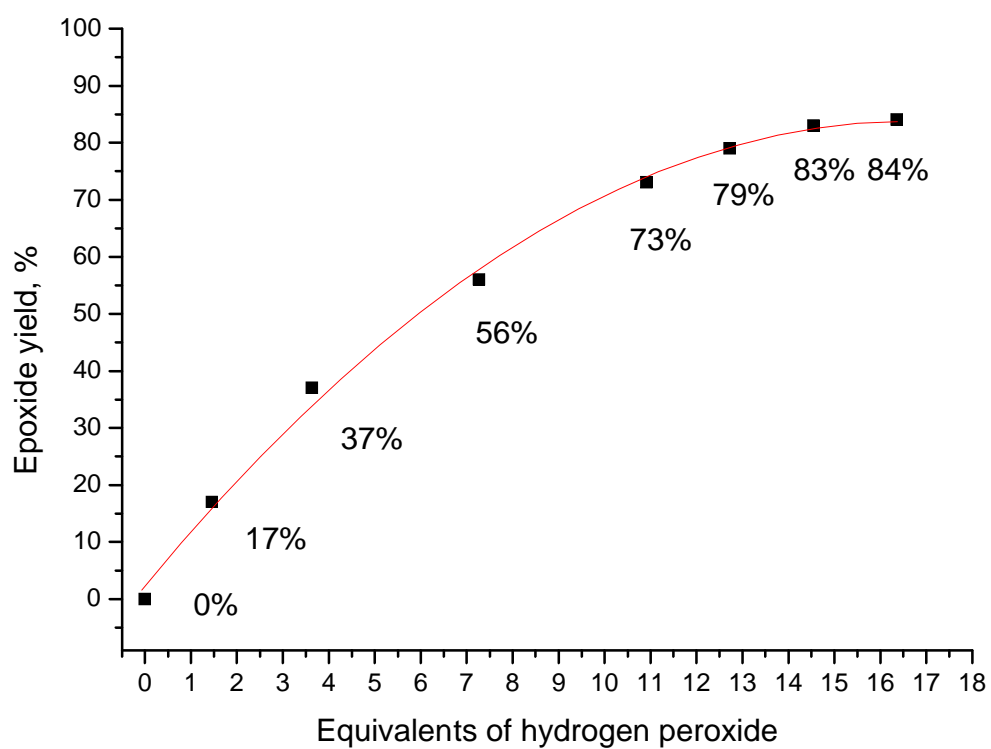
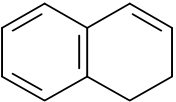
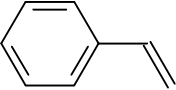
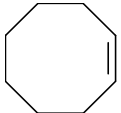
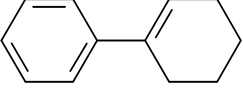
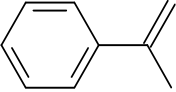
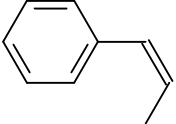
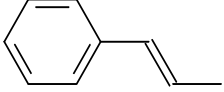
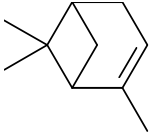
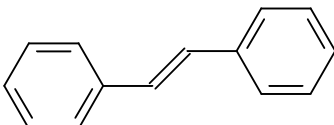



Figure 3.11 Optimization of the alkene/H₂O₂ stoichiometry. Substrate: 1,2-dihydronaphthalene (0.13 mmol). MnSO₄: 0.41 mol%.

Table 3.7 Epoxidation of various lipophilic alkenes.

Entry	Substrate	Reaction		Epoxide yield,
		Time, hr	Conversion, %	%
1	1,2-dihydronaphthalene 	4	>99	83
2	Styrene 	4	>99	84
3	Cyclooctene 	4	>99	80
4	1-phenyl-1-cyclohexene 	5	>99	90
5	α -methyl styrene 	5	95	83
6	cis- β -methyl styrene 	5	87	76
7	trans- β -methyl styrene 	5	81	71
8	α -pinene 	5	75	62

9	trans-stilbene ^a	5	44	42
				
10	1-octene	5	0	0
				

Substrate: 0.13 mmol. MnSO₄: 0.41 mol%. [H₂O₂]: 0.08 M (electrogenerated in 25 ml [bdmim][BF₄]/NaOH_(aq) mixture). Yields were calculated on the basis of converted alkenes and determined by GC-MS versus an internal standard. ^a[odmim][BF₄] was used in place of [bdmim][BF₄].

3.3.7. Recycling of the ionic liquid

Because the IL ([bdmim][BF₄]) is likely to be the most expensive component of the reaction system, it is important to demonstrate that the IL can be recovered and reused.

After product extraction, water, MnSO₄ and NaHCO₃ were retained in the yellowish ionic liquid mixture. Attempts to use the crude ionic liquid mixture for H₂O₂ electrogeneration indicated that the current efficiency dropped to 62% (Figure 3.12).

Presumably, the Mn²⁺ salt interfered with the H₂O₂ production through catalytic decomposition. Attempts were therefore made to remove the Mn²⁺ before the IL mixture was re-used for H₂O₂ electrogeneration.

Literature report indicates that ILs can be purified through extraction and separation into different phases [247]. In this study, 1 M Na₂CO_{3(aq)} was used for extraction and purification of the IL mixture (Figure 3.13). It was found that two immiscible phases were formed without the assistance of any pressurized equipment. One liquid phase was rich in IL and water, while the other was mainly water, Na₂CO₃ and Mn²⁺. This interesting biphasic behavior allows us to separate most MnSO₄ from the IL mixture in a convenient manner.

Attempts to use 1 M or saturated $\text{NaOH}_{(\text{aq})}$ for extraction of MnSO_4 from the IL mixture indicated that it is impossible to form two clear separate phases in the extraction. This is probably because of the higher solubility of NaOH in IL/water (4:1 v/v) mixture (the solubility of Na_2CO_3 and NaOH in IL/water (4:1 v/v) mixture are 0.016 M and 0.044 M respectively).

The IL mixture was extracted with 1M $\text{Na}_2\text{CO}_{3(\text{aq})}$ solution (2x15 ml). After each extraction, 85-90% of the $[\text{bdmim}][\text{BF}_4]$ was recovered and the aqueous phases were combined for further recycling. In the IL phase, the water content was always less than 20% by volume. After purification, an appropriate amount of $[\text{bdmim}][\text{BF}_4]$ or/and water was added to the mixture to adjust to the optimal IL: H_2O 8:2 v/v ratio and volume (25 ml) for H_2O_2 electrogeneration. The amount of water in the IL mixture was measured according to the density method developed by Chan and co-workers. The calibration curve for H_2O content determination is shown in Figure 3.14. As noted above, 10-15% of IL was retained in the aqueous phase. Further recovery of IL could be achieved by removing the water under vacuum and further extraction with dichloromethane.

Prior to H_2O_2 electrogeneration, the alkalinity of the recovered IL/water mixture was

adjusted to an optimal apparent pH value (~pH 9.4) by adding NaOH. The step is important because it provides a sufficiently alkaline media for effective H₂O₂ electrogeneration.

The results of epoxidation with the recovered IL/H₂O₂ mixture are summarized in Table 3.8. It can be seen that the IL mixture can be recycled for a number of times without any diminution in the epoxide yield.

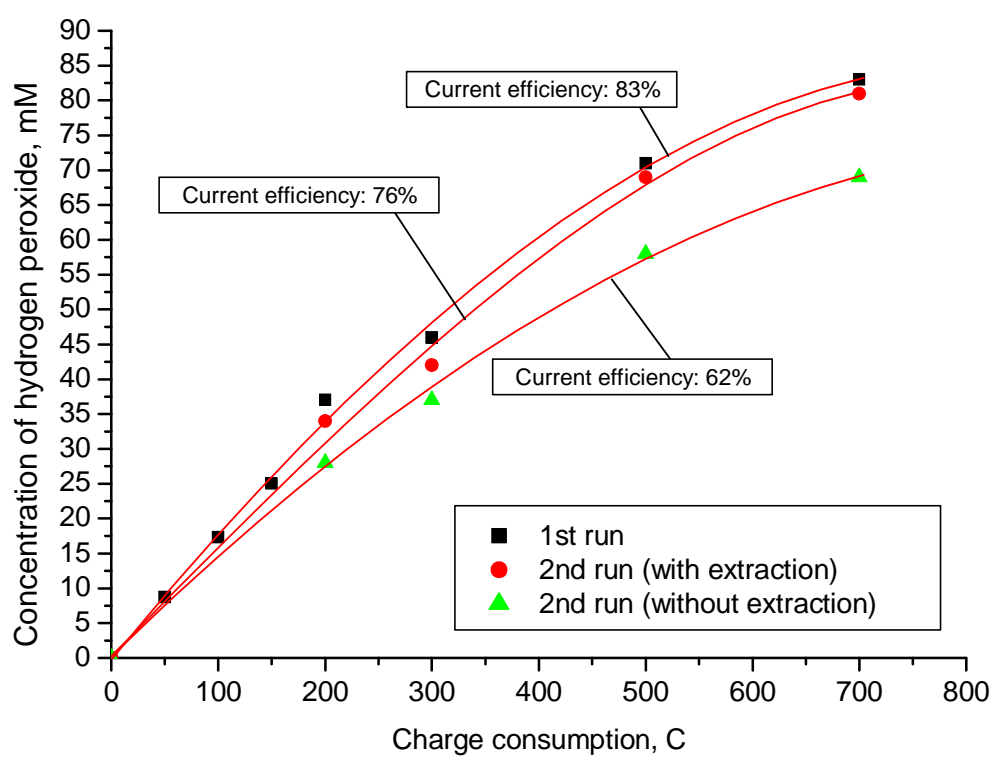


Figure 3.12 Effect of ionic liquid purity on H_2O_2 electrogeneration.

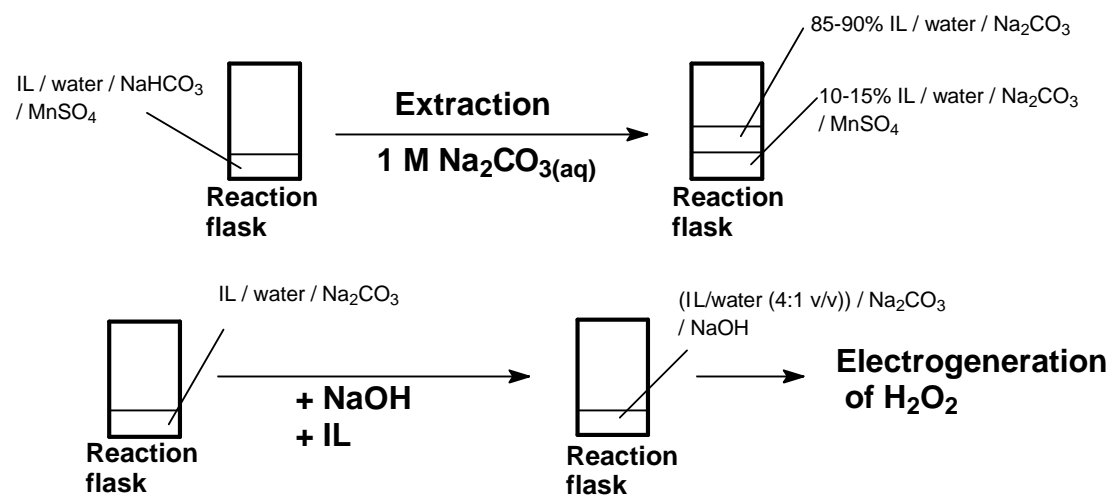


Figure 3.13 Ionic liquid purification before re-usage for H_2O_2 electrogeneration.

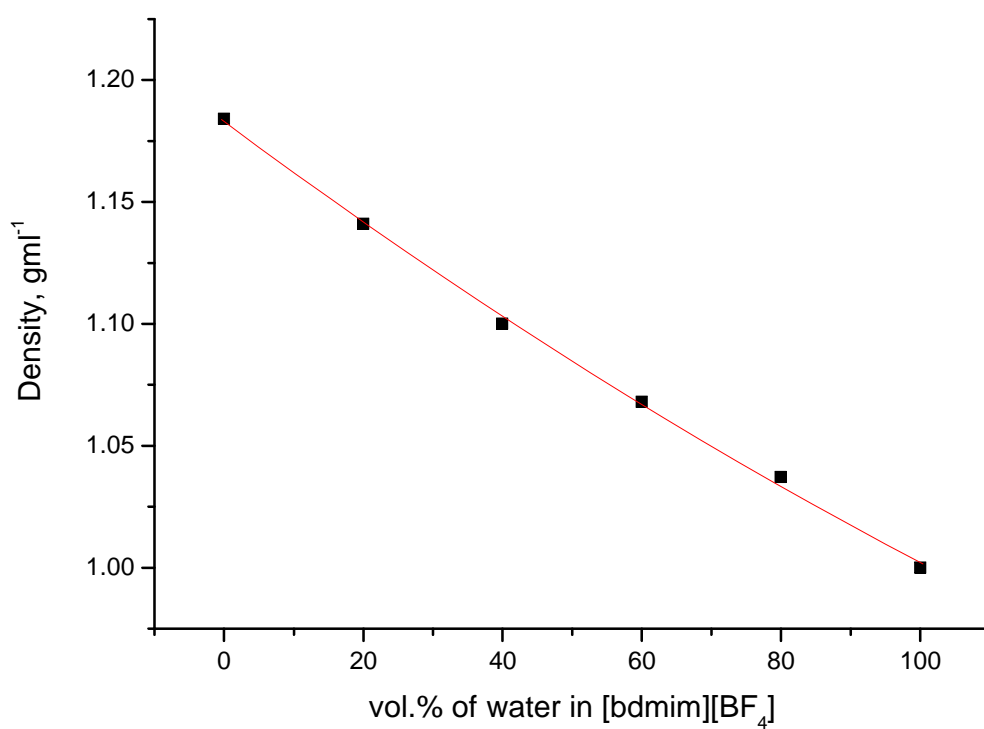


Figure 3.14 A plot of the density of [bdmim][BF₄]/Na₂CO_{3(aq)} mixture versus the volume ratio of water to [bdmim][BF₄].

Table 3.8 Recovery and reuse of [bdmim][BF₄] for 1,2-dihydronaphthalene epoxidation.

Cycle	1	2	3	4	5
Epoxide yield, %	83	86	87	84	85

Substrate: 0.13 mmol. [H₂O₂]: 0.08 M (electrogenerated in 25 ml [bdmim][BF₄]/NaOH_(aq) mixture in each cycle). MnSO₄: 0.41 mol%. Yields were calculated on the basis of converted alkenes and determined by GC-MS versus an internal standard.

3.4. Conclusion

The electrogeneration of H_2O_2 in ionic liquid ($[\text{bdmim}][\text{BF}_4]$) for epoxidation has been demonstrated. By purging CO_2 gas into the $\text{H}_2\text{O}_2/[\text{bdmim}][\text{BF}_4]/\text{NaOH}_{(\text{aq})}$ mixture, the active peroxymonocarbonate (HCO_4^-) can be generated *in-situ*, and a wide range of alkenes can be epoxidized with a simple Mn^{2+} catalyst. The ionic liquid can be recovered and reused without significant diminution in the current efficiency of H_2O_2 generation and epoxide yield.

Chapter 4

Manganese-catalyzed Epoxidation of Terminal Aliphatic Alkenes with Peracetic Acid

4.1. Introduction

Peracetic acid is widely used as an epoxidizing agent in organic synthesis [248]. It has many advantages over the peroxides including versatility, specificity and ease of preparation. The by-product acetic acid is easy to be isolated by simple extraction or vacuum evaporation. Under uncatalyzed reaction condition, peracetic acid is regarded as a strong electrophile to attack the C-C double bond of alkenes. For the electron-rich alkenes (such as di-, tri- and tetra-substituted alkenes), it gives high yields of epoxides efficiently. However, for relatively electron-deficient alkenes (such as terminal aliphatic alkenes), elevated reaction temperature and extended reaction time are usually required which significantly reduce the selectivity of the reaction [22].

Metal-catalyzed epoxidation can reduce these limitations by enhancing the selectivity and the rate of epoxidation, and lowering the reaction temperature for such alkenes [19, 22, 212, 213, 215, 249-252]. Among these, the work reported by Murphy et al. [212, 215] is of particular interest that these terminal alkenes can be epoxidized by peracetic acid with the monomeric manganese(II) complexes, $[\text{Mn}^{\text{II}}(\text{R},\text{R-mcp})](\text{CF}_3\text{SO}_3)_2$ and $[\text{Mn}^{\text{II}}(\text{mep})](\text{CF}_3\text{SO}_3)_2$ [mep = N,N'-dimethyl-N,N'-bis(2-pyridylmethyl)-ethane-1,2-diamine; R.,R-mcp =

N,N'-dimethyl-N,N'-bis(2-pyridylmethyl)-(R,R)-(+)-cyclohexane-1,2-diamine] or the dimeric iron(III) complex, $[(\text{Fe}^{\text{III}}(\text{phen})_2)_2(\mu\text{-O})(\text{H}_2\text{O})_2](\text{ClO}_4)_4$ [phen = phenanthroline] as catalysts. However, such catalysts are not easy to prepare, and some systems only work at low temperature (0°C) because of catalyst instability.

As mentioned in Chapter 2 and 3, the $\text{H}_2\text{O}_2/\text{Mn}^{2+}/\text{HCO}_3^-$ system, though simple and environmentally benign, is ineffective in the epoxidation of terminal aliphatic alkenes.

In this chapter, a modified system based on Mn^{2+} /peracetic acid was developed for the epoxidation of terminal aliphatic alkenes at ambient temperature. The effect of solvents, additives and peroxides on the reaction will be discussed.

4.2. Experimental Section

4.2.1. Materials

The solvents used were of analytical reagent (A.R.) grade and were purified according to conventional procedures [253]. All alkenes and epoxides were obtained from either Aldrich Co. or Acros Organic and were used as received unless otherwise noted. 1,2,7,8-Diepoxyoctane, 1,2,8,9-diepoxy-nonene, 1,2,9,10-diepoxydecane, 1-cyclohexyl-2,3-epoxypropane and epoxyethylcyclohexane were synthesized by literature reported methods [254, 255]. The metal salts, peracetic acid (32 wt.% in dilute acetic acid), H₂O₂ (35 wt.% solution in water), *tert*-butyl hydroperoxide (70 wt.% in water), cumene hydroperoxide (88 % in cumene) and *meta*-chloroperoxybenzoic acid (purity ~77 %) were purchased from Aldrich Co. Double deionized water was purified by passing through an ion-exchange resin purification train (Millipore).

4.2.2. Synthesis

1,2,7,8-Diepoxyoctane

3-Chloroperoxybenzoic acid (77 wt.%, 14.8 g, 66 mmol) and K_2CO_3 (2.2 g, 16 mmol) were added in small portions to 1,7-octadiene (2.01 g, 18 mmol) in dichloromethane (60 ml) at 0°C for 2 h and then stirred at room temperature for another 7 hr. After filtration, the filtrate was collected and concentrated under vacuum. The crude product was purified on a silica column using dichloromethane as eluent to give a colorless liquid. Yield: 1.4 g (53%). 1H NMR ($CDCl_3$, δ ppm): 2.84 (m, 2H), 2.68 (dd, 2H), 2.39 (dd, 2H), 1.52-1.37 (m, 8H).

1,2,8,9-Diepoxyononene

Procedures similar to the above were employed except that 1,8-nonadiene (2.23 g, 18 mmol) was used. Yield: 1.29 g (46%). 1H NMR ($CDCl_3$, δ ppm): 2.85 (m, 2H), 2.69 (dd, 2H), 2.41 (dd, 2H), 1.52-1.32 (m, 10H).

1,2,9,10-Diepoxydecane

Procedures similar to the above were employed except that 1,9-decadiene (2.48 g, 18 mmol) was used. Yield: 1.32 g (43%). 1H NMR ($CDCl_3$, δ ppm): 2.86 (m, 2H), 2.71 (dd, 2H), 2.41 (dd, 2H), 1.52-1.32 (m, 12H).

1-Cyclohexyl-2,3-epoxypropane

Procedures similar to the above were employed except that 3-chloroperoxybenzoic acid (77 wt.%, 7.4 g, 33 mmol), K₂CO₃ (1.1 g, 8 mmol) and allylcyclohexene (2.23 g, 18 mmol) were used. Yield: 1.46 g (58%). ¹H NMR (CDCl₃, δ ppm): 2.92 (m, 1H), 2.73 (dd, 1H), 2.41 (dd, 1H), 1.75-1.66 (m, 6H), 1.42-1.22 (m, 5H), 1.12-0.83 (m, 2H).

Epoxyethylcyclohexane

Procedures similar to the above were employed except that 3-chloroperoxybenzoic acid (77 wt.%, 7.4 g, 33 mmol), K₂CO₃ (1.1 g, 8 mmol) and vinylcyclohexene (2.23 g, 18 mmol) were used. Yield: 1.18 g (52%). ¹H NMR (CDCl₃, δ ppm): 2.69 (m, 2H), 2.49 (dd, 1H), 1.86 (d, 1H), 1.73-1.63 (m, 4H), 1.22-1.07 (m, 6H).

4.2.3. Instrumentation

A Hewlett-Packard 8900 GC-MS equipped with ECTM-1 or ECTM-WAX columns (Alltech Associate, Inc.) was used for yield determination and identification of the epoxidized products. ¹H and ¹³C NMR spectra were recorded on a Bruker DPX-400MHz NMR spectrometer. Tetradecane was used as an internal standard for GC-MS quantitative measurement.

EPR spectra (77K) were recorded at the X-band (9.4 GHz microwave frequency), 2mW power and 25G modulation amplitude on a Bruker EMX EPR Spectrometer. Samples were placed in a 5mm quartz tube and frozen in liquid N₂ before spectral measurement.

4.2.4. Reaction conditions for epoxidation

Solvent (2.4 ml), alkene (0.5 mmol), the metal catalyst (100 µl, 0.02 M) and additive (300 µl, 0.5 M) were added to a 5 ml round-bottle flask. The flask was sealed by a rubber septum and allowed to stand in a water bath with controlled temperature. Peracetic acid (32 wt.%) was added dropwise via a syringe over 1 min. The resulting mixture was then stirred for another 29 min. A 300 µl portion of the mixture was withdrawn and diluted with pentane to 10 ml. After mixing with internal standard (tetradecane, 100 µl of a 0.156 M solution in pentane), the sample was analyzed by GC-MS.

4.2.5. Gram-scale preparation of epoxide

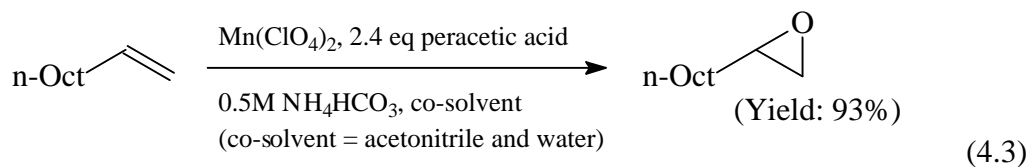
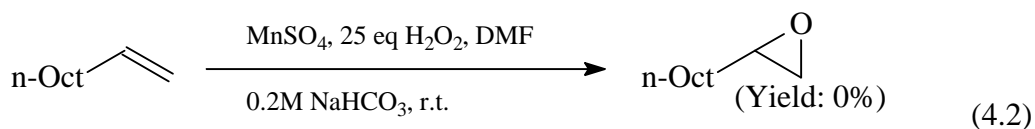
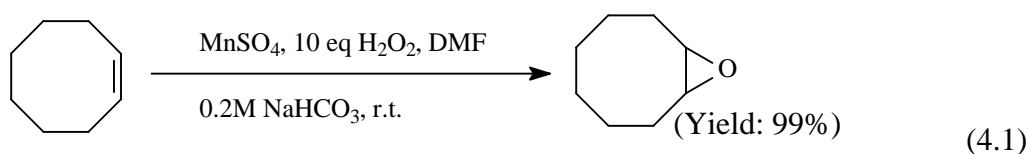
Alkene (7 mmol), acetonitrile (34 ml), 0.5 M NH₄HCO_{3(aq)} (4.2 ml), 0.02 M

$\text{Mn}(\text{ClO}_4)_2$ (1.4 ml) were placed in a 100 ml round-bottle flask equipped with a magnetic stirrer. The flask was sealed by a rubber septum before 32 wt.% peracetic acid (3.4 ml) was added dropwise via a syringe over 5 minutes. The mixture was then stirred for another 45 min till the reaction was complete. The product was extracted by pentane (3x40 ml), washed with brine, and dried over sodium sulfate. The solvent was removed under vacuum, and the crude product was purified via a silica gel column to give a colourless liquid. GC-MS and ^1H NMR were used to characterize the epoxide products.

4.3. Results and Discussion

4.3.1. Manganese-mediated epoxidation of alkenes with peracetic acid

The $\text{H}_2\text{O}_2/\text{Mn}^{2+}/\text{HCO}_3^-$ system described in Chapters 2 and 3 is capable of epoxidizing di-, tri-, tetra-substituted alkenes such as cyclooctene (eq. 4.1), but not terminal aliphatic alkenes such as 1-decene (eq. 4.2). Attempts to modify the reaction conditions by changing the catalysts, solvents and additives all failed. However, when replacing H_2O_2 with peracids, 1,2-epoxydecane was obtained in good yield with high selectivity (eq. 4.3).

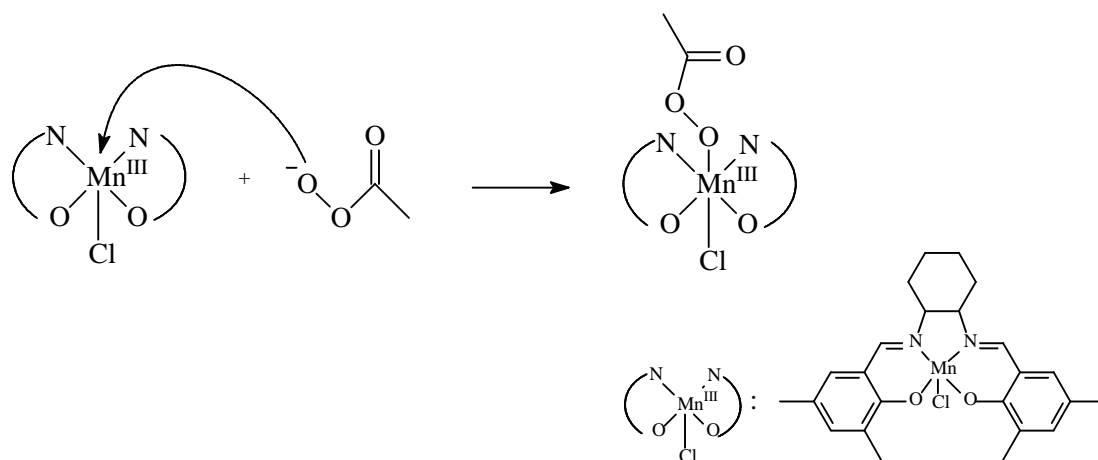


(where n-oct = n-octyl)

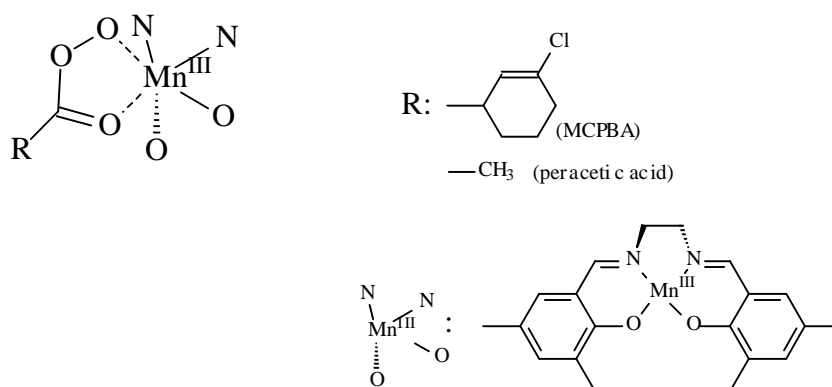
Our experiments indicated that in the presence of catalytic amount of manganese(2+) salt, the desired epoxidation reaction only occurred with peracetic acid or meta-chloroperoxybenzoic acid (MCPBA) (Figure 4.1). 1-Decene was epoxidized to give 93% yields when peracetic acid was used as the oxidant. Under the same conditions, MCPBA was not an effective oxidant and only moderate yield of 1,2-epoxydecane (47%) was obtained. The low solubility of MCPBA in acetonitrile can be a problem for this system. Moreover, MCPBA is not an environmentally friendly oxidant because of its chlorinated nature. Attempts to epoxidize 1-decene with peroxides such as cumene hydroperoxide, *tert*-butyl hydroperoxide and H₂O₂ with Mn²⁺ as catalyst all failed.

Catalytic epoxidation of alkenes with peracids using manganese-based catalysts has been extensively studied. Mechanistic studies using ¹H NMR, EPR and stopped-flow spectroscopy suggest that the peroxy oxygen transfers to the manganese complex via nucleophilic attack as shown in Scheme 4.1 [256-258]. Before transformation to a high-valent manganese-oxo species, density function study shows that the manganese acylperoxo complex (Scheme 4.2) is a possible intermediate in the course of reaction [259-261].

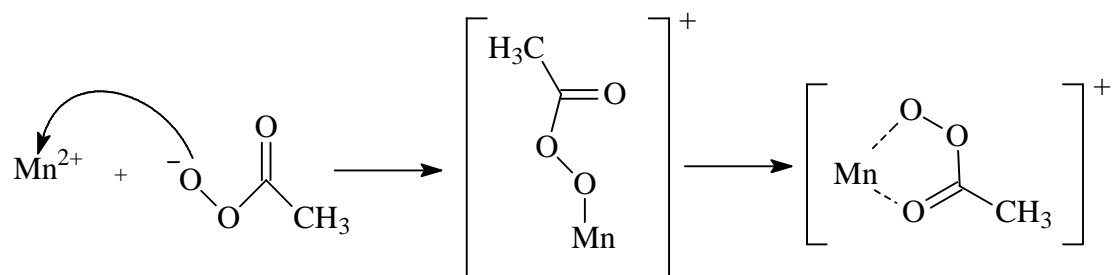
In our catalytic system, simple Mn(2+) salts were found to be good catalysts with higher selectivity for epoxidation. Similar to the mechanism with manganese complexes, it is believed that Mn(2+) binds initially to peracetate/perbenzoate to give a Mn(II) complex (Scheme 4.3), which then transforms to other high oxidation state active species for the subsequent oxidation [260-262].



Scheme 4.1



Scheme 4.2



Scheme 4.3

Figure 4.2 and Table 4.1 summarize the optimal loading of peracetic acid required in the catalytic epoxidation. When the Mn(2+) salt was combined with 2.4 equivalents of peracetic acid, efficient and rapid (< 30min) epoxidation occurred and 93% yield of 1,2-epoxydecane was obtained. The yield was far from satisfactory when less than 1.4 equivalents of peracetic acid was used, even after prolonged reaction time up to an hour.

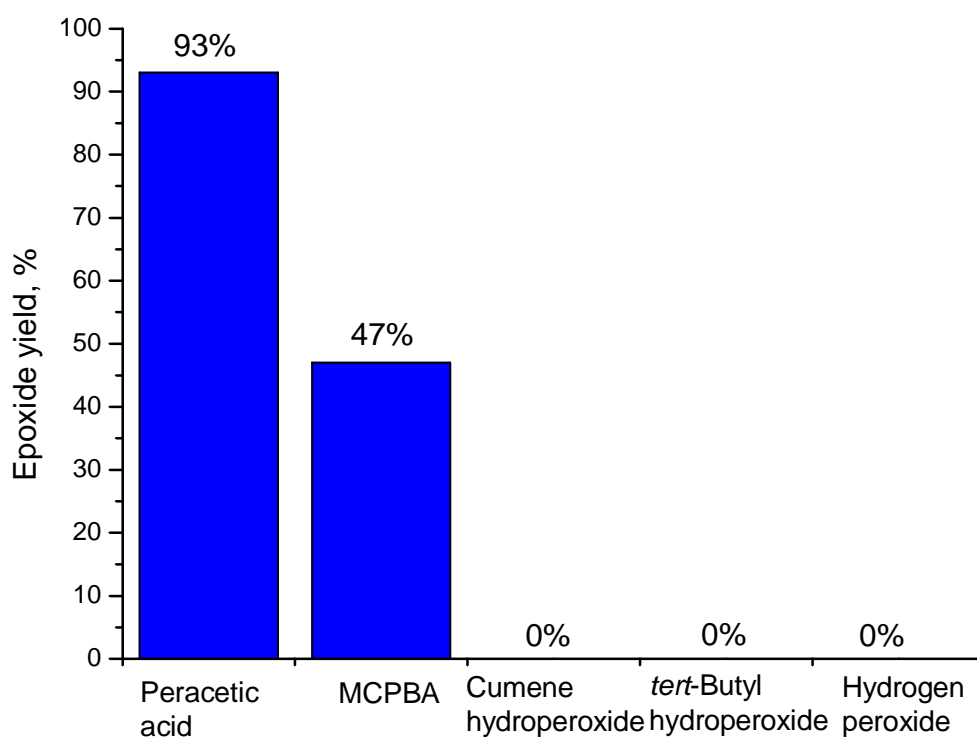


Figure 4.1 Epoxide yields with different oxidants. Solvent: acetonitrile (2.4 ml).

Additive: 0.5M $\text{NH}_4\text{HCO}_3(\text{aq})$ (300 μl). Catalyst: $\text{Mn}(\text{ClO}_4)_2$ (0.32

mol%). Substrate: 1-decene (0.5 mmol, 97 μl). Oxidants: 2.4

equivalents. Reaction time: 30 min.

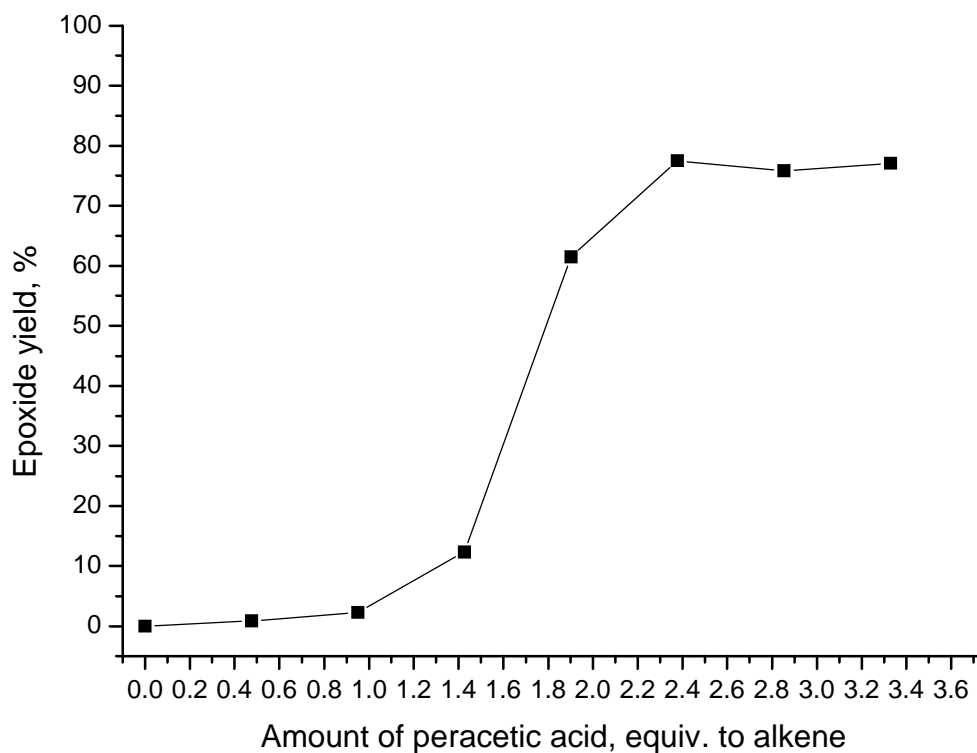


Figure 4.2 Optimization of the loading of peracetic acid for the epoxidation reaction. Solvent: acetonitrile (2.4 ml). Additive: 0.5 M $\text{NH}_4\text{HCO}_3(\text{aq})$ (300 μl). Catalyst: $\text{Mn}(\text{ClO}_4)_2$ (0.32 mol%). Substrate: 1-decene (0.5 mmol, 97 μl). Reaction time: 15 min.

Table 4.1 The effect of oxidant loading in the epoxidation reaction.

Oxidant	Amount, μl	Time, min	Epoxide yield,
	(Equiv.)		%
Hydrogen peroxide	106(2.4)	30	0
<i>tert</i> -butyl hydroperoxide	166(2.4)	30	0
Cumene hydroperoxide	200(2.4)	30	0
MCPBA	0.279g (2.4)	30	47
Peracetic acid	250(2.4)	30	93
Peracetic acid	0(0)	15	0
Peracetic acid	50(0.5)	15	1
Peracetic acid	100(1)	15	2
Peracetic acid	150(1.4)	15	12
Peracetic acid	200(1.9)	15	61
Peracetic acid	250(2.4)	15	77
Peracetic acid	300(2.9)	15	76
Peracetic acid	350(3.3)	15	77

Solvent: acetonitrile (2.4 ml). Additive: 0.5 M $\text{NH}_4\text{HCO}_3(\text{aq})$ (300 μl). Catalyst: $\text{Mn}(\text{ClO}_4)_2$ (0.32 mol%).

Substrate: 1-decene (05 mmol, 97 μl).

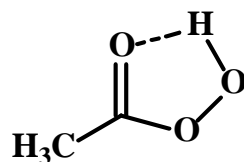
4.3.2. The role of additives in the reaction

A set of experiments has been carried out to study the significance and role of additives in the catalytic reaction (Figure 4.3 and Table 4.2). With the alkaline additives, 1-decene was efficiently epoxidized. On the other hand, no conversion was observed when acidic additives such as acetic acid, sodium dihydrogen phosphate and sodium hexametaphosphate were added to the mixture. These experimental results suggest that controlling the pH of the reaction is important.

Upon titration of the reaction mixture with NH_4HCO_3 , three inflection points could be observed at pH 2.6, 6.2 and 10.6 (Figure 4.5) which correspond to the titration endpoints of H_2SO_4 (stabilizer), acetic acid and peracetic acid respectively. Figure 4.6 is the first derivative of the titration curve, which shows the inflection points more clearly [263]. From the plot, the concentration of H_2SO_4 in peracetic acid was determined to be 0.2 M (or 0.05mmol in 250 μl peracetic acid).

In the catalysis, the concentration of NH_4HCO_3 is about 0.5M and the amount used is 0.15mmol (300 μl) (Figure 4.4), which is sufficient to neutralize all H_2SO_4 in the reaction mixture. The H_2SO_4 stabilizes peracetic acid through intramolecular

hydrogen bonding (Scheme 4.4). When all the H_2SO_4 has been neutralized, the peracetic acid is activated and the peroxy oxygen can be transferred to the catalyst more easily through complexation with Mn^{2+} .



Scheme 4.4

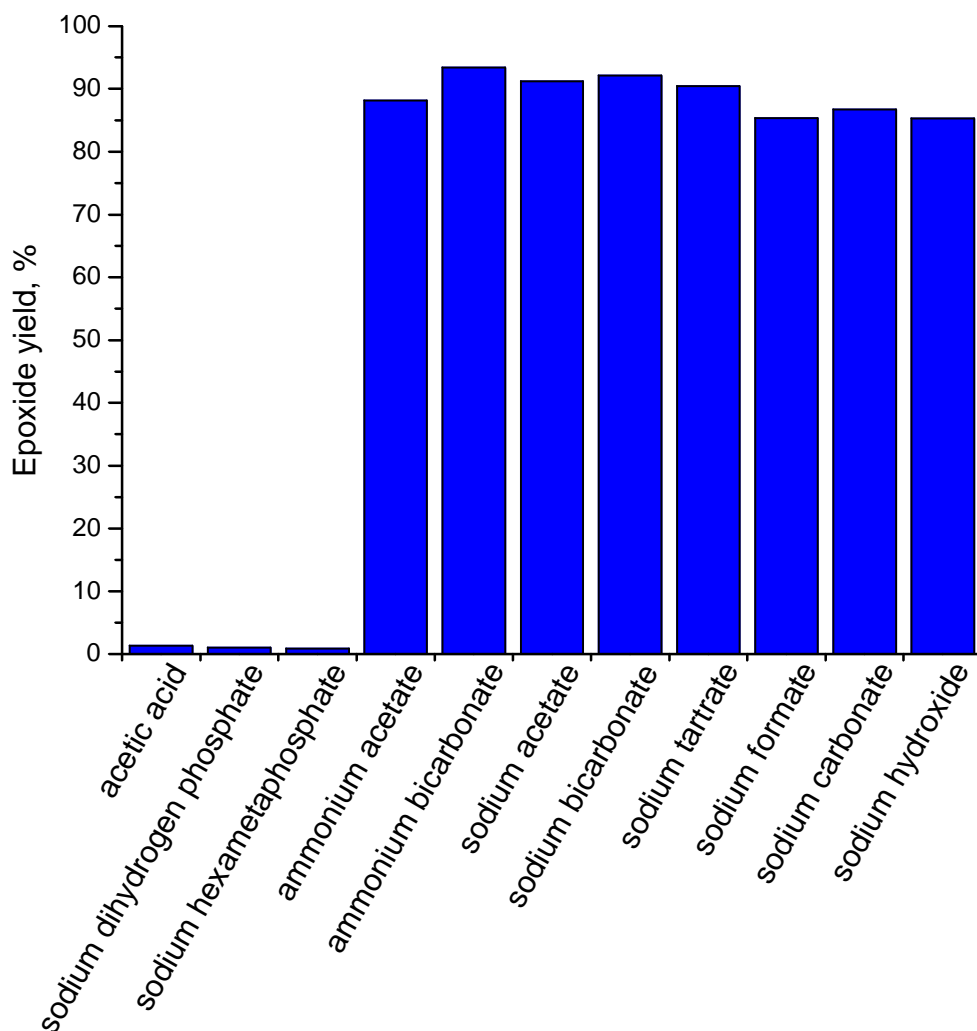


Figure 4.3 Screening of additives for the epoxidation reaction. Solvent: acetonitrile (2.4 ml). Additive: 300 μ l (0.5 M). Catalyst: $\text{Mn}(\text{ClO}_4)_2$ (0.32 mol%). Substrate: 1-decene (0.5 mmol, 97 μ l). Oxidant: 32 wt.% peracetic acid (250 μ l). Reaction time: 30 min.

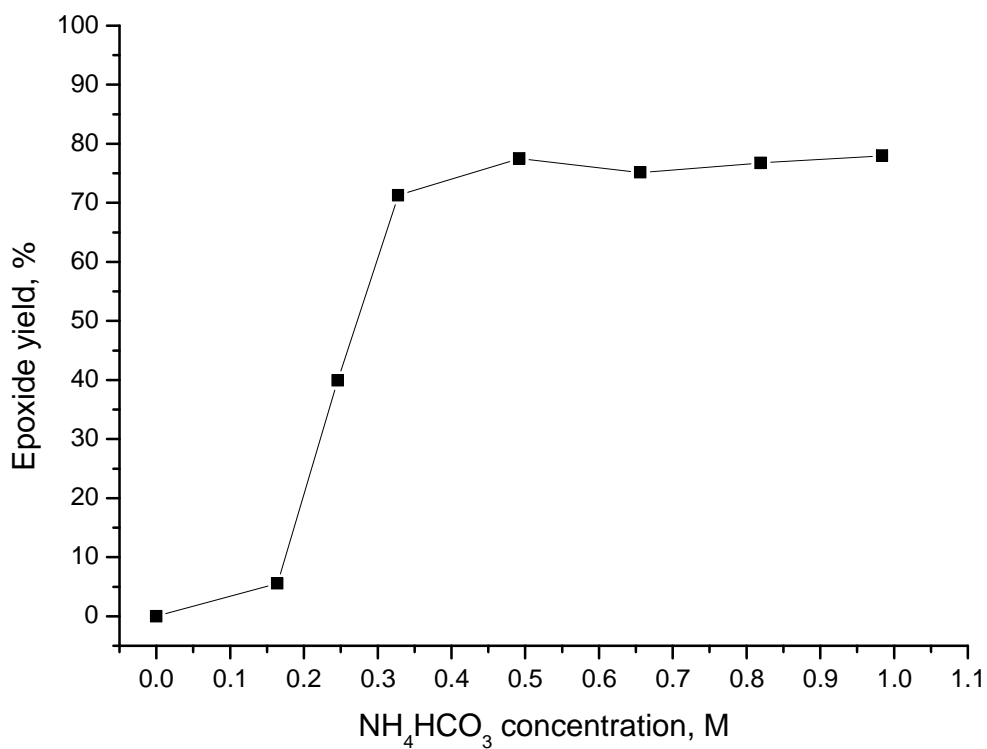


Figure 4.4 Optimization of $\text{NH}_4\text{HCO}_{3(\text{aq})}$ loading for the epoxidation reaction.

Solvent: acetonitrile (2.4 ml). Additive: $\text{NH}_4\text{HCO}_{3(\text{aq})}$ (300 μl).

Catalyst: $\text{Mn}(\text{ClO}_4)_2$ (0.32mol%). Substrate: 1-decene (0.5 mmol, 97

μl). Oxidant: 32 wt.% peracetic acid (250 μl). Reaction time: 15 min.

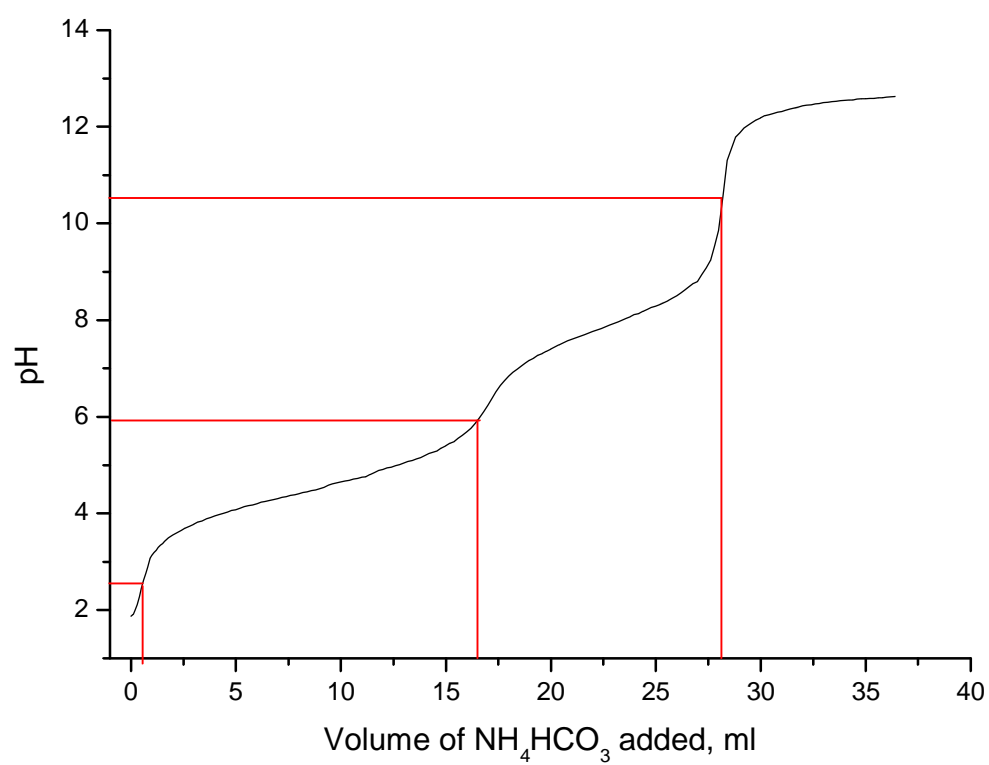


Figure 4.5 Titration curve - 0.5 M NH₄HCO_{3(aq)} against 32 wt.% of peracetic acid (500 µl).

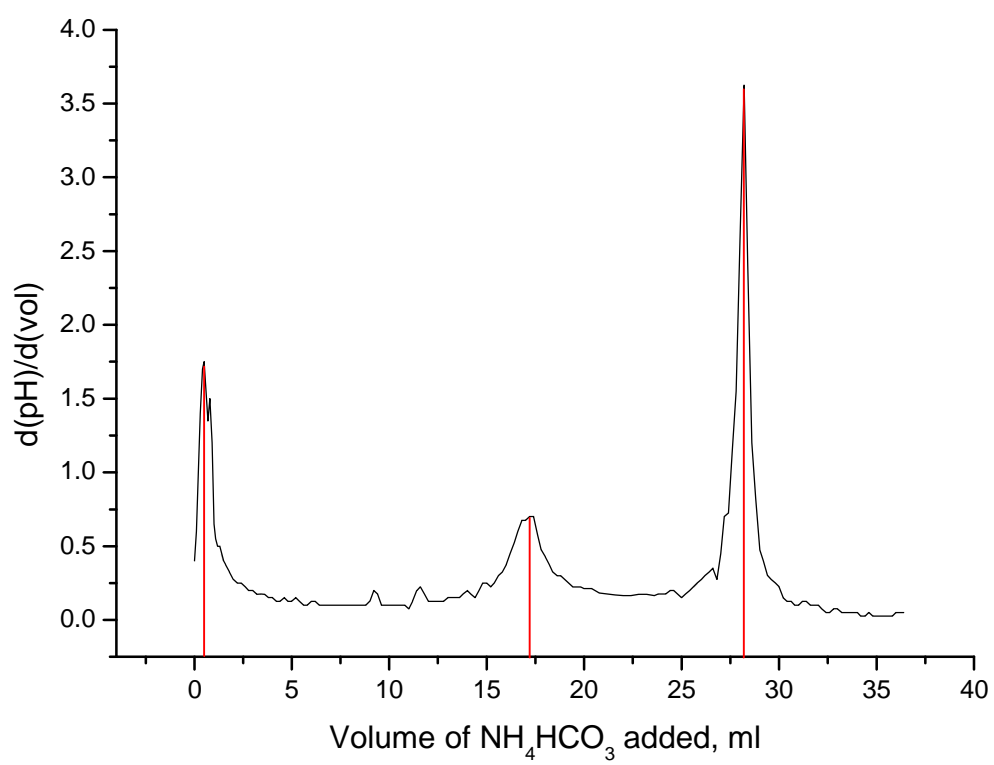


Figure 4.6 First derivative plot of the titration curve in Figure 4.5.

Table 4.2 The effect of additive loading on the epoxide yield.

Additive	Concentration,		Time, min	Epoxide
	M	pH		yield, %
Acetic acid	0.5	2.7	30	0
Sodium dihydrogen phosphate	0.5	3.8	30	0
Sodium hexametaphosphate	0.5	5.5	30	0
Ammonium acetate	0.5	7.2	30	88
Ammonium bicarbonate	0.5	7.7	30	93
Sodium acetate	0.5	7.9	30	91
Sodium bicarbonate	0.5	8.1	30	92
Sodium tartrate	0.5	8.5	30	90
Sodium formate	0.5	9.2	30	85
Sodium carbonate	0.5	11.6	30	87
Sodium hydroxide	0.5	13.4	30	85
Ammonium bicarbonate	0	-	15	0
Ammonium bicarbonate	0.16	-	15	5
Ammonium bicarbonate	0.25	-	15	40
Ammonium bicarbonate	0.33	-	15	71
Ammonium bicarbonate	0.5	-	15	77
Ammonium bicarbonate	0.66	-	15	75

Ammonium bicarbonate	0.82	-	15	77
Ammonium bicarbonate	1	-	15	78

Solvent: acetonitrile (2.4 ml). Catalyst: $\text{Mn}(\text{ClO}_4)_2$ (0.32 mol%). Substrate: 1-decene (0.5 mmol, 97 μl).

Oxidant: 32 wt.% of peracetic acid (250 μl). Volume of additive: 300 μl .

4.3.3. The effect of metal catalysts

Metal ions play a crucial role as catalysts in the epoxidation reaction. Screening of transition metal catalysts has been carried out to search for the best candidates for epoxidation (Figure 4.7). Most metal salts such as Sc(3+), Ti(4+), Cr(3+), Fe(2+), Co(2+), Ni(2+), Cu(2+) and Zn(2+) give poor epoxide yields that are only slightly higher than the uncatalyzed reaction. V(5+) gives aldehyde (5% yield) rather than epoxide as the sole product. No significant difference in the yield of 1,2-epoxydecane was observed with Mn(ClO₄)₂ and Mn(OAc)₃ which give the best epoxidation of results of 93% and 91% respectively (Table 4.3).

EPR spectroscopy was used to probe the nature of the active Mn species in the epoxidation reaction (Figure 4.8a-d). The initial solution containing Mn(2+), peracetic acid and 1-decene in acetonitrile gave a six-line pattern centered around g=2, which is consistent with a high-spin Mn(2+) (S=5/2) species. After the addition of NH₄HCO_{3(aq)}, the signal immediately diminishes in amplitude and no new esr signal was observed. EPR spectroscopic data of various high valent manganese complexes such as Mn(IV)-oxo [264, 265], Mn(V)-oxo [266], Mn(III, III)-di-μ-oxo [267], Mn(III, IV)-di-μ-oxo [268] and Mn(IV, IV)-di-μ-oxo [269] complexes have all been reported

in literature. Amongst these Mn-oxo complexes, only the Mn(V)-oxo species is a low spin species which is diamagnetic and shows no signal in the EPR spectrum [266].

Therefore, we infer that the active species might be a high-valent Mn(V)-oxo species.

The optimal loading of Mn(2+) for epoxidation was determined from the yield of epoxide (Figure 4.9 and Table 4.3). The optimal conversion efficiency could be obtained when the Mn(2+) loading was between 0.32 and 0.62 mol%. When the catalyst loading was below 0.04 mol%, no epoxide could be obtained.

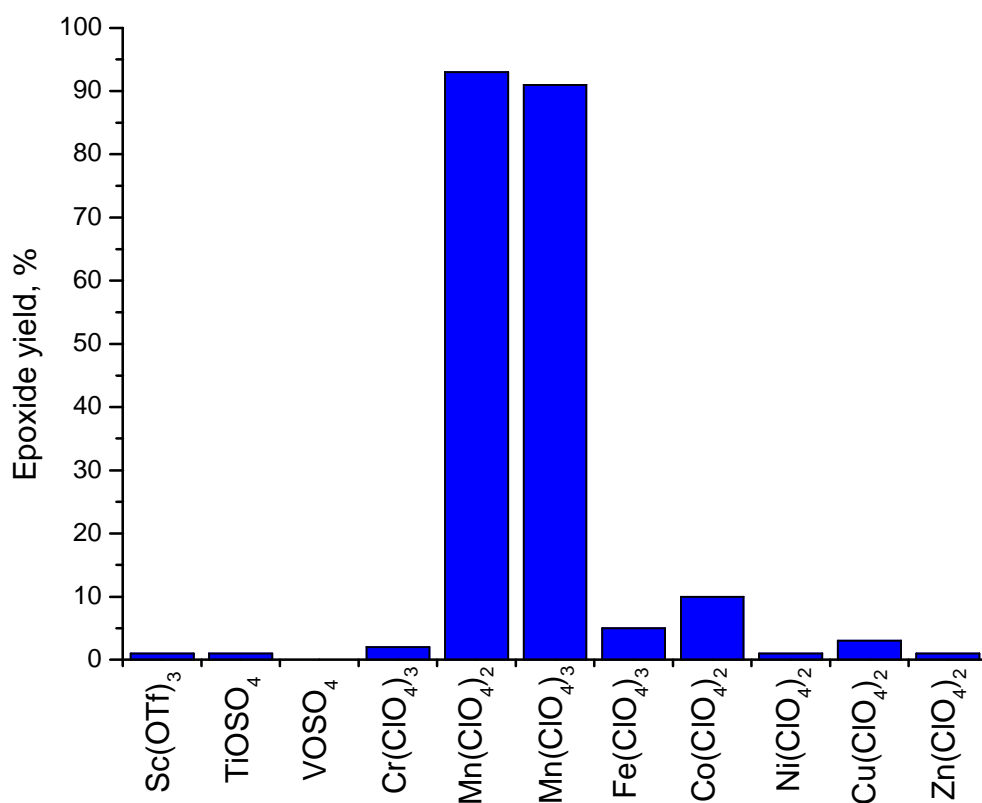


Figure 4.7 Screening of metal salts for the epoxidation reactivity. Additive: 0.5 M $\text{NH}_4\text{HCO}_3(\text{aq})$ (300 μl). Catalyst: 0.32 mol%. Substrate: 1-decene (0.5 mmol, 97 μl). Oxidant: 32 wt.% peracetic acid (250 μl). Reaction time: 30 min.

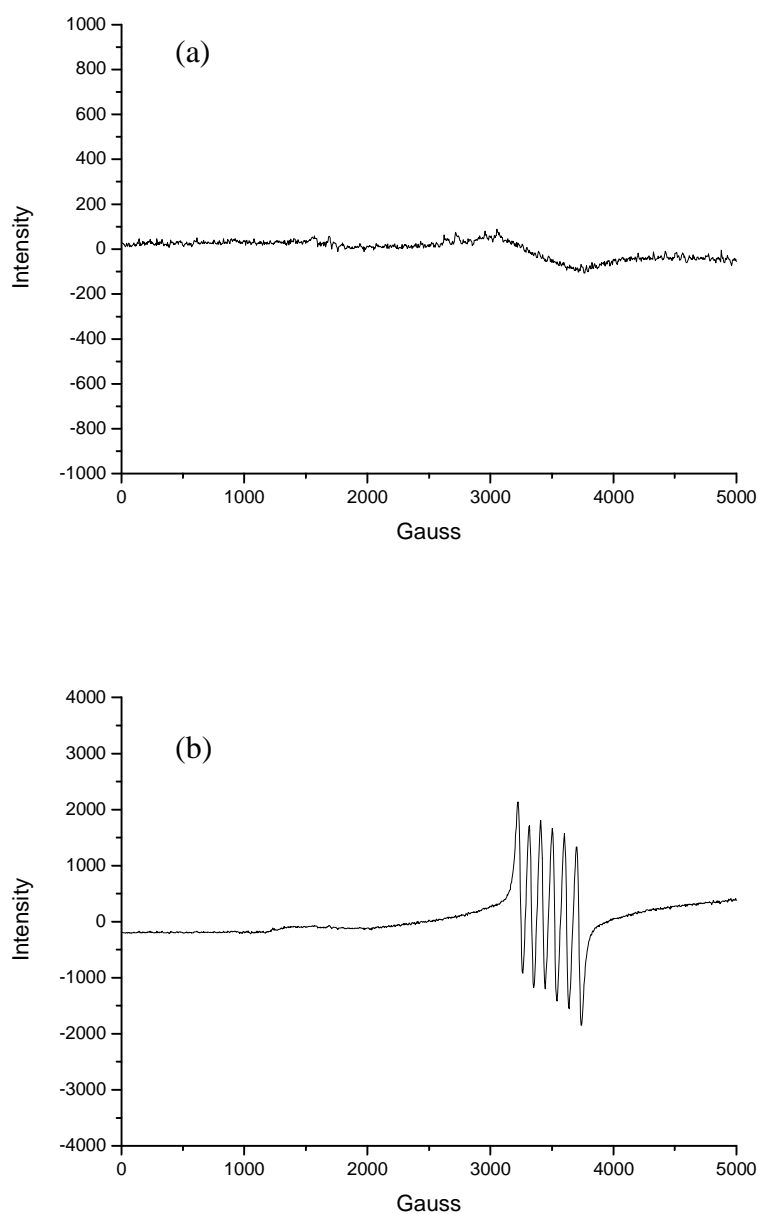


Figure 4.8 EPR spectra of a reaction mixture of (a) acetonitrile/peracetic acid/1-decene (b) acetonitrile/peracetic acid/1-decene/ $\text{Mn}(\text{ClO}_4)_2$. EPR spectra (77K) were recorded at the X-band (9.4 GHz microwave frequency), 2mW power and 25G modulation amplitude.

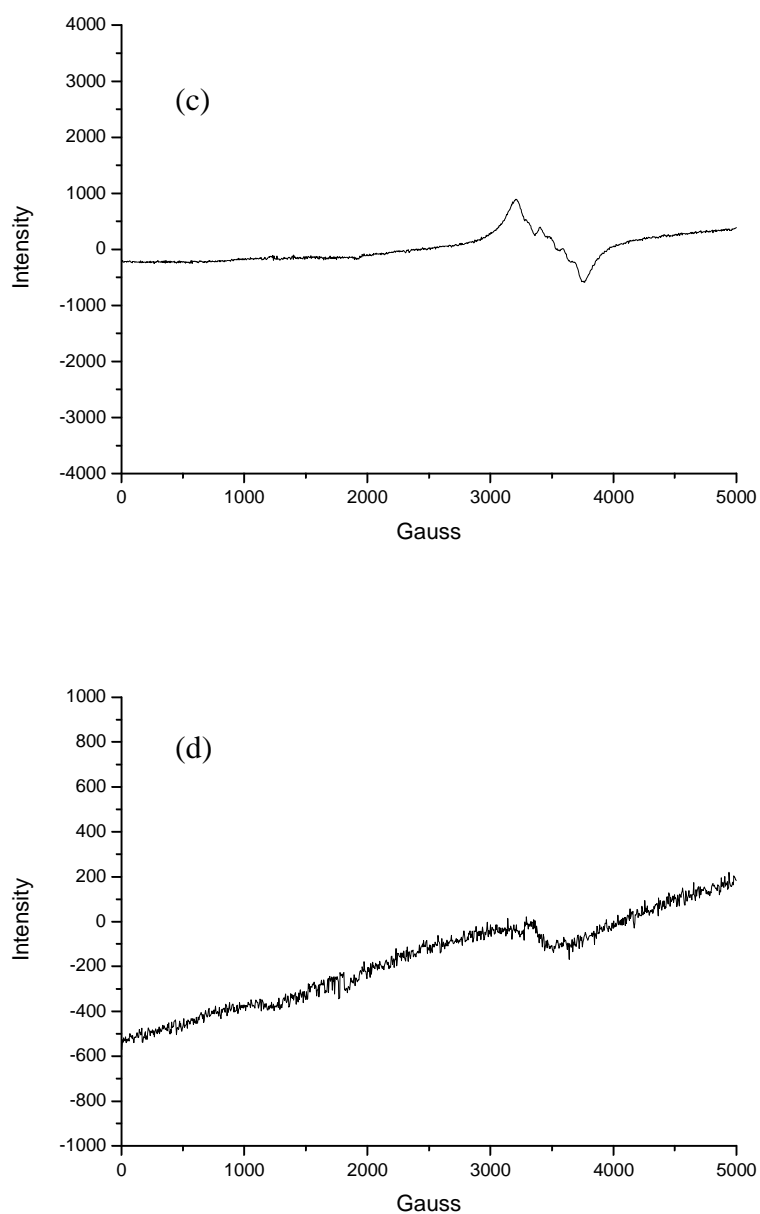


Figure 4.8 EPR spectra of a reaction mixture of (c) acetonitrile/peracetic acid/1-decene/ $\text{Mn}(\text{ClO}_4)_2/\text{NH}_4\text{HCO}_3$ at $t = 2\text{sec}$ (d) acetonitrile/peracetic acid/1-decene/ $\text{Mn}(\text{ClO}_4)_2/\text{NH}_4\text{HCO}_3$ at $t = 5\text{min}$. EPR spectra (77K) were recorded at the X-band (9.4 GHz microwave frequency), 2mW power and 25G modulation amplitude. (cont'd)

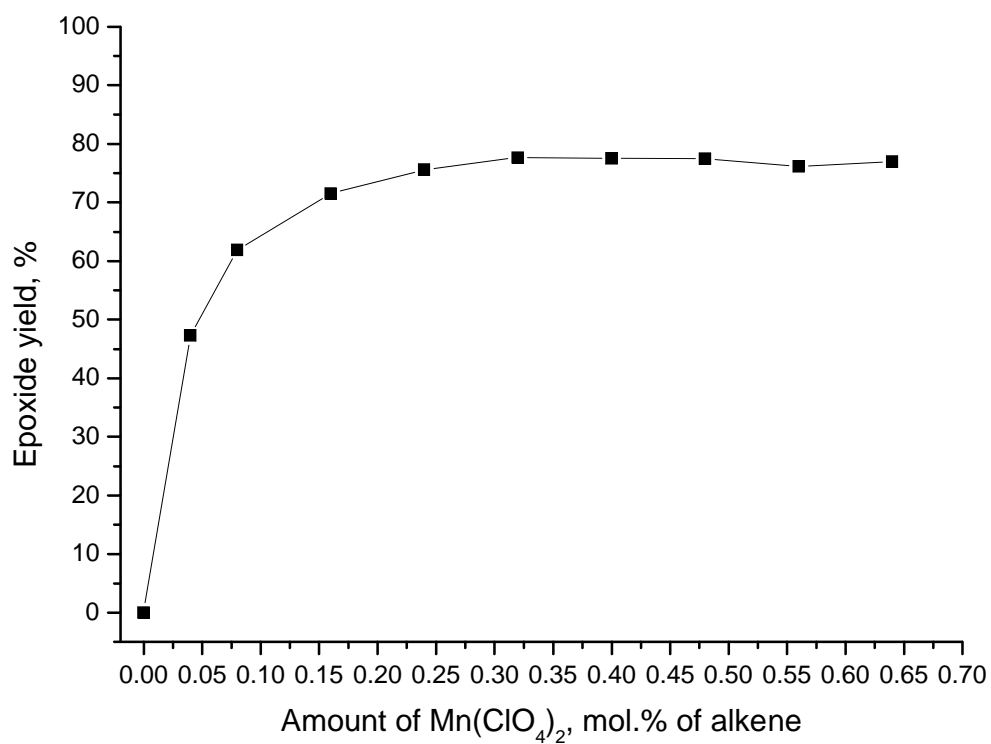


Figure 4.9 Optimization of the Mn^{2+} loading for the epoxidation reaction.

Additive: 0.5 M $\text{NH}_4\text{HCO}_3(\text{aq})$ (300 μl). Catalyst: $\text{Mn}(\text{ClO}_4)_2$. Substrate:

1-decene (0.5mmol, 97 μl). Oxidant: 32 wt.% peracetic acid (250 μl).

Reaction time: 15 min.

Table 4.3 The effect of catalyst and catalyst loading on the epoxide yield.

	Concentration,	Time, min	Epoxide
Metal salt	mol% of alkene		yield, %
Scandium(III) triflate	0.32	30	<1
Titanium(IV) oxysulfate	0.32	30	<1
Vanadium(IV) oxide sulfate	0.32	30	5 ^a
Chromium(III) perchlorate	0.32	30	2
Manganese(II) perchlorate	0.32	30	93
Manganese(III) acetate	0.32	30	91
Iron(III) perchlorate	0.32	30	5
Cobalt(II) perchlorate	0.32	30	10
Nickel(II) perchlorate	0.32	30	<1
Copper(II) perchlorate	0.32	30	3
Zinc(II) perchlorate	0.32	30	<1
Manganese(II) perchlorate	0	15	0
Manganese(II) perchlorate	0.04	15	47
Manganese(II) perchlorate	0.08	15	62
Manganese(II) perchlorate	0.16	15	72
Manganese(II) perchlorate	0.24	15	76
Manganese(II) perchlorate	0.32	15	78
Manganese(II) perchlorate	0.40	15	77
Manganese(II) perchlorate	0.48	15	77
Manganese(II) perchlorate	0.56	15	76

Manganese(II) perchlorate	0.64	15	77
---------------------------	------	----	----

Additive: 0.5 M $\text{NH}_4\text{HCO}_{3(\text{aq})}$ (300 μl). Substrate: 1-decene (0.5 mmol, 97 μl). Oxidant: 32 wt.% peracetic acid (250 μl). ^aAldehyde was formed.

4.3.4. The effect of solvents

The solvents used in the catalytic process affect the solvation environment and the complexing power of the solvated catalyst [270]. The effects of different protic and aprotic solvents on the epoxidation reaction are summarized in Figure 4.10 and Table 4.4. A quick glance of the results reveals that there is no correlation between the solvent polarity, basicity and catalytic reactivity. Besides acetonitrile and acetone (93% and 89% respectively), moderate to poor yield of 1,2-epoxydecane were obtained with most solvents.

A comparison of the results obtained with different alcohols as solvents indicate that the solvent resistance against oxidation is a crucial factor for the success of epoxidation. 2,2,2-Trifluoroethanol, the alcohol that is least susceptible towards oxidation, gives the best epoxide yield (63%). This principle also applies to methyl acetate, ethyl acetate, DMF and DMSO which are more susceptible towards oxidation than acetone and acetonitrile. Solubility of the Mn^{2+} catalyst is another crucial factor. A comparison of the organic nitriles such as acetonitrile, propionitrile, butyronitrile and valeronitrile indicate that the yields of 1,2-epoxydecane dropped sharply with the alkyl chain length. This can be attributed to the low solubility of Mn^{2+} as the

hydrophobicity of the solvent increases.

The catalytic process appears to be enhanced by the presence of an appropriate amount of water (~10%) in the reaction mixture (Figure 4.11). The presence of water assists the solubility of MnSO_4 and NH_4HCO_3 in the reaction mixture. On the other hand, too much water (>10%) causes a drop in the solubility of alkenes and hence the epoxide yield also declines (Figure 4.11).

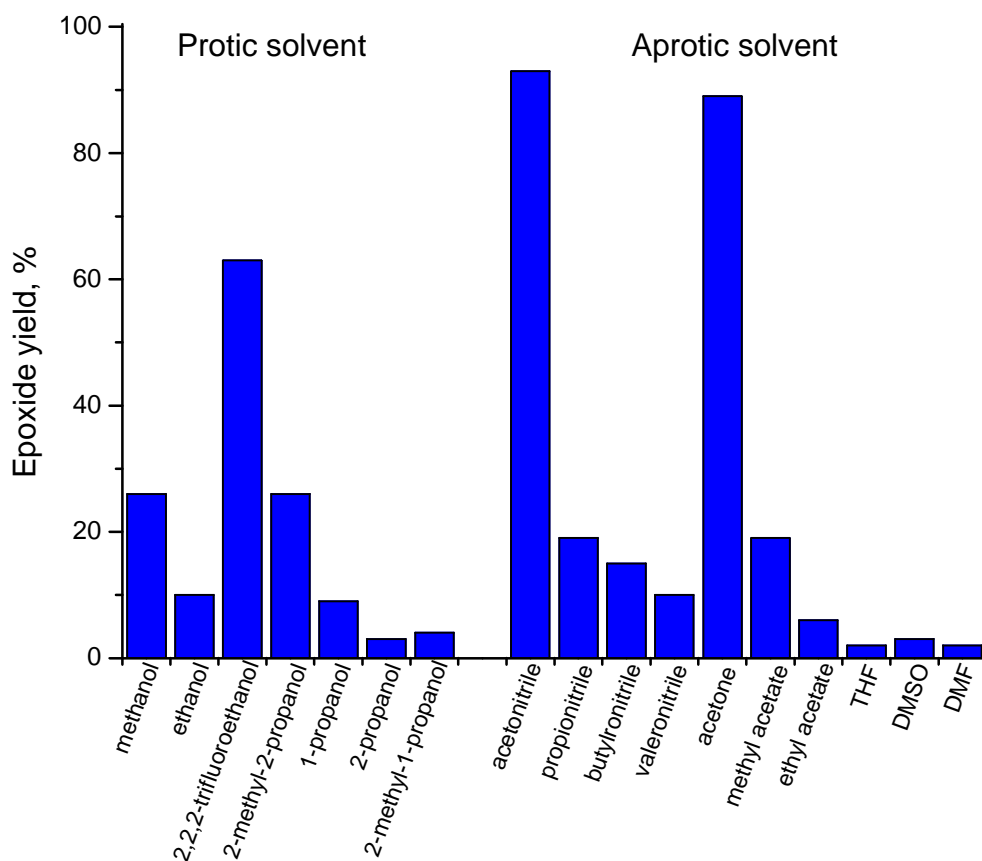


Figure 4.10 Screening of solvents for the epoxidation reaction. Solvent: 2.4 ml.

Additive: 0.5 M $\text{NH}_4\text{HCO}_3(\text{aq})$ (300 μl). Catalyst: $\text{Mn}(\text{ClO}_4)_2$ (0.32

mol%). Substrate: 1-decene (0.5 mmol, 97 μl). Oxidant: 32 wt.%

peracetic acid (250 μl). Reaction time: 30 min.

Table 4.4 The effect of solvent on the epoxidation reaction.

Solvent	Protic/aprotic solvent	Polarity	Basicity	Time, min	Epoxide yield, %
Water	Protic	0.962	0.025	30	0
Methanol	Protic	0.857	0.545	30	26
Ethanol	Protic	0.853	0.853	30	10
2,2,2-trifluoroethanol	Protic	0.912	0.107	30	63
2-methyl-2-propanol	Protic	0.829	0.928	30	26
1-propanol	Protic	0.847	0.727	30	9
2-propanol	Protic	0.832	0.762	30	3
2-methyl-1-propanol	Protic	0.829	0.828	30	4
Acetonitrile	Aprotic	0.895	0.286	30	93
Propionitrile	Aprotic	0.875	0.365	30	19
Butyronitrile	Aprotic	0.912	0.384	30	15
Valeronitrile	Aprotic	0.920	0.430	30	10
Acetone	Aprotic	0.881	0.475	30	89
Methyl acetate	Aprotic	0.785	0.527	30	19
Ethyl acetate	Aprotic	0.795	0.542	30	6
THF	Aprotic	0.838	0.591	30	2
DMSO	Aprotic	1	0.647	30	3
DMF	Aprotic	0.954	0.613	30	2

Solvent: 2.4 ml. Additive: 0.5 M $\text{NH}_4\text{HCO}_3(\text{aq})$ (300 μl). Catalyst: $\text{Mn}(\text{ClO}_4)_2$ (0.32 mol%). Substrate:

1-decene (0.5 mmol, 97 μl). Oxidant: 32 wt% peracetic acid (250 μl).

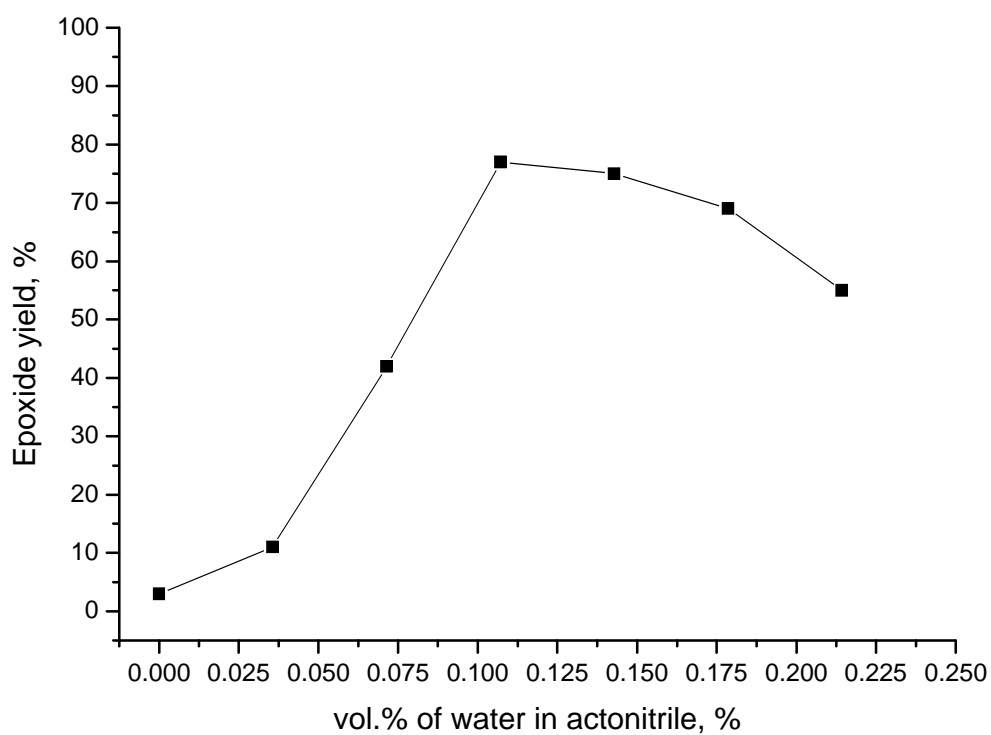


Figure 4.11 The effect of water content in acetonitrile on the epoxide yield. Solvent: 2.4 ml. Additive: $\text{NH}_4\text{HCO}_3(\text{aq})$ (0.15 mmol). Catalyst: $\text{Mn}(\text{ClO}_4)_2$ (0.32 mol%). Substrate: 1-decene (0.5 mmol, 97 μl). Oxidant: 32 wt.% peracetic acid (250 μl). Reaction time: 15 min.

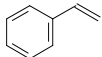
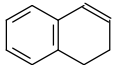
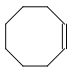
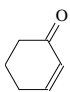
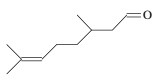
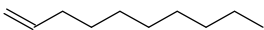
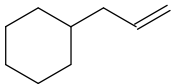
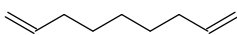
4.3.5. Epoxidation of various alkenes with this catalytic system

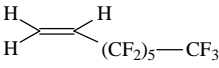
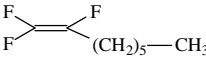
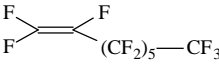
Table 4.5 summarizes the results obtained with some representative alkenes, with or without Mn(2+) salt. The epoxidation of styrene and 1,2-dihydronaphthalene (entries 1 and 2) are not promoted by the Mn^{2+} catalyst. Indeed, small amount of benzaldehyde (cleavage of carbon-carbon double bond) was observed in the presence of Mn^{2+} . The effect of Mn^{2+} on the oxidation of cyclooctene is minimal. 2-Cyclohexen-1-one is unreactive under such experimental conditions regardless the presence of Mn^{2+} (entry 4). 3,7-Dimethyl-6-octanal (entry 5) was oxidized to some unidentified products in the presence of Mn^{2+} , probably because of the reaction of aldehyde group. Entries 6-8 illustrate that unfunctionalized terminal alkenes and dienes are efficiently epoxidized. Attempts to epoxidize the electron deficient fluorinated terminal alkenes (entries 9-11) all failed except 1H,1H,2H-perfluoro-1-octene.

As shown in Table 4.6, different terminal alkenes are epoxidized in good to moderate yields under optimized conditions. In the absence of either $\text{Mn}(\text{ClO}_4)_2$ or $\text{NH}_4\text{HCO}_3(\text{aq})$, 1-decene is unreactive with peracetic acid (entries 12 and 13). In most cases (entries 14-18 and entries 27-28), 2.4 equivalents of peracetic acid is sufficient

to complete the reaction. The longer chain aliphatic alkenes (entries 19-24) are less soluble in the acetonitrile/water mixture and the epoxidation yields also decline. Entries 25-27 illustrate that terminal dienes are transformed effectively to their corresponding diepoxides. The presence of bulky groups in vinyl cyclohexane and allyl cyclohexane (entries 27-28) introduces negligible effect on the epoxidation reaction.

Table 4.5 Epoxidation of some representative alkenes.

Entry	Substrate	Epoxide yield, % ^a	
		0.4 mol % of Mn(ClO ₄) ₂	0 mol % of Mn(ClO ₄) ₂
1	Styrene 	6	17
2	1,2-dihydronaphthalene 	12	23
3	Cyclooctene 	73	67
4	2-cyclohexen-1-one 	0	0
5	3,7-dimethyl-6-octenal 	0	26
6	1-decene 	93	0
7	allyl cyclohexane 	94	0
8 ^b	1,8-nonadiene 	91 (diepoxide)	0

9	1H,1H,2H-perfluoro-1-octene	36	0
			
10	1,1,2-trifluoro-1-octene	0	0
			
11	Perfluoro-1-octene	0	0
			

Solvent: 2.4 ml acetonitrile. Additive: 0.5M $\text{NH}_4\text{HCO}_3(\text{aq})$ (300 μl). Catalyst: $\text{Mn}(\text{ClO}_4)_2$ (0.32 mol%).

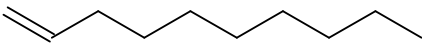
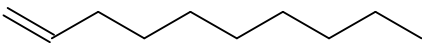
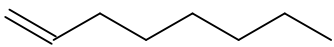
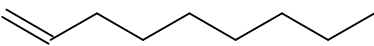
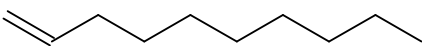
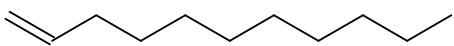
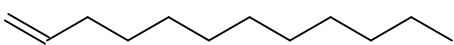
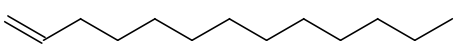
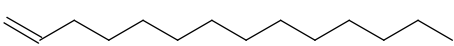
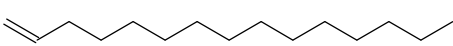
Substrate: 0.5 mmol. Oxidant: peracetic acid (250 μl). Reaction time: 15 min. ^aYields were calculated


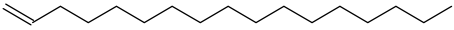
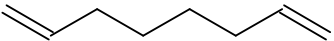
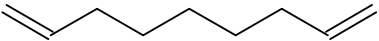
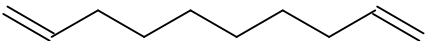
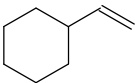
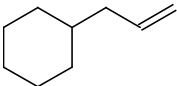
on the basis on converted alkenes and determined by GC-MS with internal standard. ^b4.8 ml

acetonitrile, 32 wt.% of peracetic acid (500 μl), $\text{Mn}(\text{ClO}_4)_2$ (0.62 mol%) and 0.5 M $\text{NH}_4\text{HCO}_3(\text{aq})$ (600

μl) were used.

Table 4.6 Epoxidation of terminal alkyl-alkenes.

Entry	Substrate	Conversion, GC yield, Isolated		
		%	% ^a	yield, % ^b
12 ^c	1-decene 	0	0	-
13 ^d	1-decene 	0	0	-
14	1-octene 	>99	86	83
15	1-nonene 	>99	91	87
16	1-decene 	>99	93	90
17	1-undecene 	>99	94	92
18	1-dodecene 	>99	92	91
19 ^e	1-tridecene 	>99	93	90
20 ^e	1-teradecene 	90	85	-
21 ^e	1-pentadecene 	75	63	-

22 ^e	1-hexadecene	65	59	-
				
23 ^e	1-heptadecene	57	48	-
				
24 ^f	1,7-octadiene	>99	78	62
				
25 ^f	1,8-nonadiene	>99	91	88
				
26 ^f	1,9-decadiene	>99	92	90
				
27	vinyl cyclohexane	>99	91	85
				
28	allyl cyclohexane	>99	94	88
				

Solvent: 2.4 ml acetonitrile. Additive: 0.5 M $\text{NH}_4\text{HCO}_3(\text{aq})$ (300 μl). Catalyst: $\text{Mn}(\text{ClO}_4)_2$ (0.32 mol%).

Substrate: 0.5 mmol. Oxidant: peracetic acid (250 μl). Reaction time: 30 min. ^aYields were calculated

on the basis on converted alkenes and determined by GC-MS with internal standard. ^bIsolated yield was

given in parenthesis. ^cControl experiment (without NH_4HCO_3) ^dControl experiment (without

$\text{Mn}(\text{ClO}_4)_2$). ^eReaction time: 40 min. ^fAcetonitrile (4.8 ml), 32 wt.% of peracetic acid 500 μl ,

$\text{Mn}(\text{ClO}_4)_2$ (0.62 mol%) and 0.5 M $\text{NH}_4\text{HCO}_3(\text{aq})$ (600 μl) were used.

4.3.6. Stereoselectivity of the epoxidation reaction

The results of epoxidizing *cis*- and *trans*-alkenes are summarized in Figure 4.12 and Table 4.7. Entry A illustrates that the terminal aliphatic alkene 1-nonene was not epoxidized in the absence of Mn^{2+} . On the other hand, the yields of epoxide for the dialkyl-substituted alkenes (entries B-E) were improved by the presence of Mn^{2+} . It is interesting to note that the improvement in epoxide yield by Mn^{2+} is more prominent for *cis*-alkenes than for *trans*-alkenes. This can be attributed to the lesser steric hindrance offered by the *cis*-alkenes upon the approach of the active manganese catalyst.

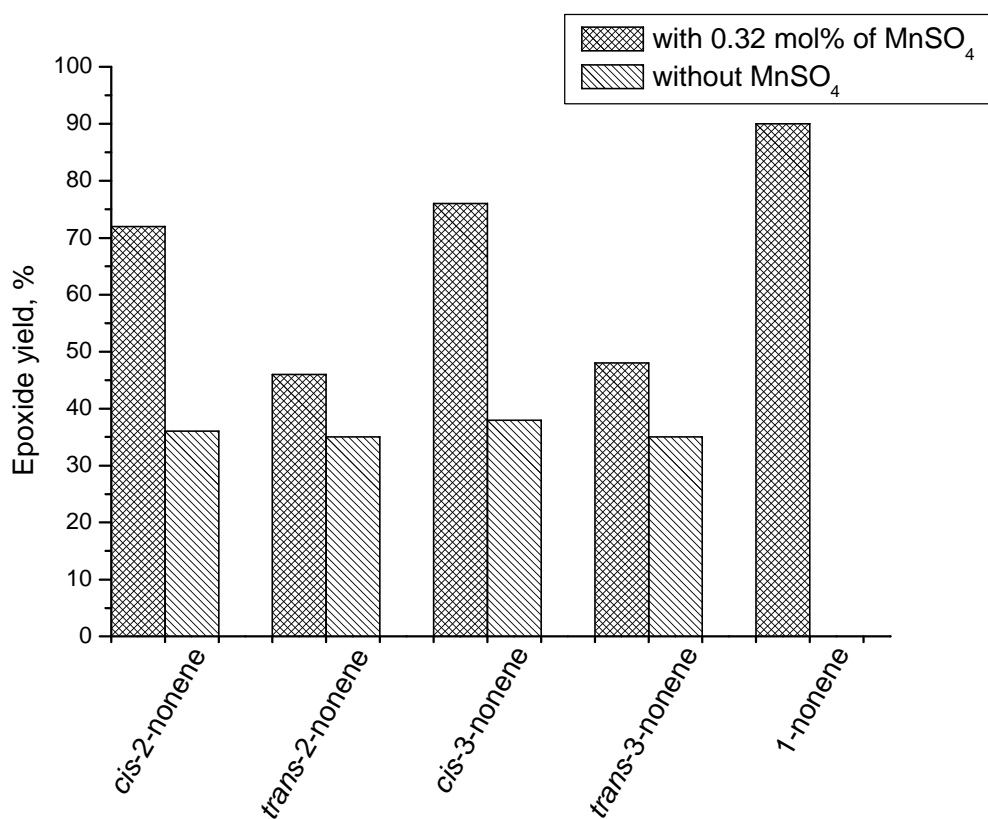


Figure 4.12 Epoxidation of various *cis*- and *trans*-alkenes. Solvent: 2.4 ml acetonitrile. Additive: 0.5 M $\text{NH}_4\text{HCO}_3(\text{aq})$ (300 μl). Catalyst: $\text{Mn}(\text{ClO}_4)_2$ (0.32 mol%). Substrate: 0.5 mmol. Oxidant: 32 wt.% peracetic acid (250 μl). Reaction time: 30 min.

Table 4.7 Epoxidation of *cis*- and *trans*-alkenes.

Entry	Substrate	Epoxide yield, %	
		0.32 mol % of	0 mol % of
		Mn(ClO ₄) ₂	Mn(ClO ₄) ₂
A	1-nonene	90	0
B	<i>cis</i> -2-nonene	72 (<i>cis</i>)	36
C	<i>trans</i> -2-nonene	46 (<i>trans</i>)	35
D	<i>cis</i> -3-nonene	76 (<i>cis</i>)	38
E	<i>trans</i> -3-nonene	48 (<i>trans</i>)	35

Solvent: 2.4 ml acetonitrile. Additive: 0.5 M NH₄HCO_{3(aq)} (300 μl). Catalyst: Mn(ClO₄)₂ (0.32 mol%).

Substrate: 0.5 mmol. Oxidant: 32 wt.% peracetic acid (250 μl). Reaction time: 30min. ^aYields were calculated on the basis on converted alkenes and determined by GC-MS with internal standard, tetradecane.

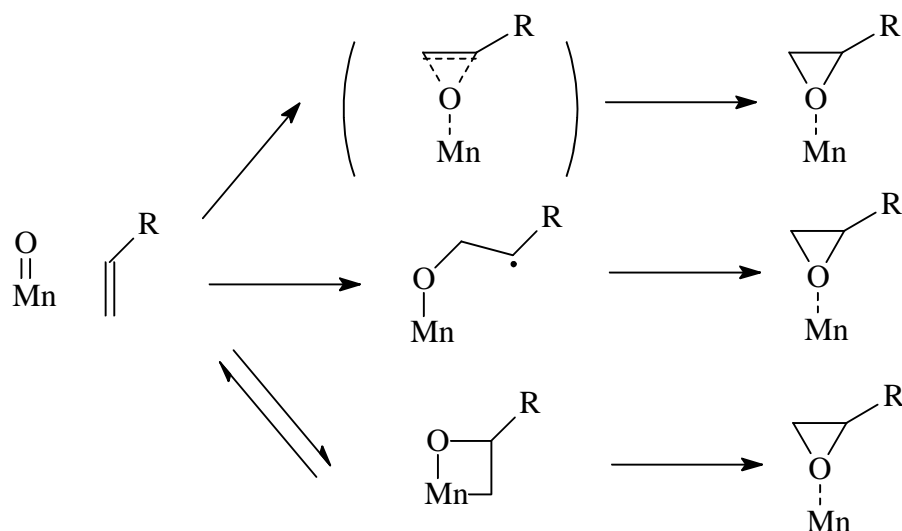
4.3.7. Proposed mechanism for the catalytic reaction

In this catalytic system, terminal aliphatic alkenes are efficiently epoxidized in acetonitrile using $\text{Mn}(\text{ClO}_4)_2$ salt as catalyst and peracetic acid as oxidant. It is generally believed that the first step in manganese-catalyzed oxidation with peracetic acid involves the formation of a manganese η^2 -acylperoxo complex (Scheme 4.3) [256, 259, 271].

The most crucial step in the epoxidation process is the oxygen delivery step. EPR study indicated that the active manganese species in the reaction is diamagnetic. Amongst the various high-valent manganese complexes, a low spin $\text{Mn}(\text{V})=\text{O}$ species is the likely species generated from the acylperoxo complex in this catalytic reaction.

In the course of oxygen transfer, the epoxidation can proceed either in a concerted manner, via a radical intermediate, or via a manganaoxetane intermediate (Scheme 4.5) [272]. The original *cis/trans* geometry of the alkenes was found to be always retained in this catalytic reaction (Table 4.7). Thus, both the concerted mechanism and the manganaoxetane pathway are favored because they can give epoxides with high stereospecificity [272-276]. These mechanisms are also consistent with the

observation that *cis*-alkenes are epoxidized more effectively than *trans*-alkenes (Table 4.7). However, we cannot completely rule out a radical mechanism at this stage because a cage-type radical intermediate can give similar products as those via a concerted mechanism or a manganaoxetane intermediate.



Scheme 4.5 Proposed pathways for the oxygen transfer step.

4.4. Conclusion

A catalytic system for the effective epoxidation of terminal aliphatic alkenes using Mn(2+) salt as catalyst and peracetic acid as oxidant has been developed. A wide range of terminal aliphatic alkenes could be efficiently epoxidized within 30-40 mins at ambient temperature. The active species is believed to be a high-valent Mn(V)=O species transforming from the manganese η^2 -acylperoxo complex.

Chapter 5

Conclusions

Manganese(2+) is considered a 'green' catalyst in alkene epoxidation because of its low toxicity. However, a truly environmentally benign catalytic system should also take into account of green solvents and oxidants. In this study, the *in-situ* electrogeneration of H₂O₂ in aqueous or aqueous/*tert*-butanol mixtures was coupled to a Mn²⁺/HCO₃⁻ system for alkene epoxidation. Oxygen was used as the primary oxygen source to generate H₂O₂ electrochemically. In the Mn²⁺/H₂O₂/HCO₃⁻ epoxidation system, the H₂O₂ should be added slowly over many hours to avoid overheating and H₂O₂ decomposition. The actual concentration of H₂O₂ present in the reaction mixture at any time should be fairly low. The electrochemical method allows the controlled release of H₂O₂ to the reaction medium in a slow and precise manner. This method presents an environmentally benign system for alkene epoxidation as electricity is used to generate H₂O₂ and the use of volatile organic solvent has been minimized.

The use of ionic liquids to replace organic solvents in the electrogenerated H₂O₂/Mn²⁺/HCO₃⁻ catalytic system has been demonstrated. Using ionic liquid as electrolyte and solvent, H₂O₂ is efficiently electrogenerated and lipophilic alkenes are effectively epoxidized. The active species peroxymonocarbonate (HCO₄⁻) can be generated *in-situ* by purging the ionic liquid/NaOH_(aq)/H₂O₂ mixture with CO₂ gas.

Most lipophilic alkenes give good yield of epoxides. The ionic liquid can be reused without significant diminution of its capacity in H_2O_2 electrogeneration and epoxidation.

As the $\text{H}_2\text{O}_2/\text{Mn}^{2+}/\text{HCO}_3^-$ catalytic system is limited to electron-rich alkenes, a relatively environmentally benign system capable of epoxidizing electron-deficient terminal alkenes has been developed. It was found that terminal aliphatic alkenes can be effectively epoxidized by peracetic acid in acetonitrile/water mixture with catalytic amount of $\text{Mn}(2+)$ salt and in the presence of NH_4HCO_3 as additive. A high valent $\text{Mn}(\text{V})=\text{O}$ species is postulated as the active intermediate. This simple system allows the effective epoxidation of terminal aliphatic alkenes at room temperature with inexpensive chemicals.

Although the Mn^{2+} /peracetic acid system is effective in the epoxidation of terminal alkenes, further improvement is necessary to make it a truly environmentally benign system. For example, the generation of acetic acid as by-product and the use of acetonitrile as solvent should be avoided. One way to achieve this is to modify this system so that it will work in ionic liquids. Recently, ionic liquids that are resistant against oxidative decomposition (e.g. pyrrolidinium-based ionic liquids) become

available. Instead of using acetic acid to generate peracetic acid from H_2O_2 , reagent-anchored ionic liquids such as those shown in Figure 5.1 can be prepared. The peracetic acid can then be generated by reaction with H_2O_2 (Scheme 5.1). As the acetic acid is now partly of the ionic liquid, the generation of acetic acid as by-product can be avoided and the reagent-anchored ionic liquids can be recycled and reused.

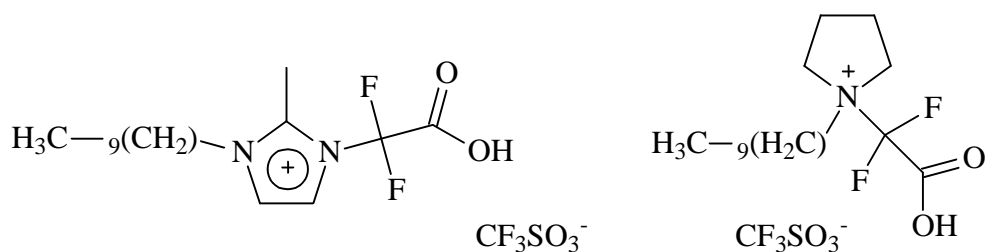
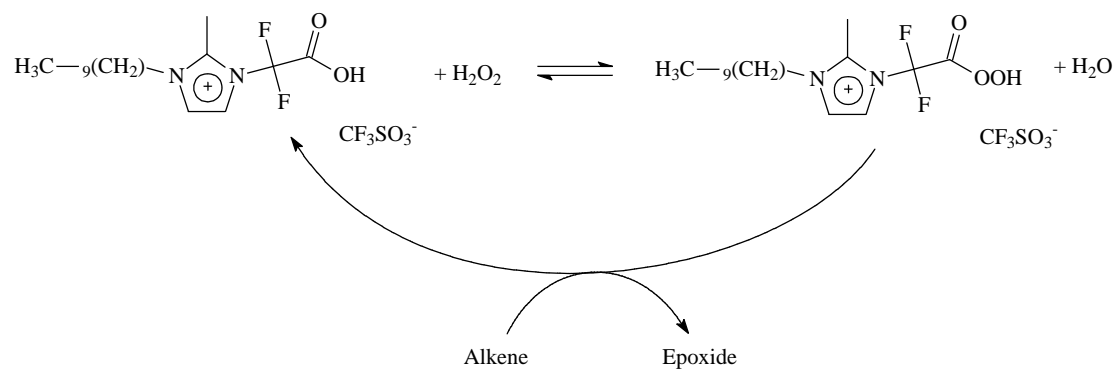


Figure 5.1 Reagent-anchored ionic liquids.



Scheme 5.1 *In-situ* formation of peracid with H_2O_2 for alkene epoxidation.

References

1. Grigoropoulou, G., Clark, J. H., Elings, J. A. Recent developments on the epoxidation of alkenes using hydrogen peroxide as an oxidant. *Green Chemistry*, 2003, **5**, 1-7.
2. Howarth, J. *Core Organic Chemistry*. New York: John Wiley & Sons, 1998.
3. Bailey, F. E. *Alkylene Oxides and Their Polymers*. New York: Dekker, 1991.
4. Young, R. V., Sessine, S. *World of Chemistry*. Detroit: Gale Group, 2000.
5. Taylor, P. *Alkenes and Aromatics*. Cambridge: Royal Society of Chemistry, 2002.
6. Hurley, S. A. *The Use of Epoxy, Polyester and Similar Reactive Polymers in Construction*. London: CIRIA, 2000.
7. Lappin, G., Sauer, J. D. *Alpha Olefins Applications Handbook*. New York: Marcel Dekker, 1989.
8. Sienel, G., Rieth, R., Rowbottom, K. T. *Ullmann's Encyclopedia of Industrial Chemistry*. Weinheim: Wiley-VCH, 1999.
9. Sheldon, R. A., Kochi, J. K. *Metal-catalyzed Oxidations of Organic Compounds: Mechanistic Principles and Synthetic Methodology Including Biochemical Processes*. New York: Academic Press, 1981.
10. Hannick, S. M., Kishi, Y. A new, effective catalytic system for epoxidation of olefins by hydrogen peroxide under phase-transfer conditions. *The Journal of Organic Chemistry*, 1983, **48**, 3831-3833.
11. Ishii, Y., Yamawaki, K., Ura, T., Yamada, H., Yoshida, T., Ogawa, M. Hydrogen peroxide oxidation catalyzed by heteropoly acids combined with cetylpyridinium chloride. Epoxidation of olefins and allylic alcohols, ketonization of alcohols and diols, and oxidative cleavage of 1,2-diols and

- olefins. *The Journal of Organic Chemistry*, 1988, **53**, 3587-3593.
12. Kozhevnikov, I. V. Heteropoly acids and related compounds as catalysts for fine chemical synthesis. *Catalysis Reviews - Science and Engineering*, 1995, **37**, 311-352.
 13. Sato, K., Aoki, M., Ogawa, M., Hashimoto, T., Noyori, R. A practical method for epoxidation of terminal olefins with 30% hydrogen peroxide under halide-free conditions. *The Journal of Organic Chemistry*, 1996, **61**, 8310-8311.
 14. Sato, K., Aoki, M., Ogawa, M., Hashimoto, T., Panyella, D., Noyori, R. A halide-free method for olefin epoxidation with 30% hydrogen peroxide. *Bulletin of the Chemical Society of Japan*, 1997, **70**, 905-915.
 15. Sato, K., Aoki, M., Noyori, R. A "green" route to adipic acid: Direct oxidation of cyclohexenes with 30 percent hydrogen peroxide. *Science*, 1998, **281**, 1646-1647.
 16. Deng, Y., Ma, Z., Wang, K., Chen, J. Clean synthesis of adipic acid by direct oxidation of cyclohexene. *Green Chemistry*, 1999, **1**, 275-276.
 17. Anelli, P. L., Banfi, S., Montanari, F., Quici, S. Synergistic effect of lipophilic carboxylic acids and heterocyclic axial ligands in alkene epoxidation by hydrogen peroxide catalyzed by manganese(III) tetraarylporphyrins. *Chemical Communications*, 1989, **12**, 779-780.
 18. Hage, R., Iburg, J. E., Kerschner, J., Koek, J. H., Lempers, E. L. M., Martens, R. J., Racherla, U. S., Russell, S. W., Swarthoff, T. Efficient manganese catalysts for low-temperature bleaching. *Nature*, 1991, **369**, 637-639.
 19. De Vos, D. E., Sels, B. F., Reynaers, M., Rao, Y. V. S., Jacobs, P. A. Epoxidation of terminal or electron-deficient olefins with H₂O₂, catalysed by Mn-trimethyltriazacyclonane complexes in the presence of an oxalate buffer.

- Tetrahedron Letters*, 1998, **39**, 3221-3224.
20. De Vos, D., Bein, T. Highly selective epoxidation of alkenes and styrenes with H_2O_2 and manganese complexes of the cyclic triamine 1,4,7-trimethyl-1,4,7-triazacyclononane. *Chemical Communications*, 1996, **8**, 917-918.
 21. Herrmann, W. A., Kratzer, R. M., Ding, H., Thiel, W., Glas, H. Methyltrioxorhenium/pyrazole - A highly efficient catalyst in the epoxidation of olefins. *Journal of Organometallic Chemistry*, 1998, **555**, 293-295.
 22. Coperet, C., Adolfsson, H., Sharpless, K. B. A simple and efficient method for epoxidation of terminal alkenes. *Chemical Communications*, 1997, 1565-1566.
 23. Rudolph, J., Reddy, K. L., Chiang, J. P., Sharpless, K. B. Highly efficient epoxidation of olefins using aqueous H_2O_2 and catalytic methyltrioxorhenium/pyridine: Pyridine-mediated ligand acceleration. *Journal of the American Chemical Society*, 1997, **119**, 6189-6190.
 24. Adolfsson, H., Coperet, C., Chiang, J. P., Yudin, A. K. Efficient epoxidation of alkenes with aqueous hydrogen peroxide catalyzed by methyltrioxorhenium and 3-cyanopyridine. *The Journal of Organic Chemistry*, 2000, **65**, 8651-5658.
 25. Al-Ajlouni, A. M., Espenson, J. H. Kinetics and mechanism of the epoxidation of alkyl-substituted alkenes by hydrogen peroxide, catalyzed by methylrhenium trioxide. *The Journal of Organic Chemistry*, 1996, **61**, 3969-3976.
 26. Abu-Omar, M. M., Hansen, P. J., Espenson, J. H. Deactivation of methylrhenium trioxide - Teroxide catalysts by diverse and competing pathways. *Journal of the American Chemical Society*, 1996, **118**, 4966-4974.
 27. Yudin, A. K., Sharpless, K. B. Bis(trimethylsilyl) peroxide extends the range of oxorhenium catalysts for olefin epoxidation. *Journal of the American*

- Chemical Society*, 1997, **119**, 11536-11537.
28. Yudin, A. K., Chiang, J. P., Adolfsson, H., Coperet, C. Olefin epoxidation with bis(trimethylsilyl) peroxide catalyzed by inorganic oxorhenium derivatives. Controlled release of hydrogen peroxide. *The Journal of Organic Chemistry*, 2001, **66**, 4713-4718.
 29. Costas, M., Tipton, A. K., Chen, K., Jo, D. H., Que, L. Modeling Rieske dioxygenases: The first example of iron-catalyzed asymmetric *cis*-dihydroxylation of olefins. *Journal of the American Chemical Society*, 2001, **123**, 6722-6723.
 30. White, M. C., Doyle, A. G., Jacobsen, E. N. A synthetically useful, self-assembling MMO mimic system for catalytic alkene epoxidation with aqueous H₂O₂. *Journal of the American Chemical Society*, 2001, **123**, 7194-7195.
 31. Chen, K., Que, L. *Cis*-dihydroxylation of olefins by a non-heme iron catalyst: A functional model for Rieske dioxygenases. *Angewandte Chemie-International Edition*, 1999, **38**, 2227-2229.
 32. Traylor, T. G., Tsuchiya, S., Byun, Y. S., Kim, C. High-yield epoxidations with hydrogen peroxide and *tert*-butyl hydroperoxide catalyzed by iron(III) porphyrins: Heterolytic cleavage of hydroperoxides. *Journal of the American Chemical Society*, 1993, **115**, 2775-2781.
 33. Nam, W., Ho, R., Valentine, J. S. Iron-cyclam complexes as catalysts for the epoxidation of olefins by 30% aqueous hydrogen peroxide in acetonitrile and methanol. *Journal of the American Chemical Society*, 1991, **113**, 7052-7054.
 34. Clerici, M. G., Ingallina, P. Epoxidation of lower olefins with hydrogen peroxide and titanium silicalite. *Journal of Catalysis*, 1993, **140**, 71-83.
 35. Sheldon, R. A., Wallau, M., Arends, I. W. C. E., Schuchardt, U. Heterogeneous

- catalysts for liquid-phase oxidations: Philosophers' stones or trojan horses? *Accounts of Chemical Research*, 1998, **31**, 485-493.
36. Arends, I. W. C. E., Sheldon, R. A. Activities and stabilities of heterogeneous catalysts in selective liquid phase oxidations: Recent developments. *Applied Catalysis A: General*, 2001, **212**, 175-187.
 37. Arends, I., Sheldon, R. A. Recent developments in selective catalytic epoxidations with H₂O₂. *Topics in Catalysis*, 2002, **19**, 133-141.
 38. Moiseev, II Hydrogen peroxide, water oxide and catalysis. *Journal of Molecular Catalysis A: Chemical*, 1997, **127**, 1-23.
 39. Huissoud, A., Tissot, P. Electrochemical reduction of 2-ethyl-9,10-anthraquinone on reticulated vitreous carbon and mediated formation of hydrogen peroxide. *Journal of Applied Electrochemistry*, 1998, **28**, 653-657.
 40. Keita, B., Nadjo, L. Catalytic synthesis of hydrogen peroxide - An attractive electrochemical and photo-electrochemical route to the reduction of oxygen. *Journal of Electroanalytical Chemistry*, 1983, **145**, 431-437.
 41. Herrmann, W. A., Kuehn, F. E., Mattner, M. R., Artus, G. R. J., Geisberger, M. R., Correia, J. D. G. Multiple bonds between transition metals and main-group elements. 163. Nitrogen-donor adducts of organorhenium(VII) oxides: Structural and catalytic aspects. *Journal of Organometallic Chemistry*, 1997, **538**, 203-209.
 42. Adolfsson, H., Converso, A., Sharpless, K. B. Comparison of amine additives most effective in the new methyltrioxorhenium-catalyzed epoxidation process. *Tetrahedron Letters*, 1999, **40**, 3991-3994.
 43. Park, S. W., Yoon, S. S. Effects of bis-oxazoline and diamine ligands in olefin epoxidation. *Journal of the Korean Chemical Society*, 2000, **44**, 81-83.

44. Abraham, M. A., Moens, L. *Clean Solvents: Alternative Media for Chemical Reactions and Processing*. Washington: American Chemical Society, 2002.
45. Anastas, P. T., Heine, L. G., Williamson, T. C. *Green Chemical Syntheses and Processes*. Washington, D.C.: American Chemical Society, 2000.
46. Clark, J., Macquarrie, D. *Handbook of Green Chemistry & Technology*. London: Blackwell Science Ltd., 2002.
47. Ichihara, J. Solvent-free epoxidation using a tungstic acid catalyst on fluoroapatite. *Tetrahedron Letters*, 2001, **42**, 695-697.
48. Ichihara, J., Kambara, A., Iteya, K., Sugimoto, E., Shinkawa, T., Takaoka, A., Yamaguchi, S., Sasaki, Y. Cetylpyridinium dodecatungstate on fluorapatite: efficient and reusable solid catalyst for solvent-free epoxidation. *Green Chemistry*, 2003, **5**, 491-193.
49. Ichihara, J., Iteya, K., Kambara, A., Sasaki, Y. New approach to environmentally benign epoxidation: the solid-phase-system using urea-H₂O₂ and recyclable dodecatungstate on apatite. *Catalysis Today*, 2003, **87**, 163-169.
50. Robles-Dutenhefner, P. A., da Silva, M. J., Sales, L. S., Sousa, E. M. B., Gusevskaya, E. V. Solvent-free liquid-phase autoxidation of monoterpenes catalyzed by sol-gel Co/SiO₂. *Journal of Molecular Catalysis A: Chemical*, 2004, **217**, 139-144.
51. Gallo, J. M. R., Paulino, I. S., Schuchardt, U. Cyclooctene epoxidation using Nb-MCM-41 and Ti-MCM-41 synthesized at room temperature. *Applied Catalysis A: General*, 2004, **266**, 223-227.
52. Aresta, M. *Carbon Dioxide Recovery and Utilization*. Boston: Kluwer Academic Publishers, 2003.
53. Haas, g. R., Kolis, J. W. Oxidation of alkenes in supercritical carbon dioxide catalyzed by molybdenum hexacarbonyl. *Organometallics*, 1998, **17**,

4454-4460.

54. Pesiri, D. R., Morita, D. K., Tumas, W., Glaze, W. Selective epoxidation in dense phase carbon dioxide. *Chemical Communications*, 1998, **9**, 1015-1016.
55. Campestrini, S., Tonellato, U. Catalytic olefin epoxidation with H₂O₂ in supercritical CO₂. Synergic effect by hexafluoroacetone and manganese-porphyrins. *Advanced Synthesis & Catalysis*, 2001, **343**, 819-825.
56. Campestrini, S., Donoli, A., Tonellato, U. Embedded Mn-porphyrins in PDMS and ORMOSILs as effective catalysts for cyclooctene epoxidation by H₂O₂ in supercritical carbon dioxide. *Letter in Organic Chemistry*, 2004, **1**, 125-128.
57. Birnbaum, E. R., Le Lacheur, r. M., Horton, A. C., Tumas, W. Metalloporphyrin-catalyzed homogeneous oxidation in supercritical carbon dioxide. *Journal of Molecular Catalysis A: Chemical*, 1999, **139**, 11.
58. Loeker, F., Leitner, W. Steel-promoted oxidation of olefins in supercritical carbon dioxide using dioxygen in the presence of aldehydes. *Chemistry - A European Journal*, 2000, **6**, 2011-2015.
59. Nolen, S. A., Lu, J., Brown, J. S., Pollet, P., Eason, B. C., Griffith, K. N., Glaser, R., Bush, D., Lamb, D. R., Liotta, C. L., Eckert, C. A., Thiele, G. F., Bartels, K. A. Olefin epoxidations using supercritical carbon dioxide and hydrogen peroxide without added metallic catalysts or peroxy acids. *Industrial & Engineering Chemistry Research*, 2002, **41**, 316-323.
60. Hancu, D., Green, H., Beckman, E. J. H₂O₂ in CO₂/H₂O biphasic systems: Green synthesis and epoxidation reactions. *Industrial & Engineering Chemistry Research*, 2002, **41**, 4466-4474.
61. van den Broeke, L. J. P., de Bruijn, V. G., Heijnen, J. H. M., Keurentjes, J. T. F. Micellar catalysis for epoxidation reactions. *Industrial & Engineering Chemistry Research*, 2001, **40**, 5240-5245.

62. Heijnen, J. H. M., de Bruijn, V. G., van den Broeke, L. J. P., Keurentjes, J. T. F. Micellar catalysis for selective epoxidations of linear alkenes. *Chemical Engineering and Processing*, 2003, **42**, 223-230.
63. Arai, S., Oku, M., Miura, M., Shioiri, T. Catalytic asymmetric epoxidation of naphthoquinone derivatives under phase-transfer catalyzed conditions. *Synlett*, 1998, **11**, 1201-1202.
64. Arai, S., Tsuge, H., Shioiri, T. Asymmetric epoxidation of α,β -unsaturated ketones under phase-transfer catalyzed conditions. *Tetrahedron Letters*, 1998, **39**, 7563-7566.
65. Denis, C., Misbahi, K., Kerbal, A., Ferrieres, V., Plusquellec, D. Epoxidation of allylic alcohols in aqueous solutions of non surfactant amphiphilic sugars. *Chemical Communications*, 2001, **23**, 2460-2461.
66. Tong, K. H., Wong, K. Y., Chan, T. H. A chemoenzymic approach to the epoxidation of alkenes in aqueous media. *Tetrahedron*, 2005, **61**, 6009-6014.
67. Prichanont, S., Leak, D. J., Stuckey, D. C. Chiral epoxide production using mycobacterium solubilized in a water-in-oil microemulsion. *Enzyme and Microbial Technology*, 2000, **27**, 134-142.
68. Yao, H. R., Richardson, D. E. Epoxidation of alkenes with bicarbonate-activated hydrogen peroxide. *Journal of the American Chemical Society*, 2000, **122**, 3220-3221.
69. Lane, B. S., Vogt, M., DeRose, V. J., Burgess, K. Manganese-catalyzed epoxidations of alkenes in bicarbonate solutions. *Journal of the American Chemical Society*, 2002, **124**, 11946-11954.
70. Liu, Y. Y., Murata, K., Inaba, M. Epoxidation of propylene with molecular oxygen in methanol over a peroxo-heteropoly compound immobilized on palladium exchanged HMS. *Green Chemistry*, 2004, **6**, 510-515.

71. Liu, Y. Y., Murata, K., Inaba, M., Mimura, N. Selective oxidation of propylene to propylene oxide by molecular oxygen over Ti-Al-HMS catalysts. *Catalysis Letters*, 2003, **89**, 49-53.
72. Welton, T. Ionic liquid in catalysis. *Coordination Chemistry Reviews*, 2004, **248**, 2459-2477.
73. Owens, G. S., Abu-Omar, M. M. Methyltrioxorhenium-catalyzed epoxidations in ionic liquids. *Chemical Communications*, 2000, **13**, 1165-1166.
74. Kuhn, F. E., Zhao, J., Abrantes, M., Sun, W., Afonso, C. A. M., Branco, L. C., Goncalves, I. S., Pillinger, M., Romao, C. C. Catalytic olefin epoxidation with cyclopentadienyl-molybdenum complexes in room temperature ionic liquids. *Tetrahedron Letters*, 2005, **46**, 47-52.
75. Valente, A. A., Petrovski, Z., Branco, L. C., Afonso, C. A. M., Pillinger, M., Lopes, A. D., Romao, C. C., Nunes, C. D., Goncalves, I. S. Epoxidation of cyclooctene catalyzed by dioxomolybdenum(VI) complexes in ionic liquids. *Journal of Molecular Catalysis A: Chemical*, 2004, **218**, 5-11.
76. Smith, K., Liu, S. F., El-Hiti, G. A. Use of ionic liquids as solvents for epoxidation reactions catalysed by a chiral Katsuki-type salen complex: Enhanced reactivity and recovery of catalyst. *Catalysis Letters*, 2004, **98**, 95-101.
77. Li, Z., Xia, C. G. Epoxidation of olefins catalyzed by manganese(III) porphyrin in a room temperature ionic liquid. *Tetrahedron Letters*, 2003, **44**, 2069-2071.
78. Tong, K. H., Wong, K. Y., Chan, T. H. Manganese/bicarbonate-catalyzed epoxidation of lipophilic alkenes with hydrogen peroxide in ionic liquids. *Organic Letters*, 2003, **5**, 3423-3425.
79. Srinivas, K. A., Kumar, A., Chauhan, S. M. S. Epoxidation of alkenes with

- hydrogen peroxide catalyzed by iron(III) porphyrins in ionic liquids. *Chemical Communications*, 2002, **20**, 2456-2457.
80. Song, C. E., Roh, E. J. Practical method to recycle a chiral (salen)Mn epoxidation catalyst by using an ionic liquid. *Chemical Communications*, 2000, **10**, 837-838.
 81. Noyori, R., Aoki, M., Sato, K. Green oxidation with aqueous hydrogen peroxide. *Chemical Communications*, 2003, **16**, 1977-1986.
 82. Venturello, C., Alneri, E., Ricci, M. A new, effective catalytic system for epoxidation of olefins by hydrogen peroxide under phase-transfer conditions. *The Journal of Organic Chemistry*, 1983, **48**, 3831-3833.
 83. Venturello, C., Ricci, M. Oxidative cleavage of 1,2-diols to carboxylic acids by hydrogen peroxide. *The Journal of Organic Chemistry*, 1986, **51**, 1599-1602.
 84. Sakaguchi, S., Nishiyama, Y., Ishii, I. Selective oxidation of monoterpenes with hydrogen peroxide catalyzed by peroxotungstophosphate (PCWP). *The Journal of Organic Chemistry*, 1996, **61**, 5307-5311.
 85. Witte, P. T., Alsters, P. L., Jary, W., Mullner, R., Pochlauer, P., Sloboda-Rozner, D., Neumann, R. Self-assembled $\text{Na}_{12}[\text{WZn}_3(\text{ZnW}_9\text{O}_{34})_2]$ as an industrial attractive multi-purpose catalyst for oxidations with aqueous hydrogen peroxide. *Organic Process Research & Development*, 2004, **8**, 524-531.
 86. Gao, S. A., Li, M., Lv, Y., Zhou, N., Xi, Z. W. Epoxidation of propylene with aqueous hydrogen peroxide on a reaction-controlled phase-transfer catalyst. *Organic Process Research & Development*, 2004, **8**, 131-132.
 87. Yadav, G. D., Pujari, A. A. Epoxidation of styrene to styrene oxide: Synergism of heteropoly acid and phase-transfer catalyst under Ishii-Venturello mechanism. *Organic Process Research & Development*, 2000, **4**, 88-93.

88. Yang, X., Gao, S., Xi, Z. W. Reaction-controlled phase transfer catalysis for styrene epoxidation to styrene oxide with aqueous hydrogen peroxide. *Organic Process Research & Development*, 2005, **9**, 294-296.
89. Mase, N., Ohno, T., Morimoto, H., Nitta, F., Yoda, H., Takabe, K. Enantioselective reactions of *tert*-butyl glycinate-benzophenone Schiff base catalyzed by chiral phase-transfer catalyst in aqueous media without any organic solvent. *Tetrahedron Letters*, 2005, **46**, 3213-3216.
90. Lu, Y., Li, M., Zhang, R. H., Xi, Z. W., Gao, S. A new quaternary ammonium heteropolyoxotungstate catalyst for propylene epoxidation to propylene oxide. *Chinese Chemical Letters*, 2004, **15**, 1491-1493.
91. Perego, G., Notari, B., Taramasso, M., US, **1981**, p. 18.
92. van Vliet, M. C. A., Mandelli, D., Arends, I., Schuchardt, U., Sheldon, R. A. Alumina: a cheap, active and selective catalyst for epoxidations with (aqueous) hydrogen peroxide. *Green Chemistry*, 2001, **3**, 243-246.
93. Cesquini, R. G., Silva, J., Woitiski, C. B., Mandelli, D., Rinaldi, R., Schuchardt, U. Alumina-catalyzed epoxidation with hydrogen peroxide: Recycling experiments and activity of sol-gel alumina. *Advanced Synthesis & Catalysis*, 2002, **344**, 911-914.
94. Wu, P., Tatsumi, T. A novel titanosilicate with MWW structure III. Highly efficient and selective production of glycidol through epoxidation of allyl alcohol with H₂O₂. *Journal of Catalysis*, 2003, **214**, 317-326.
95. Pletcher, D. *Industrial electrochemistry*. London: Chapman and Hall, 1990.
96. Pletcher, D. Indirect oxidations using electrogenerated hydrogen peroxide. *Acta Chemica Scandinavica*, 1999, **53**, 745-750.
97. Novotny, L., Navratil, T. Effect of surfactants and related biological active substances on the O₂/H₂O₂ voltammetry and its utilization for determination of

- the total surfactant content. *Electroanalysis*, 1998, **10**, 557-561.
98. Johnston, D. A., Cardosi, M. F., Vaughan, D. H. The electrochemistry of hydrogen peroxide on evaporated gold/palladium composite electrodes - manufacture and electrochemical characterization. *Electroanalysis*, 1995, **7**, 520-526.
 99. Gerlache, M., Senturk, Z., Quarin, G., Kauffmann, J. M. Electrochemical behavior of H₂O₂ on gold. *Electroanalysis*, 1997, **9**, 1088-1092.
 100. Maruyama, J., Abe, I. Cathodic oxygen reduction at the interface between Nafion (R) and electrochemically oxidized glassy carbon surfaces. *Journal of Electroanalytical Chemistry*, 2002, **527**, 65-70.
 101. Salimi, A., Eshghi, H., Sharghi, H., Golabi, S. M., Shamsipur, M. Electrocatalytic reduction of dioxygen at the surface of glassy carbon electrodes modified by some anthraquinone substituted podands. *Electroanalysis*, 1999, **11**, 114-119.
 102. Taylor, R. J., Humffray, A. A. Electrochemical studies on glassy carbon electrodes. 3. Oxygen reduction in solutions of low pH (pH less than 10). *Journal of Electroanalytical Chemistry*, 1975, **64**, 85-94.
 103. Taylor, R. J., Humffray, A. A. Electrochemical studies on glassy carbon electrodes. 2. Oxygen reduction in solutions of high pH (pH greater than 10). *Journal of Electroanalytical Chemistry*, 1975, **64**, 63-84.
 104. Taylor, R. J., Humffray, A. A. Electrochemical studies on glassy carbon electrodes. 4. Influence of solution pH and buffer capacity on reduction of oxygen. *Journal of Electroanalytical Chemistry*, 1975, **64**, 95-105.
 105. Taylor, R. J., Humffray, A. A. Electrochemical studies on glassy carbon electrodes. 1. Electron transfer kinetics. *Journal of Electroanalytical Chemistry*, 1973, **42**, 347-354.

106. Mao, L. Q., Zhang, D., Sotomura, T., Nakatsu, K., Koshiba, N., Ohsaka, T. Mechanistic study of the reduction of oxygen in air electrode with manganese oxides as electrocatalysts. *Electrochimica Acta*, 2003, **48**, 1015-1021.
107. Baez, V. B., Pletcher, D. Preparation and characterization of carbon titanium dioxide surfaces - The reduction of oxygen. *Journal of Electroanalytical Chemistry*, 1995, **382**, 59-64.
108. Zimmer, A., Monter, D., Reschetilowski, W. Catalytic epoxidation with electrochemically *in situ* generated hydrogen peroxide. *Journal of Applied Electrochemistry*, 2003, **33**, 933-937.
109. Qiang, Z. M., Chang, J. H., Huang, C. P. Electrochemical generation of hydrogen peroxide from dissolved oxygen in acidic solutions. *Water Research*, 2002, **36**, 85-94.
110. Ilea, P., Dorneanu, S., Nicoara, A. Hydrogen peroxide electrosynthesis by partial oxygen reduction in alkaline media. I - Voltammetric study on unmodified carbonaceous materials. *Revue Roumaine De Chimie*, 1999, **44**, 555-561.
111. Yeager, E. Electrocatalysts for O₂ reduction. *Electrochimica Acta*, 1984, **29**, 1527-1537.
112. Lovrecek, B., Batinic, M., Caja, J. The electrochemical oxygen reduction on the graphite electrode. *Electrochimica Acta*, 1983, **28**, 685-690.
113. Pons, S., Khoo, S. B. Reductions in aprotic media .1. Cathodic reduction limits at a platinum electrode in acetonitrile. *Electrochimica Acta*, 1982, **27**, 1161-1169.
114. Li, Y. J., Lenigk, R., Wu, X. Z., Gruendig, B., Dong, S. J., Renneberg, R. Investigation of oxygen- and hydrogen peroxide-reduction on platinum particles dispersed on poly(*o*-phenylenediamine) film modified glassy carbon

- electrodes. *Electroanalysis*, 1998, **10**, 671-676.
115. Venkatachalapathy, R., Davila, G. P., Prakash, J. Catalytic decomposition of hydrogen peroxide in alkaline solutions. *Electrochemistry Communications*, 1999, **1**, 614-617.
 116. Zecevic, S., Drazic, D. M., Gojkovic, S. Oxygen reduction on iron .4. The reduction of hydrogen-peroxide as the intermediate in oxygen reduction in alkaline solutions. *Electrochimica Acta*, 1991, **36**, 5-14.
 117. Foller, P. C., Bombard, R. T. Processes for the production of mixtures of caustic soda and hydrogen peroxide via the reduction of oxygen. *Journal of Applied Electrochemistry*, 1995, **25**, 613-627.
 118. Oloman, C. Trickle bed electrochemical reactors. *Journal of the Electrochemical Society*, 1979, **126**, 1885-1892.
 119. Oloman, C., Watkinson, A. P. Hydrogen peroxide production in trickle bed electrochemical reactors. *Journal of Applied Electrochemistry*, 1979, **9**, 117-123.
 120. McIntyre, J. A. Synthesis of hydrogen peroxide via the partial electroreduction of oxygen in alkaline solution. *Electrochemical Society Interface*, 1995, **4**, 29-33.
 121. Alcaide, F., Brillas, E., Cabot, P. L. Electrogenation of hydroperoxide ion using an alkaline fuel cell. *Journal of the Electrochemical Society*, 1998, **145**, 3444-3449.
 122. Alcaide, F., Brillas, E., Cabot, P. L. Oxygen reduction on uncatalyzed carbon-PTFE gas diffusion cathode in alkaline medium. *Journal of the Electrochemical Society*, 2002, **149**, E64-E70.
 123. Tissot, P., Huissoud, A. Proton effects in the electrochemical behaviour of 2-ethyl-9,10-anthraquinone in the medium

- dimethoxyethane-tetrabutylammonium hydroxide with and without oxygen. *Electrochimica Acta*, 1996, **41**, 2451-2456.
124. Huissoud, A., Tissot, P. Electrochemical reduction of 2-ethyl-9,10-anthraquinone (EAQ) and mediated formation of hydrogen peroxide in a two-phase medium - Part II: Production of alkaline hydrogen peroxide by the intermediate electroreduction of EAQ in a flow-by porous electrode in two-phase liquid-liquid flow. *Journal of Applied Electrochemistry*, 1999, **29**, 17-25.
 125. Huissoud, A., Tissot, P. Electrochemical reduction of 2-ethyl-9,10-anthraquinone (EAQ) and mediated formation of hydrogen peroxide in a two-phase medium - Part I: Electrochemical behaviour of EAQ on a vitreous carbon rotating disc electrode (RDE) in the two-phase medium. *Journal of Applied Electrochemistry*, 1999, **29**, 11-16.
 126. Gyenge, E. L., Oloman, C. W. Electrosynthesis of hydrogen peroxide in acidic solutions by mediated oxygen reduction in a three-phase (aqueous/organic/gaseous) system Part I: Emulsion structure, electrode kinetics and batch electrolysis. *Journal of Applied Electrochemistry*, 2003, **33**, 655-663.
 127. Gyenge, E. L., Oloman, C. W. Electrosynthesis of hydrogen peroxide in acidic solutions by mediated oxygen reduction in a three-phase (aqueous/organic/gaseous) system. Part II: Experiments in flow-by fixed-bed electrochemical cells with three-phase flow. *Journal of Applied Electrochemistry*, 2003, **33**, 665-674.
 128. AlNashef, I. M., Leonard, M. L., Matthews, M. A., Weidner, J. W. Superoxide electrochemistry in an ionic liquid. *Industrial & Engineering Chemistry Research*, 2002, **41**, 4475-4478.

129. AlNashef, I. M., Leonard, M. L., Kittle, M. C., Matthews, M. A., Weidner, J. W. Electrochemical generation of superoxide in room-temperature ionic liquids. *Electrochemical and Solid State Letters*, 2001, **4**, D16-D18.
130. Tang, C. Y., Wong, K. Y., Chan, T. H. Electrosynthesis of hydrogen peroxide in room temperature ionic liquids and *in situ* epoxidation of alkenes. *Chemical Communications*, 2005, **10**, 1345-1347.
131. Vaudano, P., Plattner, E., Comninellis, C. The industrial electrolytic regeneration of $\text{Mn}_2(\text{SO}_4)_3$ for the oxidation of substituted toluene to the corresponding benzaldehyde. *Chimia*, 1995, **49**, 12-16.
132. Kreh, R. P., Spotnitz, R. M., Lundquist, J. T. Mediated electrochemical synthesis of aromatic aldehydes, ketones, and quinones using ceric methanesulfonate. *The Journal of Organic Chemistry*, 1989, **54**, 1526-1131.
133. Spotnitz, R. M., Kreh, R. P., Lundquist, J. T., Press, P. J. Mediated electrosynthesis with cerium(IV) in methanesulfonic acid. *Journal of Applied Electrochemistry*, 1990, **20**, 209-215.
134. Steele, D. F. Electrochemical destruction of toxic organic industrial waste. *Platinum Metals Review*, 1990, **34**, 10-14.
135. Harrington, T., Pletcher, D. The removal of low levels of organics from aqueous solutions using Fe(II) and hydrogen peroxide formed *in situ* at gas diffusion electrodes. *Journal of the Electrochemical Society*, 1999, **146**, 2983-2989.
136. Alvarez-Gallegos, A., Pletcher, D. The removal of low level organics via hydrogen peroxide formed in a reticulated vitreous carbon cathode cell. Part 2: The removal of phenols and related compounds from aqueous effluents. *Electrochimica Acta*, 1999, **44**, 2483-2492.
137. Alvarez-Gallegos, A., Pletcher, D. The removal of low level organics via

- hydrogen peroxide formed in a reticulated vitreous carbon cathode cell, Part 1. The electrosynthesis of hydrogen peroxide in aqueous acidic solutions. *Electrochimica Acta*, 1998, **44**, 853-861.
138. Creager, S. E., Raybuck, S. A., Murray, R. W. An efficient electrocatalytic model cytochrome P-450 epoxidation cycle. *Journal of the American Chemical Society*, 1986, **108**, 4225-4226.
 139. Vaze, A., Parizo, M., Rusling, J. F. Enhanced rates of electrolytic styrene epoxidation catalyzed by cross-linked myoglobin-poly(L-lysine) films in bicontinuous microemulsions. *Langmuir*, 2004, **20**, 10943-10948.
 140. Estavillo, C., Lu, Z. Q., Jansson, I., Schenkman, J. B., Rusling, J. F. Epoxidation of styrene by human cyt P450 1A2 by thin film electrolysis and peroxide activation compared to solution reactions. *Biophysical Chemistry*, 2003, **104**, 291-296.
 141. Munge, B., Estavillo, C., Schenkman, J. B., Rusling, J. F. Optimization of electrochemical and peroxide-driven oxidation of styrene with ultrathin polyelectrolyte films containing cytochrome p450(cam) and myoglobin. *Chembiochem*, 2003, **4**, 82-89.
 142. Zu, X. L., Lu, Z. Q., Zhang, Z., Schenkman, J. B., Rusling, J. F. Electroenzyme-catalyzed oxidation of styrene and *cis*-beta-methylstyrene using thin films of cytochrome P450cam and myoglobin. *Langmuir*, 1999, **15**, 7372-7377.
 143. Kandzia, C., Steckhan, E. Electrochemical epoxidation of electron-poor olefins using silver bipyridine based redox mediators. *Tetrahedron Letters*, 1994, **35**, 3695-3698.
 144. Van der Eijk, J. M., Peters, T. J., De Wit, N., Colijn, H. A. Electrochemical epoxidation of olefins. *Catalysis Today*, 1988, **3**, 2-3.

145. Groves, J. T., Gilbert, J. A. Electrochemical generation of an iron(IV) porphyrin. *Inorganic Chemistry*, 1986, **25**, 123-125.
146. Tanaka, K., Miura, T., Umezawa, N., Urano, Y., Kikuchi, K., Higuchi, T., Nagano, T. Rational design of fluorescein-based fluorescence probes, mechanism-based design of a maximum fluorescence probe for singlet oxygen. *Journal of the American Chemical Society*, 2001, **123**, 2530-2536.
147. Chen, C. Y., Cheng, S. H., Su, Y. O. Electrocatalytic oxidation of styrene by a high valent ruthenium porphyrin cation radical. *Journal of Electroanalytical Chemistry*, 2000, **487**, 51-56.
148. Nishihara, H., Pressprich, K., Murray, R. W., Collman, J. P. Electrochemical olefin epoxidation with manganese *meso*-tetraphenylporphyrin catalyst and hydrogen peroxide generation at polymer-coated electrodes. *Inorganic Chemistry*, 1990, **29**, 1000-1006.
149. Zhang, X. Y., Cui, B. Q., Gu, D. P., Li, W. Cathodic indirect oxidation of organic compounds. II. Cathodic indirect epoxidation of olefin. *Dianhuaxue*, 2000, **6**, 324-328.
150. Ling, T. R., Lin, Z. C., Yang, M. C., Chou, T. C. Synthesis of propylene oxide in a paired electrolytic system: Studies on the mechanism and operating factors. *Journal of the Chinese Institute of Chemical Engineers*, 2001, **32**, 341-349.
151. Shen, Y., Atobe, M., Li, W., Nonaka, T. Paired electrosynthesis of epoxides and dibromides from olefinic compounds. *Electrochimica Acta*, 2003, **48**, 1041-1046.
152. Clerici, M. G., Bellussi, G., Romano, U. Synthesis of propylene oxide from propylene and hydrogen peroxide catalyzed by titanium silicalite. *Journal of Catalysis*, 1991, **129**, 159-167.

153. Wu, P., Tatsumi, T. Extremely high trans selectivity of Ti-MWW in epoxidation of alkenes with hydrogen peroxide. *Chemical Communications*, 2001, **10**, 897-898.
154. Wang, Y., Zhang, Q. h., Shishido, T., Takehira, K. Characterizations of iron-containing MCM-41 and its catalytic properties in epoxidation of styrene with hydrogen peroxide. *Journal of Catalysis*, 2002, **209**, 186-196.
155. Yamaguchi, K., Mizugaki, T., Ebitani, K., Kaneda, K. Heterogeneous N-oxidation of pyridines using a combined oxidant of hydrogen peroxide and nitriles catalysed by basic hydrotalcites. *New Journal of Chemistry*, 1999, **23**, 799-801.
156. Ueno, S., Yamaguchi, K., Yoshida, K., Ebitani, K., Kaneda, K. Hydrotalcite catalysis: Heterogeneous epoxidation of olefins using hydrogen peroxide in the presence of nitriles. *Chemical Communications*, 1998, **3**, 295-296.
157. Cativiela, C., Figueras, F., Fraile, J. M., Garcia, J. I., Mayoral, J. A. Hydrotalcite-promoted epoxidation of electron-deficient alkenes with hydrogen peroxide. *Tetrahedron Letters*, 1995, **36**, 4125-4158.
158. Mandelli, D., van Vliet, M. C. A., Arnold, U., Sheldon, R. A., Schuchardt, U. Epoxidation of alkenes with hydrogen peroxide catalyzed by $\text{ReO}_4\text{-SiO}_2\text{-Al}_2\text{O}_3$ and $\text{ReO}_4\text{-Al}_2\text{O}_3$. *Journal of Molecular Catalysis A: Chemical*, 2001, **168**, 165-171.
159. Reichle, W. T., Kang, S. Y., Everhardt, D. S. The nature of the thermal decomposition of a catalytically active anionic clay mineral. *Journal of Catalysis*, 1986, **101**, 352-359.
160. Lane, B. S., Burgess, K. Metal-catalyzed epoxidations of alkenes with hydrogen peroxide. *Chemical Reviews*, 2003, **103**, 2457-2473.
161. Herrmann, W. A., Fischer, R. W., Rauch, M. U., Scherer, W. Multiple bonds

- between main-group elements and transition metals. 125. Alkylrhenium oxides as homogeneous epoxidation catalysts: Activity, selectivity, stability, deactivation. *Journal of Molecular Catalysis*, 1994, **86**, 246-266.
162. Herrmann, W. A., Fischer, R. W., Marz, D. W. Multiple bonding between Main Group elements and transition metals. 100. Part 2. Methyltrioxorhenium as catalyst for olefin oxidation. *Angewandte Chemie-International Edition*, 1991, **30**, 1638-1641.
163. Gisdakis, P., Antonczak, S., Kostlmeier, S., Herrmann, W. A., Rosch, N. Olefin epoxidation by methyltrioxorhenium: A density functional study on energetics and mechanisms. *Angewandte Chemie-International Edition*, 1998, **37**, 2211-2214.
164. Wu, Y. D., Sun, J. Transition Structures of Epoxidation by $\text{CH}_3\text{Re}(\text{O})_2(\text{O}_2)$ and $\text{CH}_3\text{Re}(\text{O})(\text{O}_2)_2$ and Their Water Adducts. *The Journal of Organic Chemistry*, 1998, **63**, 1752-1753.
165. Mizuno, N., Nozaki, C., Kiyoto, I., Misono, M. Highly efficient utilization of hydrogen peroxide for selective oxygenation of alkanes catalyzed by diiron-substituted polyoxometalate precursor. *Journal of the American Chemical Society*, 1998, **120**, 9267-9272.
166. Ben-Daniel, R., Khenkin, A. M., Neumann, R. The nickel-substituted quasi-Wells-Dawson-type polyfluorooxometalate, $[\text{NiII}(\text{H}_2\text{O})\text{H}_2\text{F}_6\text{NaW}_{17}\text{O}_{55}]_9^-$, as a uniquely active nickel-based catalyst for the activation of hydrogen peroxide and the epoxidation of alkenes and alkenols. *Chemistry - A European Journal*, 2000, **6**, 3722-3728.
167. Venturello, C., D'Aloisio, R. Quaternary ammonium tetrakis(diperoxotungsto)phosphates as a new class of catalysts for efficient alkene epoxidation with hydrogen peroxide. *The Journal of Organic*

- Chemistry*, 1988, **53**, 1553-1557.
168. Gelbard, G., Raison, F., Roditi-Lachter, E., Thouvenot, R., Ouahab, L., Grandjean, D. Epoxidation of allylic alcohols by hydrogen peroxide in the presence of complexed peroxotungstic species. *Journal of Molecular Catalysis A: Chemical*, 1996, **114**, 77-85.
 169. Quenard, M., Bonmarin, V., Gelbard, G. Epoxidation of olefins by hydrogen peroxide catalyzed by phosphonotungstic complexes. *Tetrahedron Letters*, 1987, **28**, 2237-2238.
 170. Prandi, J., Kagan, H. B., Mimoun, H. Epoxidation of isolated double bonds with 30% hydrogen peroxide catalyzed by pertungstate salts. *Tetrahedron Letters*, 1986, **27**, 2617-2620.
 171. Prat, D., Lett, R. Epoxidations with 30% hydrogen peroxide catalyzed by tungstic acid in buffered media. *Tetrahedron Letters*, 1986, **27**, 707-710.
 172. Csanyi, L. J., Jaky, K. Some features of epoxidation of cyclohexene catalyzed by oxoperoxometallates under phase-transfer conditions. *Journal of Catalysis*, 1991, **127**, 42-50.
 173. Kamiyama, T., Inoue, M., Enomoto, S. Effect of amines on the epoxidation of alkenes with hydrogen peroxide in the presence of molybdenum(VI) oxide-bis(tributyltin) oxide catalysts. *Chemistry Letters*, 1989, **7**, 1129-1130.
 174. Griffith, W. P., Parkin, B. C., White, A. J. P., Williams, D. J. The crystal structures of $[\text{NMe}_4]_2[(\text{PhPO}_3)\{\text{MoO}(\text{O}_2)_2\}_2\{\text{MoO}(\text{O}_2)_2(\text{H}_2\text{O})\}]$ and $[\text{NBun}_4]_2[\text{W}_4\text{O}_6(\text{O}_2)_6(\text{OH})_2(\text{H}_2\text{O})_2]$ and their use as catalytic oxidants. *Journal of the Chemical Society, Dalton Transactions*, 1995, **19**, 3131-3138.
 175. Bortolini, O., Di Furia, F., Modena, G., Seraglia, R. Metal catalysis in oxidation by peroxides. Sulfide oxidation and olefin epoxidation by dilute hydrogen peroxide, catalyzed by molybdenum and tungsten derivatives under

- phase-transfer conditions. *The Journal of Organic Chemistry*, 1985, **50**, 2688-2690.
176. Ishii, Y., Yamawaki, K., Yoshida, T., Ura, T., Ogawa, M. Oxidation of olefins and alcohols by peroxo-molybdenum complex derived from tris(cetylpyridinium) 12-molybdophosphate and hydrogen peroxide. *The Journal of Organic Chemistry*, 1987, **52**, 1868-1870.
177. Trost, B. M., Masuyama, Y. Molybdenum catalyzed reactions. Selectivity in oxidations with hydrogen peroxide and ammonium molybdate. *Israel Journal of Chemistry*, 1984, **24**, 134-143.
178. Renaud, J. P., Battioni, P., Bartoli, J. F., Mansuy, D. A very efficient system for alkene epoxidation by hydrogen peroxide: Catalysis by manganese-porphyrins in the presence of imidazole. *Chemical Communications*, 1985, **13**, 888-889.
179. Battioni, P., Renaud, J. P., Bartoli, J. F., Reina-Artiles, M., Fort, M., Mansuy, D. Monooxygenase-like oxidation of hydrocarbons by hydrogen peroxide catalyzed by manganese porphyrins and imidazole: Selection of the best catalytic system and nature of the active oxygen species. *Journal of the American Chemical Society*, 1988, **110**, 8462-8470.
180. Gonsalves, A. M. D. R., Johnstone, R. A. W., Pereira, M. M., Shaw, J. Metal-assisted reactions. Part 21. Epoxidation of alkenes catalyzed by manganese-porphyrins: The effects of various oxidatively-stable ligands and bases. *Journal of the Chemical Society, Perkin Transactions 1*, 1991, **3**, 645-649.
181. Thellend, A., Battioni, P., Mansuy, D. Ammonium acetate as a very simple and efficient cocatalyst for manganese porphyrin-catalyzed oxygenation of hydrocarbons by hydrogen peroxide. *Chemical Communications*, 1994, **9**, 1035-1036.

182. Traylor, T. G., Xu, F. A biomimetic model for catalase: The mechanisms of reaction of hydrogen peroxide and hydroperoxides with iron(III) porphyrins. *Journal of the American Chemical Society*, 1987, **109**, 6201-6202.
183. Traylor, T. G., Fann, W. P., Bandyopadhyay, D. A Common heterolytic mechanism for reactions of iodosobenzenes, peracids, hydroperoxides, and hydrogen peroxide with iron(III) porphyrins. *Journal of the American Chemical Society*, 1989, **111**, 8009-8010.
184. Traylor, T. G., Xu, F. Mechanisms of reactions of iron(III) porphyrins with hydrogen peroxide and hydroperoxides - Solvent and solvent isotope effects. *Journal of the American Chemical Society*, 1990, **112**, 178-186.
185. Schwenkreis, T., Berkessel, A. A biomimetic catalyst for the asymmetric epoxidation of unfunctionalized olefins with hydrogen peroxide. *Tetrahedron Letters*, 1993, **34**, 4785-4788.
186. Berkessel, A., Frauenkron, M., Schwenkreis, T., Steinmetz, A., Baum, G., Fenske, D. Pentacoordinated manganese(III) dihydrosalen complexes as biomimetic oxidation catalysts. *Journal of Molecular Catalysis A: Chemical*, 1996, **113**, 321-342.
187. Irie, R., Hosoya, N., Katsuki, T. Enantioselective epoxidation of chromene derivatives using hydrogen peroxide as a terminal oxidant. *Synlett*, 1994, **4**, 255-256.
188. Pietikainen, P. Convenient asymmetric (salen)Mn(III)-catalyzed epoxidation of unfunctionalized alkenes with hydrogen peroxide using carboxylate salt cocatalysts. *Tetrahedron*, 1998, **54**, 4319-4326.
189. Pietikainen, P. Asymmetric Mn(III)-salen catalyzed epoxidation of unfunctionalized alkenes with *in situ* generated peroxycarboxylic acids. *Journal of Molecular Catalysis a-Chemical*, 2001, **165**, 73-79.

190. Pietikainen, P. Asymmetric Mn(III)-salen catalyzed epoxidation of unfunctionalized alkenes with *in situ* generated peroxycarboxylic acids. *Journal of Molecular Catalysis A: Chemical*, 2001, **165**, 73-79.
191. Hage, R., Iburg, J. E., Kerschner, J., Koek, J. H., Lempers, E. L. M., Martens, R. J., Racherla, U. S., Russell, S. W., Swarthoff, T. Efficient manganese catalysts for low-temperature bleaching. *Nature*, 1994, **369**, 637-639.
192. Berkessel, A., Sklorz, C. A. Mn-trimethyltriazacyclononane/ascorbic acid: A remarkably efficient catalyst for the epoxidation of olefins and the oxidation of alcohols with hydrogen peroxide. *Tetrahedron Letters*, 1999, **40**, 7965-7968.
193. Brinksma, J., Schmieder, L., van Vliet, G., Boaron, R., Hage, R., De Vos, D. E., Alsters, P. L., Feringa, B. L. Homogeneous *cis*-dihydroxylation and epoxidation of olefins with high H₂O₂ efficiency by a mixed manganese/activated carbonyl catalyst system. *Tetrahedron Letters*, 2002, **43**, 2619-2622.
194. Bolm, C., Meyer, N., Raabe, G., Weyhermuller, T., Bothe, E. A novel enantiopure proline-derived triazacyclononane: Synthesis, structure and application of its manganese complex. *Chemical Communications*, 2000, **24**, 2435-2436.
195. Bolm, C., Kadereit, D., Valacchi, M. Enantioselective olefin epoxidation with chiral manganese-1,4,7-triazacyclononane complexes. *Synlett*, 1997, **6**, 687-688.
196. Bolm, C., Meyer, N., Raabe, G., Weyhermuller, T., Bothe, E. A novel enantiopure proline-derived triazacyclononane: Synthesis, structure and application of its manganese complex. *Chemical Communications*, 2000, **24**, 2435-2436.
197. Argouarch, G., Gibson, C. L., Stones, G., Sherrington, D. C. The synthesis of

- chiral annulet 1,4,7-triazacyclononanes. *Tetrahedron Letters*, 2002, **43**, 3795-3798.
198. Pradhan, B. P., Chakraborty, S., Weyerstahl, P. Studies on oxidation of triterpenoids. Part VII. Transformation of oleanane and ursane skeletons to 11a,12a-oxidotriterpenoids with hydrogen peroxide and selenium dioxide and their carbon-13 NMR data. *Tetrahedron*, 1987, **43**, 4487-4495.
 199. Betzemeier, B., Lhermitte, F., Knochel, P. A selenium-catalyzed epoxidation in perfluorinated solvents with hydrogen peroxide. *Synlett*, 1999, **4**, 489-491.
 200. Wten Brink, G. J., Fernandes, B. C. M., van Vliet, M. C. A., Arends, I. W. C. E., Sheldon, R. A. Selenium catalyzed oxidations with aqueous hydrogen peroxide. Part I. Epoxidation reactions in homogeneous solution. *Journal of the Chemical Society, Perkin Transactions 1*, 2001, **3**, 224-228.
 201. Itakura, J., Tanaka, H., Ito, H. Epoxidation of eight- and twelve-membered cyclic olefins with hydrogen peroxide in the presence of metal oxide catalysts. *Bulletin of the Chemical Society of Japan*, 1969, **42**, 1604-1608.
 202. Berkessel, A., Andreae, M. R. M. Efficient catalytic methods for the Baeyer-Villiger oxidation and epoxidation with hydrogen peroxide. *Tetrahedron Letters*, 2001, **42**, 2293-2295.
 203. Jacobson, S. E., Mares, F., Zambri, P. M. Biphasic and triphasic catalysis. Arsonated polystyrenes as catalysts for epoxidation of olefins by aqueous hydrogen peroxide. *Journal of the American Chemical Society*, 1979, **101**, 6946-6950.
 204. Lane, B. S., Burgess, K. A cheap, catalytic, scalable, and environmentally benign method for alkene epoxidations. *Journal of the American Chemical Society*, 2001, **123**, 2933-2934.
 205. Banfi, S., Montanari, F., Quici, S., Barkanova, S. V., Kaliya, O. L.,

- Kopranenkov, N., Luk'yanets, E. A. Porphyrins and azaporphines as catalysts in alkene epoxidations with peracetic acid. *Tetrahedron Letters*, 1995, **36**, 2317-2320.
206. Banfi, S., Cavazzini, M., Coppa, F., Barkanova, S. V., Kaliya, O. L. Manganese-porphyrins and -azaporphyrins as catalysts in alkene epoxidations with peracetic acid. Part 2. Kinetics and mechanism. *Journal of the Chemical Society, Perkin Transactions 2*, 1997, **8**, 1577-1583.
207. Banfi, S., Cavazzini, M., Pozzi, G., Barkanova, S. V., Kaliya, O. L. Kinetic studies on the interactions of manganese-porphyrins with peracetic acid. Part 1. Epoxidation of alkenes and hydroxylation of aromatic rings. *Journal of the Chemical Society, Perkin Transactions 2*, 2000, **4**, 871-877.
208. Banfi, S., Cavazzini, M., Pozzi, G., Barkanova, S. V., Kaliya, O. L. Kinetic studies on the interactions of manganese-porphyrins with peracetic acid. Part 2. The influence of acetic acid and porphyrin substituents. *Journal of the Chemical Society, Perkin Transactions 2*, 2000, **4**, 879-885.
209. Barkanova, S. V., Kaliya, O. L. Naphthalene oxidation by peracetic acid catalyzed by Mn(III) porphine-like complexes: Nature of intermediates and pathways of their formation. *Journal of Porphyrins and Phthalocyanines*, 1999, **3**, 180-187.
210. Barkanova, S. V., Kaliya, O. L., Luk'yanets, E. A. Naphthalene oxidation by peracetic acid catalyzed by Mn^{3+} porphinoid complexes. *Mendeleev Communications*, 2001, **3**, 116-118.
211. Barkanova, S. V., Makarova, E. A. Mechanism of the interaction of Mn tetraazaporphines with peracetic acid. The comparative reactivity of Mn(III) porphinoid complexes in the formation of Mn-oxenes. *Journal of Molecular Catalysis A: Chemical*, 2001, **174**, 89-105.

212. Murphy, A., Dubois, G., Stack, T. D. P. Efficient epoxidation of electron-deficient olefins with a cationic manganese complex. *Journal of the American Chemical Society*, 2003, **125**, 5250-5251.
213. Murphy, A., Pace, A., Stack, T. D. P. Ligand and pH influence on manganese-mediated peracetic acid epoxidation of terminal olefins. *Organic Letters*, 2004, **6**, 3119-3122.
214. Takeya, T., Egawa, H., Inoue, N., Miyamoto, A., Chuma, T., Kotani, E. Iron(III)picolinate-catalyzed oxygenation of cholesteryl acetate with hydrogen peroxide or peracetic acid. *Chemical & Pharmaceutical Bulletin*, 1999, **47**, 64-70.
215. Dubois, G., Murphy, A., Stack, T. D. P. Simple iron catalyst for terminal alkene epoxidation. *Organic Letters*, 2003, **5**, 2469-2472.
216. Lam, P. K. H., George, M. H., Barrie, J. A. Sulfonated polyurethane ionomers with new ionic diols. *Polymer*, 1989, **30**, 2320-2323.
217. Westbroek, P., Temmerman, E. Mechanism of hydrogen peroxide oxidation reaction at a glassy carbon electrode in alkaline solution. *Journal of Electroanalytical Chemistry*, 2000, **482**, 40-47.
218. Sawyer, D. T., Seo, E. T. One-electron mechanism for the electrochemical reduction of molecular oxygen. *Inorganic Chemistry*, 1977, **16**, 499-501.
219. Pardo, J., Mainar, A. M., Lopez, M. C., Royo, F., Urieta, J. S. Solubility of gases in butanols IV. Solubilities of nonpolar gases in 2-methyl-2-propanol at 303.15 K and 101.33 kPa partial pressure of gas. *Fluid Phase Equilibria*, 1999, **155**, 127-137.
220. Kutsche, I., Gildehaus, G., Schuller, D., Schumpe, A. Oxygen solubilities in aqueous alcohol solutions. *Journal of Chemical and Engineering Data*, 1984, **29**, 286-287.

221. Swatloski, R. P., Visser, A. E., Reichert, W. M., Broker, G. A., Farina, L. M., Holbrey, J. D., Rogers, R. D. Solvation of 1-butyl-3-methylimidazolium hexafluorophosphate in aqueous ethanol - A green solution for dissolving 'hydrophobic' ionic liquids. *Chemical Communications*, 2001, **20**, 2070-2071.
222. Visser, A. E., Holbrey, J. D., Rogers, R. D. Hydrophobic ionic liquids incorporating N-alkylisoquinolinium cations and their utilization in liquid-liquid separations. *Chemical Communications*, 2001, **23**, 2484-2485.
223. Papageorgiou, N. A., Y.; Armand, M.; Bonhote, P.; Pettersson, H.; Azam, A.; Graetzel, M. The performance and stability of ambient temperature molten salts for solar cell applications. *Journal of the Electrochemical Society*, 1996, **143**, 3099-3108.
224. Hagiwara, R., Hirashige, T., Tsuda, T., Ito, Y. Acidic 1-ethyl-3-methylimidazolium fluoride: A new room temperature ionic liquid. *Journal of Fluorine Chemistry*, 1999, **99**, 1-3.
225. Wheeler, C., West, K. N., Eckert, C. A., Liotta, C. L. Ionic liquids as catalytic green solvents for nucleophilic displacement reactions. *Chemical Communications*, 2001, **10**, 887-888.
226. Song, C. E., Roh, E. J., Lee, S. G., Shim, W. H., Choi, J. H. Ionic liquids as powerful media in scandium triflate catalysed Diels-Alder reactions: significant rate acceleration, Selectivity improvement and easy recycling of catalyst. *Chemical Communications*, 2001, **12**, 1122-1123.
227. Schofer, S. H., Kaftzik, N., Kragl, U., Wasserscheid, P. Enzyme catalysis in ionic liquids: lipase catalysed kinetic resolution of 1-phenylethanol with improved enantioselectivity. *Chemical Communications*, 2001, **5**, 425-426.
228. Barhdadi, R., Courtinard, C., Nedelec, J. Y., Troupel, M. Room-temperature ionic liquids as new solvents for organic electrosynthesis. The first examples

- of direct or nickel-catalysed electroreductive coupling involving organic halides. *Chemical Communications*, 2003, **12**, 1434-1435.
229. Doherty, A. P., Brooks, C. A. Electrosynthesis in room-temperature ionic liquids: Benzaldehyde reduction. *Electrochimica Acta*, 2004, **49**, 3821-3826.
 230. Davison, J. B., Kacsir, J. M., Peercelanders, P., Jasinski, R. J. A voltammetric investigation of oxygen reduction in a trickle bed electrochemical reactor. *Journal of the Electrochemical Society*, 1982, **129**, C119-C119.
 231. Gyenge, E. L., Oloman, C. W. Influence of surfactants on the electroreduction of oxygen to hydrogen peroxide in acid and alkaline electrolytes. *Journal of Applied Electrochemistry*, 2001, **31**, 233-243.
 232. Dzyuba, S. V., Bartsch, R. A. Expanding the polarity range of ionic liquids. *Tetrahedron Letters*, 2002, **43**, 4657-4659.
 233. Headley, A. D., Jackson, N. M. The effect of the anion on the chemical shifts of the aromatic hydrogen atoms of liquid 1-butyl-3-methylimidazolium salts. *Journal of Physical Organic Chemistry*, 2002, **15**, 52-55.
 234. Cammarata, L., Kazarian, S. G., Salter, P. A., Welton, T. Molecular states of water in room temperature ionic liquids. *Physical Chemistry Chemical Physics*, 2001, **3**, 5192-5200.
 235. *Determination of Hydrogen Peroxide By Potassium Permanganate Titration*. The American Association of Textile Chemists and Colorists, 102-2002, 2002.
 236. Sawyer, D. T., Sobkowiak, A., Roberts, J. L. *Electrochemistry for chemists*. New York: Wiley Interscience, 1995.
 237. Buzzeo, M. C., Hardacre, C., Compton, R. G. Use of room temperature ionic liquids in gas sensor design. *Analytical Chemistry*, 2004, **76**, 4583-4588.
 238. Camper, D., Scovazzo, P., Koval, C., Noble, R. Gas solubilities in room-temperature ionic liquids. *Industrial & Engineering Chemistry Research*,

- 2004, **43**, 3049-3054.
239. Hultgren, V. M., Mariotti, A. W. A., Bond, A. M., Wedd, A. G. Reference potential calibration and voltammetry at macrodisk electrodes of metallocene derivatives in the ionic liquid [bmim][PF₆]. *Analytical Chemistry*, 2002, **74**, 3151-3156.
 240. Zhang, J., Bond, A. M., Belcher, J., Wallace, K. J., Steed, J. W. Electrochemical studies on the modular podand 1,3,5-tris(3-((ferrocenylmethyl)amino)pyridiniumyl)-2,4,6-triethylbenzene hexafluorophosphate in conventional solvents and ionic liquids. *Journal of Physical Chemistry B*, 2003, **107**, 5777-5786.
 241. Amyes, T. L., Diver, S. T., Richard, J. P., Rivas, F. M., Toth, K. Formation and stability of N-heterocyclic carbenes in water: The carbon acid pK_a of imidazolium cations in aqueous solution. *Journal of the American Chemical Society*, 2004, **126**, 4366-4374.
 242. Nishida, T., Tashiro, Y., Yamamoto, M. Physical and electrochemical properties of 1-alkyl-3-methylimidazolium tetrafluoroborate for electrolyte. *Journal of Fluorine Chemistry*, 2003, **120**, 135-141.
 243. Huddleston, J. G., Visser, A. E., Reichert, W. M., Willauer, H. D., Broker, G. A., Rogers, R. D. Characterization and comparison of hydrophilic and hydrophobic room temperature ionic liquids incorporating the imidazolium cation. *Green Chemistry*, 2001, **3**, 156-164.
 244. Scovazzo, P., Camper, D., Kieft, J., Poshusta, J., Koval, C., Noble, R. Regular solution theory and CO₂ gas solubility in room-temperature ionic liquid. *Industrial & Engineering Chemistry Research*, 2004, **43**, 6855-6860.
 245. Espinal, L., Suib, S. L., Rusling, J. F. Electrochemical catalysis of styrene epoxidation with films of MnO₂ nanoparticles and H₂O₂. *Journal of the*

- American Chemical Society*, 2004, **126**, 7676-7682.
246. Wekesa, M., Ni, Y. H. Mechanism of hydrogen peroxide decomposition by manganese dioxide. *Tappi Journal*, 2003, **2**, 23-26.
 247. Scurto, A. M., Aki, S. N. V. K., Brennecke, J. F. Carbon dioxide induced separation of ionic liquids and water. *Chemical Communications*, 2003, **5**, 572-573.
 248. Swern, D. *Organic peroxides*. Toronto: John Wiley & Sons, 1970.
 249. Jorgensen, K. A. Transition metal-catalyzed epoxidations. *Chemical Reviews*, 1989, **89**, 431-458.
 250. Lai, T. S., Lee, S. K. S., Yeung, L. L., Liu, H. Y., Williams, I. D., Chang, C. K. Remarkable axial ligand effect on regioselectivity towards terminal alkenes in epoxidation of dienes by a robust manganese porphyrin. *Chemical Communications*, 2003, 620-621.
 251. Calvente, R. M., Campos-Martin, J. M., Fierro, J. L. G. Effective homogeneous molybdenum catalyst for linear terminal alkenes epoxidation with organic hydroperoxide. *Catalysis Communications*, 2002, **3**, 247-251.
 252. Rose, E., Ren, Q. Z., Andrioletti, B. A unique binaphthyl strapped iron-porphyrin catalyst for the enantioselective epoxidation of terminal olefins. *Chemistry - A European Journal*, 2004, **10**, 224-230.
 253. Perrin, D. D., Armarego, W. L. F., Perrin, D. R. *Purification of laboratory chemicals*. Oxford: Pergamon Press Ltd., 1980.
 254. Lennon, P., Rosenblum, M. Carbon-carbon bond formation by condensation at metal-activated olefins. Regio- and stereoselectivity of cycloaddition reactions. *Journal of the American Chemical Society*, 1983, **105**, 1233-1241.
 255. Chow, S., Kitching, W. Hydrolytic kinetic resolution of terminal mono- and bis-epoxides in the synthesis of insect pheromones: Routes to (-)-(R)- and

- (+)-(S)-10-methyldodecyl acetate, (-)-(R)-10-methyl-2-tridecanone, (-)-(R)-(Z)-undec-6-en-2-ol (Nostrenol), (-)-(1R,7R)-1,7-dimethylnonyl propanoate, (-)-(6R,12R)-6,12-dimethylpentadecan-2-one, (-)-(2S,11S)-2,11-diacetoxytridecane and (+)-(2S,12S)-2,12-diacetoxytridecane. *Tetrahedron : Asymmetry*, 2002, **13**, 779-793.
256. Bryliakov, K. P., Babushkin, D. E., Talsi, E. P. ^1H NMR and EPR spectroscopic monitoring of the reactive intermediates of (Salen) Mn^{III} catalyzed olefin epoxidation. *Journal of Molecular Catalysis A: Chemical*, 2000, **158**, 19-35.
257. Groves, J. T., Watanabe, Y., McMurry, T. J. Oxygen activation by Metalloporphyrins. Formation and decomposition of an acylperoxymanganese(II) complex. *Journal of the American Chemical Society*, 1983, **105**, 4489-4490.
258. Groves, J. T., Lee, J., Marla, S. S. Detection and characterization of an oxomanganese(V) porphyrin complex by rapid-mixing stopped-flow spectrophotometry. *Journal of the American Chemical Society*, 1997, **119**, 6269-6273.
259. Khavrutskii, I. V., Musaev, D. G., Morokuma, K. Epoxidation of unfunctionalized olefins by Mn(salen) catalyst using organic peracids as oxygen source: A theoretical study. *Proceedings of the National Academy of Sciences (USA)*, 2004, **101**, 5743-5748.
260. Khavrutskii, I. V., Musaev, D. G., Morokuma, K. Cooperative pull and push effects on the O-O bond cleavage in acylperoxo complexes of [(Salen) Mn^{III} L]: Ensuring formation of manganese(V) oxo species. *Inorganic Chemistry*, 2005, **44**, 306-315.

261. Khavrutskii, I. V., Musaev, D. G., Morokuma, K. Insights into the structure and reactivity of acylperoxo complexes in the kochi-jacobsen-katsuki catalytic system. A density functional study. *Journal of the American Chemical Society*, 2003, **125**, 13879-13889.
262. Khavrutskii, I. V., Rahim, R. R., Musaev, D. G., Morokuma, K. Axial ligand and solvent effects on the O-O bond activation in acylperoxo complexes of [(Salen)Mn^{III}L]: Mn^{IV} versus Mn^V oxo species. *Journal of Physical Chemistry B*, 2004, **108**, 3845-3854.
263. Rilbe, H. *pH and Buffer Theory : A New Approach*. New York: John Wiley & Sons, 1996.
264. Groves, J. T., Stern, M. K. Olefin epoxidation by manganese(IV) porphyrin: evidence for two reaction pathways. *Journal of the American Chemical Society*, 1987, **109**, 3812-3814.
265. Schappacher, M., Weiss, R. Formation of manganese(IV)-oxo-porphyrin derivatives by decomposition of peroxycarbonate complexes. *Inorganic Chemistry*, 1987, **26**, 1189-1190.
266. Lansky, D. E., Mandimutsira, B., Ramdhanie, B., Clausen, M., Penner-Hahn, J. E., Zvyagin, S. A., Telser, J., Krzystek, J., Zhan, R., Ou, Z. P., Kadish, K. M., Zakharov, L., Rheingold, A. L., Goldberg, D. P. Synthesis, characterization, and physicochemical properties of manganese(III) and manganese(V)-oxo corrolazines. *Inorganic Chemistry*, 2005, **44**, 4485-4498.
267. Gultneh, Y., Ahvazi, B., Khan, A. R., Butcher, R. J., Tuchagues, J. P. Modeling the multinuclear redox-active manganese enzymes - Synthesis, structure, and properties of a Bis(Dinuclear Mn(III)- μ -oxo-Bis(μ -acetato)) Complex. *Inorganic Chemistry*, 1995, **34**, 3633-3645.
268. Hureau, C., Blondin, G., Charlot, M. F., Philouze, C., Nierlich, M., Cesario, M.,

- Anxolabehere-Mallart, E. Synthesis, structure, and characterization of new mononuclear Mn(II) complexes. Electrochemical conversion into new oxo-bridged Mn₂(III,IV) complexes. Role of chloride ions. *Inorganic Chemistry*, 2005, **44**, 3669-3683.
269. Glerup, J., Goodson, P. A., Hazell, A., Hodgson, D. J., McKenzie, C. J., Michelsen, K., Rychlewska, U., Toftlund, H. Synthesis and characterization of bis(μ -oxo)dimanganese(III,III), -(III,IV), and -(IV,IV) complexes with ligands related to N,N'-bis(2-pyridylmethyl)-1,2-ethanediamine (bispicen). *Inorganic Chemistry*, 1994, **33**, 4105-4111.
270. Osokin, M. Y., Karpov, O. P., Osokin, Y. G., Surovtsev, A. A., Bychkov, B. N., Kryukov, S. I. Epoxidation of 5-vinyl-2-norbornene with *tert*-butyl hydroperoxide, catalyzed with transition metal compounds. *Russian Journal of Applied Chemistry*, 2001, **74**, 834-838.
271. Bryliakov, K. P., Kholdeeva, O. A., Vanina, M. P., Talsi, E. P. Role of Mn^{IV} species in Mn(salen) catalyzed enantioselective aerobic epoxidations of alkenes: An EPR study. *Journal of Molecular Catalysis A: Chemical*, 2002, **178**, 47-53.
272. Linde, C., Arnold, M., Norrby, P., Akermark, B. Is there a radical intermediate in the (salen)Mn-catalyzed epoxidation of alkenes? *Angewandte Chemie-International Edition*, 1997, **36**, 1723-1725.
273. Ostovic, D., Bruice, T. C. Mechanism of alkene epoxidation by iron, chromium, and manganese higher valent oxo-metalloporphyrins. *Accounts of Chemical Research*, 1992, **25**, 314-320.
274. Limberg, C. The role of radicals in metal-assisted oxygenation reactions. *Angewandte Chemie-International Edition*, 2003, **42**, 5932-5954.
275. Norrby, P., Linde, C., Akermark, B. On the chirality transfer in the

- epoxidation of alkenes catalyzed by Mn(salen) complexes. *Journal of the American Chemical Society*, 1995, **117**, 11035-11036.
276. Backvall, J. E., Bokman, F., Blomberg, M. R. A. Metallaoxetanes as possible intermediates in metal-promoted deoxygenation of epoxides and epoxidation of olefins. *Journal of the American Chemical Society*, 1992, **114**, 534-538.